TEXTILE RESEARCH JOURNAL

Publication of

TEXTILE RESEARCH INSTITUTE

VOLUME XXIX MARCH 1959 NUMBER 3

TEXTILE RESEARCH JOURNAL

VOL. XXIX *March 1959* NUMBER 3

Editor: **Julian S. Jacobs**

Assistant Editor: **Richard K. Toner**

Production Editor: **Candida Frenking**

Advisory Board

H. J. Ball
Earl E. Berkley
Henry Eyring
W. J. Hamburger
Milton Harris
K. L. Hertel
Harold P. Lundgren
H. Mark
E. R. Schwarz

TEXTILE RESEARCH JOURNAL, published monthly at Prince and Lemon Streets, Lancaster, Pa., is devoted to the interest of research in textile and allied industries. It is published by Textile Research Institute.

Manuscripts and communications should be sent to the Publications Department, P.O. Box 625, Princeton, N. J.

Second-class postage paid at Lancaster, Pa.

Subscription rates: $25.00 per year; additional for postage, 50 cents to Canada, $1.00 to all other countries. Single copies, $2.50 each.

Contents copyrighted © 1959 by Textile Research Institute. Advertising rates supplied on request.

IN THIS ISSUE

Theoretical Analysis of Rate of Liquid Absorption by Capillary Absorbing Media. *Allen R. Winch* 193

Concerning the Mechanism of Fiber and Yarn Lubrication. *C. Schlatter, R. A. Olney, and B. N. Baer* 200

Stiffness and Resiliency of Wet and Dry Fibers as a Function of Temperature. *G. M. Bryant and A. T. Walter* 211

Improved Instrument to Measure the Moisture Content of Lint Cotton, Seed Cotton, and Cottonseed. *J. A. Reddick, S. C. Mayne, Jr., and Earl E. Berkley* 219

A Two-Phase Structure for Keratin Fibers. *M. Feughelman* 223

Density Changes in Cellulose Treated With Urea-Formaldehyde Resins. *Richard Steele and Raymond P. Schiwall* 228

A Study of the Relationship Between Breaking Time and Breaking Load for Fabrics Tested on CRE and CRT Machines. *Audrey S. Tweedie, Margaret T. Mitton, and J. Margaret Fry* 235

Rheological Interpretation of the Mechanism of Crease Recovery of Fiber. *Hiroshi Sobue and Kenkichi Murakami* 251

Effects of Heat-Drying on the Physical and Chemical Properties of Cotton. *Mary L. Nelson, Frederick R. Andrews, and James N. Grant* 260

Phosphonomethylation of Cotton. *George L. Drake, Jr., Wilson A. Reeves, and John D. Guthrie* 270

The Effects of Gamma Radiation on Cotton. *Part II:* Base Exchange Properties of Irradiated Cotton. *Robert J. Demint and Jett C. Arthur, Jr.* 276

LETTERS TO THE EDITOR

A Useful Stain for Inclusion and Surface Damage Detection in Viscose Rayon Filaments. *E. Corwith Jolliff* 279

A Note on the Degradation of Jute Cellulose on Storage. *H. Chatterjee and A. K. Mazumdar* 282

The Hydrogen → Deuterium Exchange Reaction in Stretched Keratin. *G. G. S. Dutton and I. H. Rogers* 284

Book Reviews 286

REPRINT REQUESTS SHOULD BE DIRECTED TO THE AUTHORS

SEE ARTICLES FOR ADDRESSES

MARCH 1959
VOL. XXIX NO. 3

TEXTILE RESEARCH JOURNAL

Theoretical Analysis of Rate of Liquid Absorption by Capillary Absorbing Media

Allen R. Winch

Celanese Corporation of America, New York 16, N. Y.

Abstract

A theoretical analysis of rate of capillary absorption by absorbent media is presented which emphasizes the critical importance of environmental factors to the rate of liquid absorption (as well as factors which are specific to the structure of the absorbent mass). The theoretical relationships of environmental factors and capillary structure are combined in an over-all rate of flow equation. From this equation many theoretical conclusions of interest may be drawn. The equation also suggests principles for design of capillary structures for optimum rate of absorption in proper relationship to external or competing environmental factors.

Introduction

Measurement and theory of absorbency of cotton fabrics have been discussed, and an interesting testing apparatus and procedure have been described previously by Buras, Goldthwait, and Kraemer [1]. Their paper points out many of the problems associated with absorption rate studies. It is our purpose in this paper to shed further light on this problem by using a different approach. We have pursued the analysis of a fluid flow system using a broader theoretical approach in order to encompass most of the environmental factors, as well as those factors which are specific to the structure of the absorbent mass, which affect the rate of liquid absorption. The environment can never really be neglected in rate analysis or in design for optimum rate.

This analysis presents no new basic knowledge, but, we hope, a better understanding of important relationships. Various elements of the problem, such as capillarity, frictional resistance to fluid flow, etc., have been treated extensively by others. However, fluid flow equations have been developed for steady state conditions, and capillary studies have been devoted primarily to equilibrium conditions. But here we are dealing with a dynamic, changing system as fluid is absorbed into a capillary absorbent system. Hence, some caution must be used to adjust our basic theoretical relationships for steady state and equilibrium in order to modify and assemble them for unsteady state where rate of flow tends to change with time. This paper assembles the basic elements into a proper framework and presents an analysis which should be of general interest.

It was rather awkward to approach the problem until the boundaries of a thermodynamic system were defined in the manner noted in this analysis.

The boundaries were chosen to avoid dealing with the surface energy changes occurring as the liquid wets *dry* walls. The only surface energy change of interest is that component which is actually used to draw liquid into the "wetted walls" of empty capillaries. Hence only the surface energy released by reducing the liquid–air interface (i.e., the reduction in interfacial area as the "wetted wall" capillaries fill up) is considered as contributing to the capillary driving force. This energy factor is actually introduced by using the relationship of Equation 9.

This definition of boundaries and the idealized assumptions permitted a relatively straightforward and simple solution. Reality may, of course, depart from the idealized assumptions to varying degrees. When and if it does, this treatment should focus attention on the nature of the departure and enable us to examine and understand the deviations from theory more readily.

The effect of air flow resistance as it is expelled by the advancing liquid has been neglected in this treatment. Furthermore, the equation assumes that open end capillaries are under consideration with atmospheric pressure at both ends essentially the same.

Two very important general conclusions which we shall point out in this analysis are given. First, for maximum rate of liquid absorption there is an optimum effective capillary diameter or pore size. This optimum size depends upon environmental conditions of use external to the absorbing media, such as hydrostatic head, capillary tension of the supply source, and friction of fluid flow in the source. Second, because of the above, considerable caution should be used in the method of testing absorbent media for rate of fluid absorption. If an arbitrary test method is used which "prefers" one optimum pore size or capillary diameter for maximum rate of absorption, and the material being tested will actually be used with another environmental condition which "prefers" another optimum pore size, then the rate testing device can rank the various absorbing media incorrectly for the end use application.

Existing rate testing methods should be examined carefully in the light of this type of analysis to determine whether they are properly designed to give meaningful data for end use application of the materials being tested.

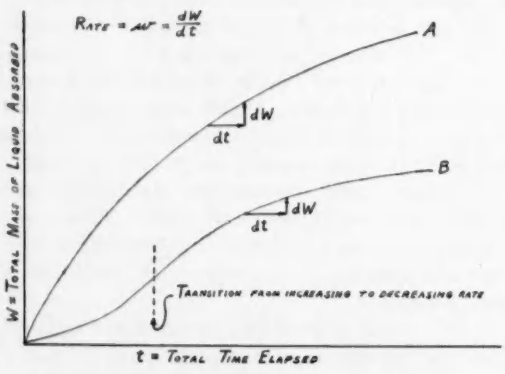

Fig. 1. Liquid absorbed vs. time elapsed.

A New Approach to the Analysis

If we plot W, the total mass of liquid absorbed, as the ordinate versus t, the total time required to absorb W, as the abscissa we obtain flow curves typified in Figure 1. Since the mass rate of fluid flow, w, at any given moment equals the differential fraction dW/dt, the instantaneous rate of absorption w can be represented by the instantaneous slope of the W–t curve. Such flow curves may be obtained by appropriate testing devices.

We are very much interested in the shape of this W–t curve. First we must understand the significance of its shape and the factors influencing it if we are to interpret test data intelligently and translate this evaluation properly for end use applications. Second, we are very much interested in changing the shape of this curve by designing the absorbent mass to suit our purposes. For these reasons we need a theoretical explanation or equation (rather than an empirical equation) which relates all of the factors affecting the rate of fluid flow.

To attack this problem we have therefore set up two different and distinct idealized models which can be analyzed in classical terms of thermodynamics and hydrodynamics.

Model A assumes that the liquid immediately wets the capillary walls of the absorbing medium; i.e., the contact angle at the liquid–solid–air interface is constant. For such a case the rate controlling factor may be considered to be the frictional resistance to fluid flow. This case is a falling rate process, and it is of considerable interest because highly absorbent materials undoubtably approach this condition.

Model B assumes the liquid is absorbed at a *constant* rate of linear diffusion. This case is usually an *increasing total mass* rate flow process. In this case the rate controlling factors are those which affect the rate of mass transfer at the liquid–gas–solid interface of the advancing liquid. Since this rate may be increased by merely increasing the area of the interface across which mass transfer is occurring, the total mass rate of the flow can increase with time in those cases where the flow pattern is one of an expanding hemisphere, disc, etc.; i.e., a flow pattern which enlarges the advancing wetted frontier as more liquid is absorbed.

Of course there are probably many cases where the absorption process begins with the rate of mass transfer at the advancing interface as the controlling factor, but then, as the wetted perimeter grows larger and the rate of flow increases, the retarding frictional forces in the rear may become the dominant rate controlling factor, and the flow curve may pass from an increasing rate zone into a decreasing rate zone. Surface tension, contact angle, and viscosity should influence the point at which this transition occurs. We are interested in this model because we believe that some relatively nonabsorbent materials approach this condition.

Most of our discussion pertains to Model A. Figure 2 represents a generalized liquid absorption system including environmental effects symbolized by the "plumbing" leading up to the absorbent mass. This system is defined thermodynamically, and the equation is developed showing the overall energy balance which exists when a unit mass of liquid is absorbed by the absorbing medium. From this energy balance an overall flow equation is derived which brings all of the elements affecting rate of liquid absorption into a proper framework as they relate to one another.

This frame of reference for the various elements affecting flow rate is of general practical importance to anyone who wishes to either measure or control rate of fluid absorption.

Some of the elements attached to this frame are not well defined with respect to reality. However, this analysis helps call attention to these areas and should stimulate further experimental investigation of these elements.

Analysis

A generalized thermodynamic picture of a fluid flow system is outlined in Figure 2 showing a liquid source of supply contained in a glass tube connected to an orifice by a length of rubber tubing. As liquid is absorbed by capillary action into the absorbing medium at the advancing meniscus (2), liquid is simultaneously withdrawn from the glass capillary tube as indicated by the retreating meniscus (1).

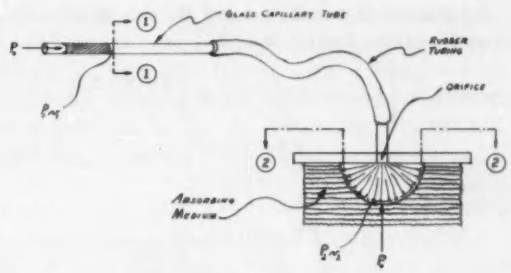

Fig. 2. Generalized thermodynamic picture of fluid flow absorption system.

For a simple thermodynamic analysis the system is defined as the liquid mass bounded by the *wetted walls* of the glass capillary tubing, the rubber tubing, and the wetted walls of the absorbing medium. This liquid mass is also bounded by a film of liquid a differential distance in advance of the retreating meniscus and also by a film of liquid a differential distance behind the advancing meniscus. The equations below are obtained from an energy balance for the system when the boundaries of the system move to displace a unit mass of liquid from the source (glass capillary tube) into the absorbing medium.

An over-all energy balance is given by Equation 1; symbols are defined, along with consistent units, in the Appendix.

$$\P = (z_1 - z_2) + \left(\frac{P_1 - P_2}{\rho}\right) = F_s + F_1 + \Delta I \qquad (1)$$

An over-all generalized fluid flow relationship is given by Equation 2.

$$w = \left[(Z_1 - Z_2)\left(\frac{g_L}{g_c}\right) + \left(\frac{\psi\sigma\cos\theta_2}{\rho}\right) - \left(\frac{4\sigma\cos\theta_1}{\rho D_c}\right) - F_1 - \Delta I\right] \div \left[k_0\int_0^{L_s}\left(\frac{dL_s}{A_s}\right)\right] \qquad (2)$$

Equation 3 in terms of t and W may be obtained from Equation 2 since $w = dW/dt$.

$$t = k_9 H \div \left[(Z_1 - Z_2)\left(\frac{g_L}{g_c}\right) + \left(\frac{\psi\sigma \cos\theta_2}{\rho}\right) - \left(\frac{4\sigma \cos\theta_1}{\rho D_c}\right) - F_1 - \Delta I \right] \quad (3)$$

where

$$H = \int_{,}^{W} \int_{0}^{L_s} \left(\frac{dL_s}{A_s}\right)(dW) \quad (4)$$

If the absorbing medium is isolated from environmental effects of hydrostatic head, capillarity of the liquid source, frictional resistance to fluid flow in the source "plumbing," and inertia or kinetic energy effects, Equation 2 simplifies to Equation 5.

$$w = \left(\frac{\psi}{k_2 k_8}\right)\left(\frac{\rho\sigma \cos\theta_2}{\mu}\right)\left[\frac{1}{\int_0^{L_s}\left(\frac{dL_s}{A_s}\right)}\right] \quad (5)$$

Equation 6, in terms of t and W, may be obtained from Equation 5.

$$t = \left(\frac{\rho k_9 H}{\psi\sigma \cos\theta_2}\right) \quad (6)$$

General Remarks and Conclusions

In Equation 1, the driving force for liquid absorption, ¶, is equal to the potential energy term $(z_1 - z_2)$ plus the energy term $(P_1 - P_2)/\rho$, which results from the net differences in capillary tension between the absorbing medium and the liquid source. This driving force is balanced by a number of resisting forces. These are the frictional resistance to fluid flow in the absorbing medium and the source or supply "plumbing," F_s and F_1 respectively, and also the inertia or kinetic energy term, ΔI.

Since it can be shown that

$$F_s = wk_9 \int_0^{L_s}\left(\frac{dL_s}{A_s}\right) \quad (7)$$

$$(z_1 - z_2) = (Z_1 - Z_2)(g_L/g_c) \quad (8)$$

and

$$\left(\frac{P_1 - P_2}{\rho}\right) = \left[\left(\frac{\psi\sigma \cos\theta_2}{\rho}\right) - \left(\frac{4\sigma \cos\theta_1}{\rho D_c}\right)\right] \quad (9)$$

Equation 2 develops immediately from Equation 1.

Since this is *not* a standard case of steady state fluid flow, the term ΔI cannot be handled as simply as is usually done in the Bernoulli flow equation. Considerable caution should be used before neglecting this kinetic energy or inertia term, ΔI, since we must deal with the energy changes occurring within the *entire* liquid system per unit mass of liquid absorbed, rather than the mere change in kinetic energy of the unit mass absorbed.

The term F_1 may be neglected under some conditions; under other conditions F_1 may not be negligible. If it is not negligible, an equation for F_1 in terms of w and the plumbing constants (and also W if the capillaries of the source are emptying, hence growing shorter) can be derived and substituted into Equation 2.

The term ΔI also may be negligible under many conditions; however, where a testing apparatus such as that employed by Buras [1] is used, large masses of liquid in the long plumbing supply lines must be accelerated. It is preferable to modify the testing apparatus to minimize the effects of ΔI rather than to attempt to incorporate the cumbersome relationship between ΔI, w, and the geometry of the plumbing into Equation 2.

Equation 5 is an interesting, enlightening simplification in which the absorbing medium is completely divorced from environmental effects of plumbing, inertia, and hydrostatic head. However, it must be used with considerable caution, always keeping in mind the simplifying assumptions. Since there are always environmental effects present in any end use application, generalized conclusions based on Equation 5 can be highly misleading. It is, nevertheless, interesting to examine Equation 5. Here it can be seen that (if the absorbing medium is divorced from supply plumbing effects, inertia effects, and hydrostatic head effects) the mass rate of flow, w, of the liquid depends upon three basic factors: (1) the factor $(\psi/k_2 k_8)$ which characterizes the physical structure of the absorbing medium, (2) the factor $(\rho\sigma \cos\theta_2/\mu)$ which characterizes the liquid in terms of its density ρ, its surface tension σ, its viscosity μ, and its contact angle θ_2 with the absorbing medium (i.e., the facility with which it wets or is attracted by the absorbing medium), and (3) the factor $\int_0^{L_s}\left(\frac{dL_s}{A_s}\right)$ which characterizes the flow pattern in the absorbing medium. L_s is the path length of fluid flow through which liquid is flowing. The values which can be obtained for this integral depend upon the size and shape of the orifice delivering liquid to the absorbent

mass, upon the flow pattern peculiar to the method of preparing the test specimen (or the design of the absorbent mass, etc.), and upon the degree of departure from isotropic absorption characteristics of the absorbing medium. The third factor can be readily integrated for a number of different shapes or flow patterns since both L_s and A_s are functions of W, the total mass of liquid absorbed.

If the Kozeny-Carman relationship [2] holds true, $(\psi/k_2k_8) = (g_c/5)(\psi\epsilon^3/S^2)$, and for parallel rods or fibers where liquid is flowing parallel to the length of the rods or fibers, $\psi = S/\epsilon$, and therefore $(\psi/k_2k_8) = (g_c/5)(\epsilon^2/S)$.

If environmental effects are neglected, Equation 5 suggests that maximum rate w will be obtained for maximum values of (ψ/k_2k_8) which in turn means maximum values of (ϵ^2/S). However, if environmental effects exist, which of course is usually the case, Equation 2 must be used. Equation 2 can be rearranged and rewritten in terms of ϵ and S to give Equation 10 for parallel rods or fibers.

$$w = \left\{\frac{\left(\frac{\rho^2}{\mu}\right)\left(\frac{g_c}{5}\right)\left(\frac{\epsilon^3}{S^2}\right)}{\int_0^{L_s}\left(\frac{dL_s}{A_s}\right)}\right\}\left\{\left(\frac{S}{\epsilon}\right)\left(\frac{\sigma\cos\theta_2}{\rho}\right) + (Z_1 - Z_2)\left(\frac{g_L}{g_c}\right) - \left(\frac{4\sigma\cos\theta_1}{\rho D_c}\right) - F_1 - \Delta I\right\} \quad (10)$$

Now it is easy to see that making the voidage, ϵ, larger or making the surface area, S, smaller will increase the value of factor (ϵ^3/S^2), but that it will decrease the value of (S/ϵ). Hence, there is an optimum value for ϵ and S which will give maximum flow rate w, and this optimum value will depend upon the relative magnitudes of the factors in the numerator of the right-hand side of Equation 10, viz., the hydrostatic head, the capillary tension of the source plumbing, the inertia of the total liquid mass, and the friction of the source plumbing on the one hand and the capillary tension of the absorbing medium on the other.

The fact that the optimum capillary diameter, pore size, or ϵ-to-S relationship for maximum rate of absorption depends upon environmental conditions external to the absorbing medium is of considerable importance in the design of a rate testing apparatus and the method of using such a device to rank the efficiency of various absorbing media. Where end use environment of hydrostatic head, inertia of the liquid mass, capillary tension of the source, or fluid flow friction of the source are significantly different from the environmental conditions imposed by the test method, serious errors in ranking can result.

Acknowledgment

The author wishes to thank Dr. Edmund Buras, Jr. of Harris Research Laboratories for his constructive criticisms and helpful comments.

Appendix: Symbols, Definitions, Units, and Abbreviations Used in Fluid Flow Analysis for Absorption Rates

Letter symbols are listed alphabetically, followed by definitions and explanations. The equations are set up using the gravitational conversion constant (g_c) which has converted the potential energy and the frictional energy terms to gravitational units of gram force-centimeters for the c.g.s. system. The units for pressure and surface tension have been specified in gravitational units for consistency. The units for viscosity, however, must be absolute units by definition of the dimensionless Reynolds number. The net result is that all energy terms in the equations as derived in this discussion are in the gravitational system. Care must therefore be used when using surface tension data that such data be converted to gram force/centimeter as indicated in the notation following the symbol for surface tension, σ.

For those who prefer to use absolute units of force and energy throughout, the gravitational units of force and energy can be converted to absolute units by multiplying the gravitational units by the factor (g_c).

Only the c.g.s. units are given with the alphabetical list of symbols; the following abbreviations have been used.

centimeter:	cm.
gram mass:	gmm. or gm.
gram force:	gmf.
second:	sec.

Alphabetical List of Symbols With Definitions, Units

A = cross-sectional area of duct, tube, pipe, channel, or bed through which liquid is flowing, this area being perpendicular to the path of fluid flow [cm.^{2}]

A_0 = superficial value of A for granular, fibrous, or porous bed which assumes that the entire area is open and free for fluid flow

A_s = A_0 for absorbing sample or medium being tested or used

A_T = A for connecting tubing between glass capillary and the absorbing medium or sample

A_2 = $A_0 = A_s$ for absorbing medium or sample
= A at Boundary ②, the downstream boundary of the fluid flow system

A_1 = A at Boundary ①, the upstream boundary of the fluid flow system

D = the diameter of duct, tube, or medium through which liquid is flowing [cm.]

$D_c = D$ for glass capillary tube

F = total mechanical energy converted by frictional flow within the system into heat per unit mass of liquid absorbed by the absorbing medium $\left[\frac{\text{gmf.-cm.}}{\text{gmm.}}\right]$

$F_c = F$ for glass capillary tube

$F_s = F$ for absorbing sample or medium

$F_T = F$ for connecting tubing between glass capillary and absorbing sample

$F_1 = (F_c + F_T) = F$ for "plumbing" leading up to the absorbing medium

g_c = gravitational conversion factor, a dimensional constant in Newton's law of "force = $\left(\frac{\text{mass} \times \text{acceleration}}{g_c}\right)$," where the force is expressed in gravitational units of force such as the "pound of force" or "the gram of force"

$$g_c = \left[\frac{980.6 \text{ gmm.-cm.}}{\text{gmf.-sec.}^2}\right] = \left[\frac{980.6 \text{ dynes}}{\text{gmf.}}\right]$$

g_L = the local acceleration of gravity; approximately 980.6 cm./sec.^{2}

$\left(\frac{g_L}{g_c}\right)$ = gravitational force acting upon unit mass

Since g_L usually varies from g_c by such a small numerical amount, the numerical value of (g_L/g_c) is usually assumed to be unity. Another way of viewing the dimension of (g_L/g_c) is as follows:

$$(g_L/g_c) = \left[\frac{980 \text{ cm./sec.}^2}{980.6 \text{ dynes/gmf.}}\right] \approx 1.000 \left[\frac{\text{gmf.}}{\text{gmm.}}\right]$$

$$H = \left[\int_0^W \int_0^{L_s} \left(\frac{dL_s}{A_s}\right)(dW)\right] \left[\frac{\text{gmm.}}{\text{cm.}}\right]$$

This double integral represents the summation of (flow path length/flow area) integrated over the entire path length from $L_s = 0$ to $L_s = L_s$ for each moment of time t; this integral is again integrated for the time interval $t = 0$ to $t = t$ corresponding to the liquid mass absorbed from $W = 0$ to $W = W$. Integrated values of H for various flow patterns can readily be obtained since both L_s and A_s are functions of W

I = kinetic energy or inertia of the total liquid mass in the entire system [gmf.-cm.]

$I_c = I$ for total liquid mass in glass capillary tube

$I_T = I$ for total liquid mass in rubber connecting tubing

$I_s = I$ for total liquid mass in the absorbing medium or sample

$\Delta I = (I_2 - I_1)$ = change in kinetic energy or inertia of the entire system per unit mass of liquid absorbed by the absorbing medium $\left[\frac{\text{gmf.-cm.}}{\text{gmm.}}\right]$

$k_2 = \left(\frac{32}{g_c}\right)$ = constant in Darcy flow equation [gmf.-sec.^{2}/gmm.-cm.]

$k_3 = \left(\frac{\mu}{\rho^2}\right)$ = fluid constant in Darcy flow equation [cm.^{5}/gmm-.sec.]

$k_s = \left(\frac{5S^2}{32\epsilon^3}\right)$ = specific resistance constant of absorbing medium [cm.$^{-2}$]

$k_p = (k_2 k_3 k_s) = \left(\frac{32}{g_c}\right)\left(\frac{\mu}{\rho^2}\right)\left(\frac{5S^2}{32\epsilon^3}\right)$ = combined specific resistance constant for the liquid-absorbing medium system $\left[\frac{\text{gmf.-sec.-cm.}^2}{\text{gmm.}^2}\right]$

L = length of duct, tube, or medium through which liquid is flowing [cm.]

L_s = superficial L for absorbing medium, porous bed, etc.

P = static pressure [gmf./cm.^{2}]

P_0 = atmospheric pressure

P_1 = pressure in liquid in glass capillary tube a differential distance in front of the retreating meniscus

P_2 = pressure in the liquid in the absorbing medium a differential distance behind the advancing meniscus

$(P_1 v_1)$ = work done by the retreating boundary on the liquid-system per unit mass of liquid absorbed by the absorbing medium [gmf.-cm./gmm.]

$(P_2 v_2)$ = work done by the liquid on the advancing boundary in the absorbing medium per unit mass of liquid absorbed by the absorbing medium [gmf.-cm./gmm.]

S_0 = area of particle or fiber surface per unit volume of solid particle of fiber [cm.$^{-1}$]

$S = S_0(1 - \epsilon)$ = area of particle or fiber surface per unit volume of absorbing sample [cm.$^{-1}$]

t = total time required to absorb W mass of liquid [sec.]

$v = (1/\rho)$ = specific volume of liquid $\left[\frac{\text{cm.}^3}{\text{gmm.}}\right]$

W = total weight of liquid absorbed by absorbing medium in time t [gmm.]

w = total mass rate of liquid flow [gmm./sec.]
$w = (dW/dt)$

Z = height above any arbitrary datum plane [cm.]

Z_1 = height of liquid at Boundary ①

Z_2 = height of liquid at Boundary ②

$(Z_2 - Z_1)$ = vertical distance a unit mass of liquid moves; see note below regarding $(z_2 - z_1)$

z = potential energy of the total liquid mass in the system [gmf.-cm.]

$(z_2 - z_1)$ = change in potential energy of the total liquid mass in the system per unit mass of liquid absorbed by the absorbing medium [gmf.-cm./gmm.]

Note: $(z_2 - z_1) = (Z_2 - Z_1) \times (g_L/g_c)$ since, when unit mass of liquid is absorbed, the net change in potent tial energy of the entire system is the same as if a unimass were moved directly from height Z_1 to height Z_2.

ϵ = voidage or fractional free volume in the absorbing medium (dimensionless)

θ = contact angle between the wetted solid surface and the meniscus as measured within the liquid

$\theta_1 = \theta$ for liquid–air–solid at retreating boundary interface

$\theta_2 = \theta$ for liquid–air–solid at advancing boundary interface

ρ = density of the liquid [gmm./cm.^{3}]

σ = surface tension of the liquid (i.e., the interfacial tension between the liquid and the air at the air–liquid interface [gmf./cm.]

Note: $\sigma = \frac{\sigma'}{g_c} = \left(\frac{\sigma'}{980.6}\right)$ gmf./cm., where σ' = surface tension of the liquid in dynes/cm. $= \left(\frac{\text{gmm.-cm.}}{\text{sec.}^2\text{-cm.}}\right)$

μ = absolute viscosity of liquid [gmm./cm.-sec.]
1 Poise = 1 dyne-sec./cm.^{2} = 1 gmm./cm.-sec.

ψ = wetted *effective* perimeter of the advancing meniscus in the absorbing medium per unit *liquid* area (perpendicular to the path of fluid flow) at the air–liquid–solid interface [cm.$^{-1}$]

¶ = the driving force for fluid flow, equal, in effect, to the net energy available from potential and surface energy changes to overcome or supply the energy used up in frictional fluid flow and the fluid inertia changes;
$(z_1 - z_2) + \left(\frac{P_1 - P_2}{\rho}\right)\left[\frac{\text{gmf.-cm.}}{\text{gmm.}}\right]$

Literature Cited

1. Buras, E. M., Goldthwait, C. F., and Kraemer, R. M., TEXTILE RESEARCH JOURNAL **20**, 239–248 (1950).
2. Carman, P. C., *Disc. Faraday Soc.*, 72–77 (1948).
3. *Chemical Engineers' Handbook*, John H. Perry, ed., McGraw-Hill, New York, 799 (1941).

Manuscript received November 22, 1957.

MIT Summer Program

Materials for Parachute and Retardation Devices

July 20–31, 1959

This program is planned for technical personnel of the aircraft or missile fields who are interested in the design, development, and application of parachutes or other retardation devices. The topics will provide a survey of the properties of materials such as synthetic organic fibers, metallic and other inorganic fibers, plastic film, etc. Specific subjects to be discussed include static mechanical properties, general rheological behavior, behavior under impact loads, resistance to repeated loads, and high temperature characteristics.

The program will be under the supervision of Dr. Stanley Backer, Associate Professor of Mechanical Engineering, MIT, Cambridge 39, Massachusetts, from whom additional information may be obtained.

Concerning the Mechanisms of Fiber and Yarn Lubrication

C. Schlatter

Textile Consultant

R. A. Olney and B. N. Baer

Atlas Powder Co., Wilmington 99, Delaware

Abstract

In the past, the main approach to the problems of friction and its modification, as they apply to textile structures, has been to determine the coefficient of friction and to develop a general determinant for this constant. It is suggested in this paper that a quantitative measure of the frictional relationships between fiber and fiber or between fiber and some other material, rather than being a reasonably constant quantity, is a highly unreasonable variable. This is especially true if the fiber is coated with a finish, which is usually the case; then in addition to depending on such variables as contact pressure and area, stress–strain characteristics of the fiber, etc., the coefficient of friction will depend on such factors as the physical and chemical characteristics of the finish, the amount of finish present, the relative speeds of the surfaces in frictional contact, and so on.

The authors feel that it may be of greater practical significance to evaluate qualitatively the changes that take place in the frictional characteristics (type as well as magnitude) with given changes in the above-described variables. The observed behavior may then be related to performance in the various unit processes employed in textile manufacturing. Evidence justifying this point of view is presented in the paper, and some rather speculative explanations correlating finish properties and frictional behavior are given.

Introduction

The components of most physical systems seek to adjust themselves to a position offering maximum stability at minimum energy level. Thus, if due to excessive friction during manufacture, the component fibers and yarns of a fabric are not allowed sufficient mobility to adjust, strains are introduced into the fabric which often lead to puckering, uneven dyeing, decreased strength, or unpleasing esthetic qualities. The first function, therefore, of what may be called "component mobility" is to prevent the formation of undesirable tensions during the spinning, twisting, or weaving operations.

A second function of component mobility is to enable the fibers or yarns to shift smoothly and evenly relative to one another or to parts of the processing mechanism in such operations as carding, drafting, and weaving. If this mobility is impaired by excessive friction, the result will be abrasion, fiber breakage, or weak and uneven yarns and fabrics.

The third function of component mobility is to give flexibility and thereby drape and softness, where this is desirable, to fabrics. If the fibers and yarns in a fabric are not permitted to move over very short distances relative to each other (as would be the case in a heavily starched material where the fibers and yarns have actually been "glued" together) a stiff, rigid structure is the result. Fabric handle is, of course, also determined by the flexibility of the fiber itself. Plasticization of the fiber to improve fabric softness characteristics is seldom practiced, however, since this is an expensive method, leading to actual chemical modification of the fiber, and is not very effective unless fiber and yarn mobility exist to begin with.

It should not be inferred from the foregoing that low friction is the only desirable condition. Rather, it is the correct degree of friction at a particular stage of processing that is important. For example, in the sliver stage it is desirable that the fibers move easily and uniformly in relation to one another to permit proper drafting. Once the sliver has been

twisted into a yarn, however, the fibers should no longer move relative to each other (except reciprocally over very small distances to give softness or flexibility where this is desirable) so that the yarn will have strength. Thus the term lubrication, when applied to textiles, should be taken to mean the modification, but not necessarily the elimination, of the frictional characteristics of fibers.

In the case of textile structures, the degree of component mobility is almost entirely governed by the frictional relationships between the fibers and yarns themselves, and between them and parts of the processing equipment. If these materials were plastic solids, that is, perfectly inelastic, and their surfaces reasonably smooth, uniform, and free of foreign matter, the governing frictional force would be determined by

$$F = \mu P$$

where F = the total force due to friction, μ = a constant for the pair of materials in contact (usually referred to as the coefficient of friction), and P = the force (normal to the plane in which the surfaces are moving relative to each other) with which the bodies are pressed together.

This is the well-known Amonton equation, which does not apply to textile processing [6, 8], since fibers are elastic in nature and the surfaces involved are never free of foreign materials. Processors, in fact, take great pains to provide the fibers and yarns they manipulate with a coating, commonly referred to as the finish, designed to give them optimum processing characteristics.

Much of the work done to determine coefficients of friction [1, 5, 6, 7, 8, 9, 12, 15, 17, 18] has been done by running yarns or filaments over a cylindrical surface and measuring the tensions in them before and after frictional contact. The equation often used to derive the coefficient from the relationship between these tensions is the well-known "belt" or "pulley" formula

$$\frac{T_2}{T_1} = e^{\mu\theta}$$

where T_1 = the tension in the yarn just before frictional contact, T_2 = the tension just after frictional contact, e = the base of the natural logarithms, μ = the coefficient of friction (a constant), and θ = the angle of lap, in radians, of the yarn over the cylinder. Since this formula is based on Amonton's law, it cannot be expected to hold for textile materials, and it is generally acknowledged that it can lead to very erroneous estimates of T_2/T_1 when applied in practice.

Bowden and Young [2] have developed an equation which has been shown to apply to textile materials [8, 9, 11, 13, 14]

$$F = aP^n$$

where F and P are the same as in Amonton's equation, a = a constant which is equal to μ when $n = 1$, and n = a measure of the elasticity or plasticity of the materials in frictional contact. $n = 1$ for two perfectly plastic substances and $n = 0.67$ for two perfectly elastic ones.

Using this formula, Howell [6] and Lincoln [9] calculated that

$$\frac{T_2}{T_1} = \left[1 + (1 - n)a\theta\left(\frac{r}{T_1}\right)^{1-n}\right]^{1/(1-n)}$$

where r = the radius of the cylinder. As $n \to 1$

$$\frac{T_2}{T_1} = e^{a\theta(r/T_1)^{1-n}} \qquad (7)$$

which corresponds to the special case described by the "pulley" formula [1] when

$$\mu = a\left(\frac{r}{T_1}\right)^{1-n}$$

or when $n = 1$. Thus T_2/T_1 is not constant but depends on the normal force as determined by T_1, on r, and on n. This has been experimentally and theoretically substantiated [10, 16, 17]. Honegger [5] has shown that, in addition to the above factors, yarn twist and velocity may also affect the ratio.

These equations cannot be applied to finished fibers, however, since the concept of n presupposes the free and random interaction of the asperities or points of adhesion of the surfaces in frictional contact. A finish or other foreign matter present on the surfaces will hinder or completely prevent this.

When the complexities of the frictional interaction of partially or totally coated surfaces with each other or with initially uncoated surfaces are considered, it becomes difficult to see how anything but a highly complex mathematical relationship can be derived. Such an equation may be of value from a theoretical point of view if it could be used to calculate certain friction factors. It seems to the authors, however, that a study of the behavior of the dependent variables (the magnitude and type of friction) in relation to the more or less independent variables (the type

amount of finish, the type of fiber, the contact pressure, and the surface speed, to name a few) may result in information having a more direct bearing on the problems of those engaged in the lubrication of fibers, yarns, and fabrics under actual production conditions. It is in this spirit that this paper is written.

The data presented here are the result of efforts aimed at defining the nature and scope of a systematic study of the manner in which lubricants affect the frictional behavior of textile materials, under a variety of conditions. The data are of necessity preliminary in character and should be regarded in a qualitative rather than quantitative light. It is hoped that future efforts, the direction of which has been indicated by this work, will make it possible to predict accurately the changes to be expected in the frictional relationships of the components of a textile assembly with a given change in one or more of the variables listed in the preceding paragraph.

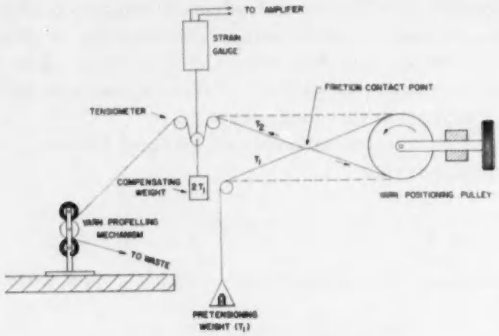

Fig. 1. Yarn-to-yarn friction setup.

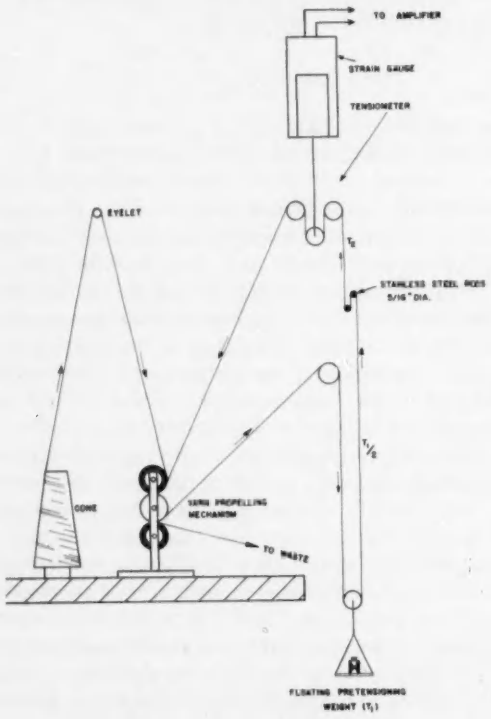

Fig. 2. Yarn-to-metal friction setup.

Experimental

The work reported here consisted essentially of applying various finishes to clean rayon yarn and measuring the friction of this yarn against itself and against stainless steel at various values of T_1 (the initial tension applied to the yarn which governs the pressure at the contact point). Also included were experiments in which heat or solvents were applied at the friction point to assess their effect on the lubricating behavior of the finishes.

The yarn used in this work was continuous filament rayon, 150 den., 40 filaments, with 2.5 turns of Z twist, supplied by the American Viscose Corporation in cake form and free of any finish. This yarn was wound into skeins to which the lubricants were applied by immersion in 0.75% aqueous dispersions of the materials and centrifuging out the excess to a wet pick-up of 90–100%. No analysis of the actual finish applied was made. Subsequent to the application, the skeins were dried for ½ hr. at 80° C. and then wound onto cones for more convenient storage.

The finish formulations and individual compounds applied are described in Table I, and require no explanation. The experimental set-ups are shown schematically in Figures 1 and 2.

In the yarn-to-yarn friction set-up (Figure 1), the yarn was made to move at a speed of 1 cm./min. (2 cm./min. relative yarn speed at the crossover point). A weight was attached to the yarn, which was then passed over a series of pulleys, initially following the path of the dotted line. The yarn positioning pulley was then rotated 540° to insert 1½ turns of S twist (corresponding to $\theta = 2\pi$) and force the yarn into contact with itself. Beyond this contact point, the yarn passed over a pulley arrange-

ment which permitted the measurement of the force, due to friction, hindering the exit of the yarn from the contact point. The signal from the strain gauge was amplified by a Universal Amplifier and recorded by a direct writing Magnetic Oscillograph (both by the Brush Electronics Company). The compensating weight, equal to twice the pretensioning weight (since T_1 acts on both sides of the pulley attached to

TABLE I. Description of the Materials Applied as Finishes

Compositions of the finishes applied to the yarn	%	Abbreviation	Viscosity, cps. 25° C.	50° C.	70° C.	90° C.	Melting point, ° C.
100 SSU white mineral oil (Textiline 100—L. Sonneborn & Sons)	90	MO+Tw 65	38	17	9	5	<25
Tween® 65 (polyoxyethylene (20) tristearate—Atlas Powder Company)	10						
100 SSU white mineral oil (as above)	70	MO+3780+Sp 80	114	30	15	8	<25
G-3780 (polyoxyethylene alkyl amine—Atlas Powder Company)	20						
Span® 80 (sorbitan monooleate—Atlas Powder Company)	10						
100 SSU white mineral oil (as above)	80	MO+263+GDO	68	30	16	11	<25
G-263 Anh. (N-cetyl-N-ethyl morpholinium ethosulfate—Atlas Powder Company)	10						
Glycerol dioleate	10						
Refined mineral oil	75	MO+MOS	159	36	16	10	<25
Mineral oil sulfonate	20						
Coupling agent+water	5						
Refined mineral oil	70	MO+EOS	54	20	10	5	<25
Ester oil sulfate	25						
Coupling agent+water	5						
Span® 40 (sorbitan monopalmitate—Atlas Powder Company)	67	Sp 40+NaOl	Solid	Solid	Solid	Too visc. to meas.	102
Sodium oleate	33						
Span® 40 (as above)	50	Sp 40+Tw 65	Solid	149	67	34	38
Tween® 65 (as above)	50						
Diglycol monostearate	50	DGMS+Tw 65	Solid	44	20	13	41
Tween® 65 (as above)	50						
Span® 60 (sorbitan monostearate—Atlas Powder Company)	60	Sp 60+1300	Solid	Solid	128	91	51
G-1300 (polyoxyethylene castor oil—Atlas Powder Company)	40						
G-3531 (complex cationic amine condensate—Atlas Powder Company)	100	3531	Solid	Solid	Too visc. to meas.	69	61
Igepon® T (sodium N-methyl-N-oleoyl taurate—Antara Chemicals, Div. of General Aniline & Film Corp.)	100	IT	Solid	Solid	Solid	Solid	
Sodium lauryl sulfate (salt free)	100	SLS	Solid	Solid	Solid	Solid	170 (?)
G-1300 (as above)	100	1300	Solid	972	571	431	41
Tween® 65 (as above)	100	Tw 65	Solid	55	28	14	31

the strain gauge), was added to make it possible to run a series, in which T_1 was varied, without having to change the amplification scale. At higher amplification, most of the available recording space on the chart would be used up by even moderate values of T_1 if no compensation were made. The mechanical means used was found to be superior to adjusting the zero electronically.

The yarn-to-metal friction set-up (Figure 2) differed from the above in four respects: (1) the yarn passed over two polished, stainless steel pins of $\frac{5}{16}$ in. diameter rather than over itself, the total arc of contact being 360° (2π radians), 180° around each pin; (2) a floating pretension instead of a dead weight was used; (3) the yarn speed was 10 m./min. (500 times greater than the relative speed of the yarn-to-yarn measurements); (4) no compensating weight was used.

The yarn propelling mechanism in both cases consisted of a miniature squeeeze roll arrangement of two rubber covered idler rolls and a center brass driving roll. This mechanism was driven by a constant speed motor. The pressure on the rolls could be adjusted and was maintained reasonably constant throughout the work at such a level as to insure slippage-free operation without causing undue yarn distortion. All tests were carried out at room temperature and approximately 50% RH.

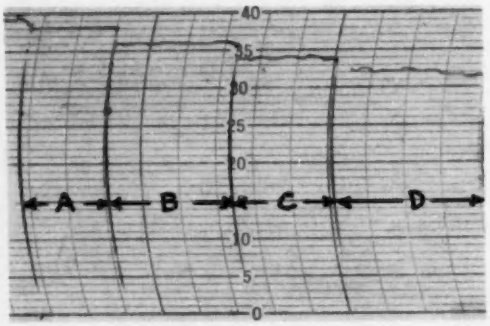

Fig. 3. Example of smooth yarn-to-yarn friction (3531).

Results and Discussion

Figures 3 and 4 are examples of the oscillograph tracings obtained from yarn-to-yarn measurements. Figure 3 illustrates the smooth type of friction obtained with a highly effective lubricant. Sections A, B, C, and D of this graph show the typical increase in friction level with an increase in T_1. An increase in frictional force is indicated by progression of the tracings toward the bottom of the chart. Due to a modification of the recording instrument, the numbers printed on the chart are in reverse order. In Figure 3, initial tensions of 10, 20, 30, and 50 g. produced frictional forces ($T_2 - T_1$) of 6, 12, 18, and 20 g. respectively. As the character of the tracings indicate, the friction was of the smooth type at all levels. By way of contrast, Figure 4 illustrates the "stick-slip" type of friction obtained with a less effective lubricant. Sections A, B, and C were obtained with T_1 values of 10, 20, and 30 g. respectively. Each one of the zigzags represents a gradual increase in tension until static friction is overcome and the yarn begins to move; then there is a rapid drop in the tension (apparently due to the fact that the dynamic friction is lower than static friction in this case) until a level is reached where the dynamic friction is sufficient to stop the yarn from moving, and then the cycle is repeated. The stick-slip type of friction is always obtained with finish-free yarns; the tracings obtained, however, show a much higher level and magnitude of stick-slip and are not nearly as uniform as the tracings in Figure 4.

Where this type of friction was obtained, $T_2 - T_1$ was taken as the average of the peaks of the tracing (the points of the zigzag closest to the bottom of the chart). Sections A, B, and C of Figure 4 yield average $T_2 - T_1$ values of 19, 55, and 92 g. re-

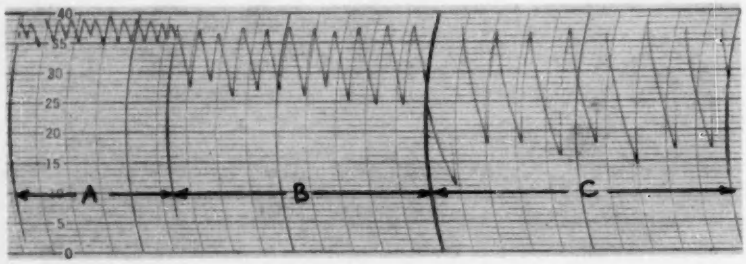

Fig. 4. Example of stick-slip yarn-to-yarn friction (DGMS + Tw 65).

spectively. It was reasoned that stick-slip friction could not occur with the test method employed unless at least one of the materials being tested possessed elastic deformation characteristics. This, in turn, suggested that the magnitude of the stick-slip (the distance between the valleys and peaks of the zigzag), but not the peak level, was greatly dependent on the stress–strain characteristics of the fiber and the length of yarn under test. A series of experiments, in which the distance between the yarn positioning pulley and the strain gauge pulley was varied, confirmed this. As the distance was decreased, the magnitude of the stick-slip effect increased, and when the distance was increased, it decreased proportionately. At no time, however, was there a change in the level of the peaks, that is, $T_2 - T_1$.

Figure 5 shows typical curves obtained in the yarn-to-metal work. Here again the expected increase of T_2 with an increase in T_1 is obtained. T_2 was determined from an "average" line drawn through the tracings. The average T_2 values, in grams, derived from each section are indicated at the bottom of the chart strip.

Figure 6 is a graphic presentation of yarn-to-yarn and yarn-to-metal friction data obtained at various

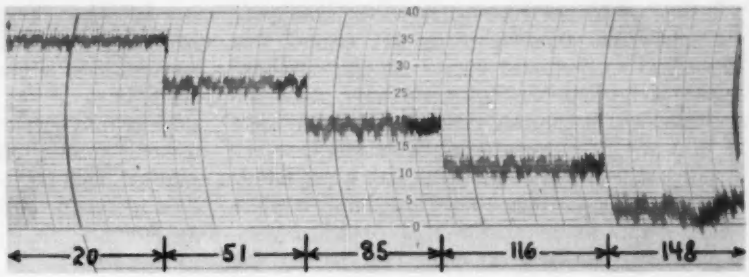

Fig. 5. Example of yarn-to-metal friction (MO + 263 + GDO).

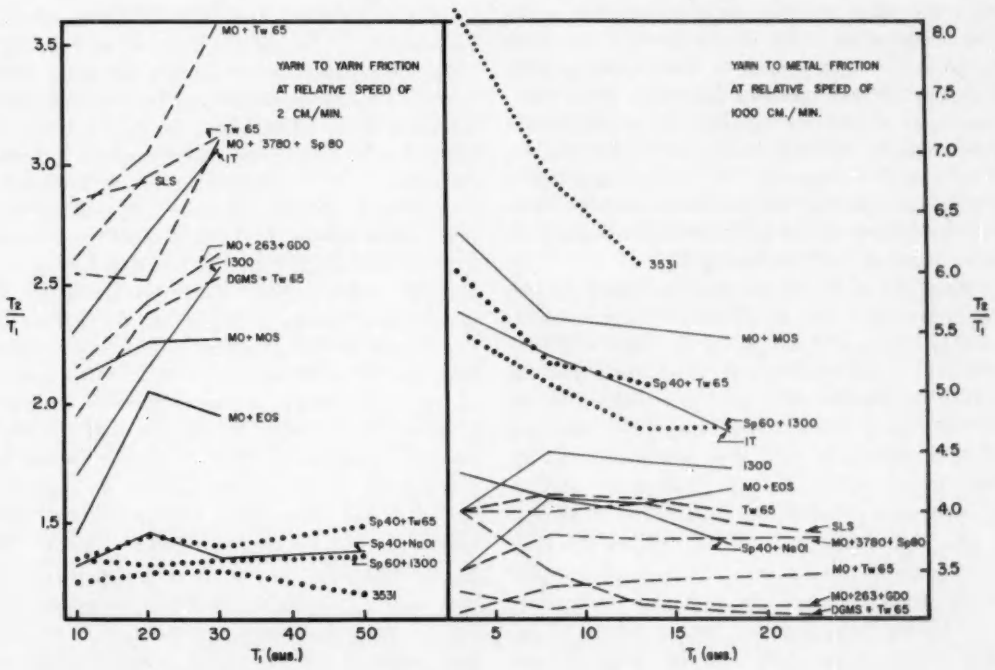

Fig. 6. Yarn-to-yarn and yarn-to-metal results; T_1 vs. T_2/T_1.

values of T_1, with the finishes listed in Table I. The quantity T_2/T_1 was chosen as the dependent variable, since in a plot against T_1, T_2 would merely give the standard positive slope curve; the use of the ratio, however, should result in curves the slopes of which are related to lubricating efficiency. The values of T_1 chosen for the yarn-to-yarn work were 10, 20, 30, and 50 g., and for the yarn-to-metal studies, 3, 8, 13, 18, and 23 g. Often the highest level of T_1 used is below 50 g. for yarn-to-yarn or 23 g. for yarn-to-metal friction; this is due to the fact that at the higher levels of friction the yield point of the yarn was exceeded, and measurements beyond this point were considered meaningless.

It appears from Figure 6 that the finishes group themselves into three more or less distinct sets. These sets are indicated by the dashed, solid, and dotted curves representing, respectively, those finishes which are at the high end of the friction order in yarn-to-yarn measurements but at the low end in yarn-to-metal friction, those finishes which do not markedly change order, and those finishes which yield low yarn-to-yarn friction results but high yarn-to-metal values. Of great interest is the fact that the slopes of the yarn-to-yarn curves are essentially zero at the lower friction levels but positive at the higher levels, whereas the yarn-to-metal curves have either zero or negative slopes. This seems to indicate that at the slow speed (2 cm./min.) of the yarn-to-yarn tests, the lubricating efficiency of some of the finishes remains constant while that of the rest decreases with an increase in T_1. At the much higher speed (10 m./min.) of the yarn-to-metal tests, however, the efficiency of the finishes either remains constant or increases with increasing T_1.

With regard to the finishes that are liquid at room temperature and are represented in the dashed curves in Figure 6 (MO + Tw 65, MO + 3780 + Sp 80, MO + 263 + GDO), the mechanism whereby this type of lubricant acts may be explained by results obtained by Hansen and Tabor [4]. Working with oil lubricants on yarn, they established that the hydrodynamic mechanism of lubrication applies. This is the same principle that governs the oil lubrication of a shaft riding in a bearing. When the shaft is not turning or turning very slowly, there is metal-to-metal contact between the shaft and the bearing, the oil having been displaced to the sides and top by the weight of the shaft. At this stage, the so-called boundary type of lubrication is active and friction is at a maximum. When the rotational speed is increased, however, the oil is forced under the shaft, and at a certain speed sufficient pressure will have been built up to counteract the weight of the shaft, which will now be surrounded by a continuous film of oil sufficiently thick so that its flow is governed by the laws of hydrodynamics. At this point, the hydrodynamic mechanism of lubrication is in effect and friction is at a minimum.

This same principle can be used to explain the behavior of the three oil finishes mentioned above. At the slow speed of the yarn-to-yarn measurements, the lubricant is displaced, fiber contacts fiber, and high friction results. This is evidenced by the fact that all three oils gave stick-slip friction. As T_1 is increased, the fiber-to-fiber contact pressure is increased, also resulting in the disproportionate increase in the T_2/T_1 ratio and the sharply increasing slope of the curves. At the high speed of the yarn-to-metal studies, on the other hand, there is not sufficient time for the oil to be displaced, and it may even be forced into the contact area. At any rate, the film of lubricant remains intact, and low smooth friction results.

Two liquid finishes do not fit this picture. They are the MO + MOS and MO + EOS oils which are represented in the solid set of curves. As can be seen, these materials do not reverse order between yarn-to-yarn and yarn-to-metal friction, but maintain a median level. The reason for this is not entirely clear, but assuming the hydrodynamic lubrication theory to apply, it certainly seems that lubricant film rupture was greatly minimized, compared to the other liquid finishes, in the slow speed measurements. This is substantiated by the fact that both oils give smooth friction results. This must mean that these films possess greater strength than the others. That this is not merely a matter of viscosity is evident from the 25° C. figures in Table I. An explanation of these phenomena appears, therefore, to involve a second mechanism. It may be that the film or micelle forming tendencies of the emulsifiers used play a part. There is some evidence to support this theory in the order, from highest friction level to lowest, in which the liquid finishes are placed. Tween 65, the emulsifier for the finish giving highest friction values, is a highly branched surfactant which, due to steric hindrance, probably does not orient very well. G-3780 is also a branched chain compound, but to a lesser extent than the Tween, and

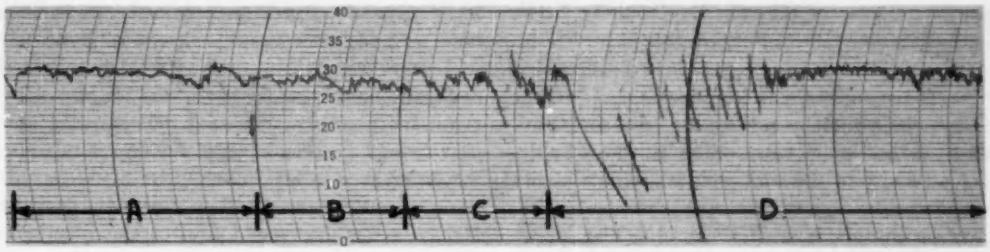

Fig. 7. Effect of heat and isopropanol on the yarn-to-yarn friction behavior of yarns treated with MO + EOS finish.

should orient somewhat more easily. G-263 is an ionic straight chain material and should orient still more. The sulfonates of the MO + MOS and MO + EOS formulations should encourage the formation of strong micelles or films since they are highly ionic and not greatly sterically hindered. There is some support for this line of reasoning in the results obtained by Fogg [3], who studied the lubricating behavior of a homologous series of esters on metal surfaces. It is not known to what extent the magnitude of emulsifier content influenced the order in which the ionic formulations placed; it seems quite likely, however, that an optimum value exists at which the lubricant possesses maximum efficiency (film strength) at a desired level of lubricity. It is possible that the MO + 263 + GDO would have behaved more like the MO + MOS and MO + EOS formulations if the G-263 content had been brought up to a comparable level (about 20%). On the other hand, it is quite possible that due to their substantivity for cellulosics, cationics do not orient on rayon in a manner favorable to strong film formation. It remains to be assessed what effect emulsifier–fiber affinity has on film strength. In fact, the more general question of the effect on lubricity of the substantivity and consequent orientation on the fiber of a finish as a whole would seem to bear thorough investigation.

There appears to be some support for the film strength theory in the data shown in Figure 7. These tracings illustrate the effect of heat and isopropanol applied to MO + EOS treated yarn at the crossover point in yarn-to-yarn tests. If the strength of the lubricant film is indeed due to the orientation and film forming properties of the EOS and not the viscosity of the oil, then heat should have little or no effect. A solvent, on the other hand, would disrupt the micellar structure of the film by swelling or dissolving it. In Section A of Figure 7, the normal friction curve of the finish is shown. Sections B and C illustrate the negligible effect on frictional characteristics of two levels of heat (exact temperature not known, but in the range of 80° C. for B and 175° C. for C). Section D shows the marked effect of the addition of a minute quantity of isopropyl alcohol to the yarn at the crossover point and the return to normal as the alcohol evaporates.

With regard to the Tw 65 and DGMS + Tw 65 finishes, these materials are pliable waxes which exhibit sticking or cohering tendencies when rubbed over themselves. The Tw 65 is the stickier material. By referring again to Figure 6, it can be seen that these materials have friction curves similar to those of the weak film strength oil finishes. In the yarn-to-yarn work, stick-slip friction was obtained which was markedly greater for the Tw 65 than the DGMS + Tw 65.

It seems difficult to believe that the yarn-to-yarn friction characteristics exhibited by these materials can be due to rupture of the lubricant film since they are solids and should possess considerable film strength. It seems unlikely also that the work done in overcoming friction at the slow speed produces sufficient heat to melt the finishes, causing them to be squeezed out of the contact area. Considering the pliable, cohesive nature of these waxes, the following mechanism for the low speed may explain their behavior: wherever the finish coated yarns come in contact, points of cohesion (sticking) are established. As the yarn attempts to move, it is opposed by the sum of the forces at the cohesion points and can move only as much as permitted by the flow properties of the finish. This flow is not sufficient, however, to relieve the tension, which continues to rise until it reaches a level at which it succeeds in overcoming the forces of cohesion. At that instant, the points at which the wax films were sticking together rupture and the yarn slips. Movement

continues until the tension has been relieved; then the cycle is repeated. In this mechanism, an increase of T_1 or the cohesiveness of the finish would increase the number and/or effectiveness of the cohesion points, thereby raising the level and magnitude of the stick-slip effect. The hardness or degree of plasticity of the wax would affect its ability to influence T by flow. This effect should be small, however, with this type of material. The higher position of the Tw 65 curve in Figure 6 is probably due mainly to its greater cohesiveness.

As far as the yarn-to-metal behavior of the DGMS + Tw 65 and Tw 65 finishes is concerned, this can be readily explained by the hydrodynamic friction mechanism. It can be calculated that at the 10 m./min. speed of the test, sufficient heat is generated to melt the waxes. A comparison of their melt viscosities to those of the oil finishes indicates that their friction curves should be at a comparable level, and indeed they are. It will also be noticed, however, that whereas the melt viscosities of the two waxes are very close, their curves diverge significantly, the indication being that the DGMS + Tw 65 is the more efficient lubricant. There does not appear to be a satisfactory explanation for this nor for the differences in level among the liquid finishes in general; certainly no correlation with viscosity exists. It may be that the type of flow, turbulent or laminar, of the lubricant film has a measurable effect, or the factor of orientation on the fiber surface and consequent micellar structure of the film may enter into the picture.

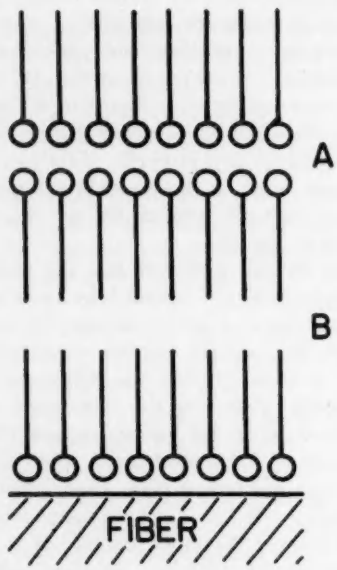

Fig. 8. Possible micelle structure in 3531 film.

The case of 3531 is somewhat more involved. This material can also be classified as a pliable wax with cohesive tendencies. However, its behavior did not even faintly resemble that of the above waxes. It gave a very low, smooth, yarn-to-yarn friction and the highest yarn-to-metal readings of the finishes tested. Two more or less plausible reasons for the yarn-to-yarn friction behavior of this wax may be advanced: it possesses greater flow properties than the Tw 65 or the DGMS + Tw 65 and it orients to a high degree on the surface of the rayon, forming a film containing a large number of micelles of the configuration indicated in Figure 8. This orientation may take place in a similar manner to that described by Fogg [3] and is probably influenced by the affinity of the finish for the fiber.

Cleavage of the micelles in the regions indicated by A is difficult due to the forces acting between the polar groups, but should be relatively easy in the areas indicated by B. Areas of the type indicated by A located on the surface of the film would provide points for cohesion when a corresponding area on another film of the same material is brought in contact with it. When a shearing force is now applied, relative motion would occur by cleavage within the films along the hydrocarbon planes indicated by B. It is conceivable that this would proceed smoothly at slow speeds and that it is not greatly affected by T_1. At the higher velocities of the yarn-to-metal

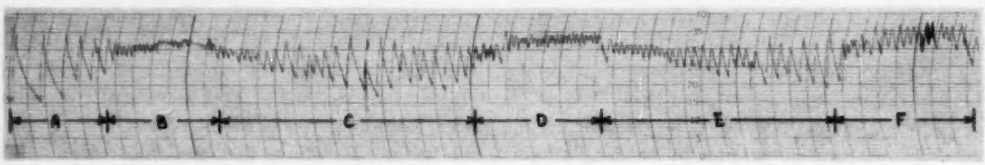

Fig. 9. Effect of heat on the yarn-to-yarn friction behavior of yarns treated with finish 1300.

tests, however, the films may not have time for either flow or uniform film cleavage.

Referring to Table I, it can be seen that the 3531 will also not melt readily; therefore the hydrodynamic lubricating mechanism does not apply. At increasing T_1, however, more heat is generated, flow increases, and film cleavage is facilitated. This may account for the downward slope of the curve. It is also quite likely that at the higher speed not sufficient time or intimate contact are allowed for the formation of effective cohesion points.

The salt-free SLS might be expected to form micellar films similar to those of 3531 and to possess a degree of tackiness. It does not behave in the same manner as 3531, however, probably due to the fact that it is a considerably harder material having shorter hydrocarbon chain length. This means that it flows less and that film cleavage is more difficult. As a result, the films move past each other by rupture of the cohesion points, thus accounting for the stick-slip oscillograph tracings and positive-slope curve obtained in the yarn-to-yarn work. Being a harder, less tacky wax than 3531, it is not surprising to find that the SLS gives yarn-to-metal results at a lower level of friction. Its considerably smaller slope can probably be explained by the fact that the SLS has an extremely high melting (or decomposition) point and thus is not nearly as sensitive to the increasing temperature at the friction point brought about by the increasing T_1.

With regard to Sp 40 + Tw 65, Sp 40 + NaOl, and Sp 60 + 1300, these materials may be classified as plastic waxes (hard but not brittle), similar to SLS, but not tacky. As a result, the films of these materials slide by one another smoothly in the slow speed measurements. These materials, due to their plasticity, are also capable (as are all the previously discussed waxes) of being distributed over the surface of the fiber during frictional contact. This action may be very important, as it tends to minimize the effect of the topography of the yarn (by building up layers of finish around the asperities and filling in the crevasses) and any unevenness of application of the finish. In the yarn-to-metal tests, the heat generated causes these waxes to become more plastic. This has the effect of making the Sp 40 + Tw 65 and the Sp 60 + 1300 tacky at the low T_1. This accounts for their initially higher yarn-to-metal friction level. As T_1 is increased, however, the finishes become more plastic and flow more readily, which results in a friction curve of negative slope.

The low yarn-to-metal friction of the Sp 40 + NaOl finish may be due to the fact that this material has a high melting point and/or does not become as tacky as the other waxes as it is plasticized by the heat generated during the test.

Two finishes remain, 1300 and IT. These are hard, probably brittle, waxes. Two mechanisms that may account for their high yarn-to-yarn friction stick-slip behavior suggest themselves. When the finish is applied, it coats the fiber with a thin film which outlines the irregularities of the surface. When frictional contact occurs, the coated asperities are forced into contact. Unlike the more plastic waxes, the finish does not redistribute itself over the surface to minimize the friction effects of the topography of the fiber and any unevenness in finish application. The interaction of the "hard-coated" asperities results in the stick-slip friction, which may be expected to (and does) increase with increasing T_1. The second mechanism involves the continuity of the finish film. Assuming the wax to have been applied as a perfectly uniform, smooth film (which, of course, it is not), subsequent flexing or stretching of the fiber will cause the film to rupture and become discontinuous due to its brittleness. This should also cause high stick-slip friction. Figure 9 may lend some support to this and the general concept of the importance of plasticity in that it illustrates the significant effect of heat. These tracings show how the frictional characteristics of yarn treated with 1300 change on the application of heat at the crossover point in yarn-to-yarn tests. Section A shows the normal stick-slip behavior of 1300, Section B the elimination of stick-slip and significant reduction in level of friction due to the application of heat (exact temperature unknown), Sections C and E the return to stick-slip when the heat is removed, Section D the behavior on the application of greater heat than applied previously, and Section F illustrates the frictional behavior on using still higher heat. Here it appears that the lubricant film has been softened (possibly liquified) to the extent that it is beginning to rupture, and the stick-slip friction typical of the low film strength liquid finishes is obtained. It is interesting to note that the friction level in Section B approaches that of Sp 60 + 1300 at the same T_1. Span 60 may be thought to perform the same function as the heat; that is, plasticization.

The behavior of the 1300 and IT finishes in the yarn-to-metal tests can probably be explained by the same mechanism as that suggested for the plastic waxes.

Conclusions

Hansen and Tabor's findings [4] that the hydrodynamic mechanism of friction applies to oil-soaked yarns has been used to explain the frictional behavior of liquid lubricated yarns at higher speeds. The lubricating properties of liquids vary considerably, but independently of viscosity. At the low speed of the yarn-to-yarn tests, effectiveness appears to be dependent on film strength. This in turn may be provided by the emulsifier through an orientation mechanism similar to that proposed by Fogg. This mechanism as well as flow characteristics may also contribute to the widely varying results obtained with the oils in yarn-to-metal testing. This is mere speculation, however.

There seems little doubt that a number of friction mechanisms also govern the behavior of the solid lubricants. The significant differences in behavior of these materials, as charted in Figure 6, support this view.

The data indicate clearly that the physical properties of the finish such as hardness, film strength, cohesiveness, flow, ionic character, etc. are the factors that determine the friction mechanism in a given situation. The relative speed of the surfaces in contact and the force with which they are pressed together influence the mechanism mainly insofar as they alter (e.g., by heat) the physical properties or behavior of the finish.

The friction mechanisms proposed for the solid finishes must not be thought of as explanations for their behavior but merely as speculations, the proof or negation of which will constitute the basis of future research efforts. In this regard, one of the most important phases of a program aimed at the correlation of the physical properties of a lubricant with its frictional behavior is the determination of those properties under various conditions and then classifying the lubricant according to some logical system.

The usefulness of a classification of finishes by lubricant behavior under various conditions can hardly be overestimated, especially if this can be correlated with performance in the many textile processes where the maintenance of the proper level of friction is of utmost importance.

Acknowledgment

The authors wish to express their thanks to Miss J. L. Spang and Mr. J. J. Crumlish, who carried out the tests; to Mr. W. C. Griffin for his encouragement and many helpful suggestions; and to the Atlas Powder Company for permission to publish.

Literature Cited

1. Baird, M. E. and Mieszkis, K. W., *J. Textile Inst.* **46**, P101 (1955).
2. Bowden, F. P. and Young, J. E., *Proc. Roy. Soc.* **A208**, 444 (1951).
3. Fogg, A., *Proc. Phys. Soc.* **52**, 239 (1940).
4. Hansen, W. W. and Tabor, D., TEXTILE RESEARCH JOURNAL **27**, 300 (1957).
5. Honegger, E., *Textil-Rundschau* **10**, 551 (1957).
6. Howell, H. G., *J. Textile Inst.* **44**, T359 (1953).
7. Howell, H. G., *J. Textile Inst.* **45**, T575 (1954).
8. Howell, H. G. and Mazur, J., *J. Textile Inst.* **44**, T59 (1953).
9. Lincoln, B., *J. Textile Inst.* **45**, T92 (1954).
10. Lodge, A. S. and Howell, H. G., *Proc. Phys. Soc.* **B67**, 89 (1954).
11. Lord, E., *J. Textile Inst.* **46**, P41 (1955).
12. Lyne, D. G., *J. Textile Inst.* **46**, P112 (1955).
13. Mazur, J., *J. Textile Inst.* **46**, T712 (1955).
14. Pascoe, M. W. and Tabor, D., *Research* **8**, S15 (1955).
15. Röder, H. L., *J. Textile Inst.* **46**, P84 (1955).
16. Rubinstein, C., *Proc. Phys. Soc.* **B69**, 921 (1956).
17. Rubinstein, C., *J. Textile Inst.* **49**, T13 (1958).
18. Rubinstein, C., *J. Textile Inst.* **49**, T181 (1958).
19. Warzee, M. and Quintelier, G., *J. Textile Inst.* **46**, P123 (1955).

Manuscript received September 8, 1958.

Stiffness and Resiliency of Wet and Dry Fibers as a Function of Temperature[1]

G. M. Bryant and A. T. Walter

Research Department, Union Carbide Chemicals Company, South Charleston, West Virginia

Introduction

Hot, wet conditions are frequently encountered by textile fibers and fabrics—in the wet spinning of man-made fibers, dyeing, scouring, wet finishing and laundering, and in certain end-use applications. The ability of a fiber to resist stretching or shrinkage under such conditions is frequently of critical importance. In some cases (for example, the regenerated protein fibers), the properties of a fiber having good performance under normal conditions may be so seriously lowered under the action of water as to limit the utility of the fiber.

Most of the work reported in the literature on the effects of ambient conditions on mechanical properties of fibers has been carried out on natural and regenerated fibers, which are greatly softened by water but are relatively unaffected by temperature, either wet or dry. The effect of temperature on properties of the hydrophobic synthetic fibers has been studied to a considerable extent [2, 4, 8], but the influence of water at elevated temperatures on synthetic fiber properties has received less attention, probably due to the minor influence of water at room temperature. As will be shown, these minor effects sometimes become quite important at higher temperatures.

The only systematic study of fiber stiffness modulus over a range of temperatures in water appears to be that of Guthrie [7], who studied a variety of natural, regenerated, and synthetic fibers in water over the temperature range 22–100° C. However, only a few measurements were made on dry fibers, and these were insufficient for separate assessment of the effects of temperature and water. Other related studies include those of Farrow [6] on the extensometric and elastic properties of a wide variety of fibers in water at 20° and 95° C., Cheetham and Edwards [3] on the temperature–extension behavior of acrylic fabrics in processing baths, and Meldrum and Ward [9] on the compressibility of acrylic staple fiber under hot, wet conditions.

The present paper presents stiffness modulus and mechanical loss measurements on a number of fibers in air and in water, and interprets the results in terms of glass transition behavior. To the extent that features of the stiffness and resiliency versus temperature curves measured in air may be attributed solely to the influence of temperature, comparison of the wet and air-dry measurements permits the effects of temperature and water to be judged separately. In the case of the more hydrophilic fibers, the loss of moisture on heating in air will have an appreciable influence on stiffness moduli below 100° C. However, the glass transition regions of interest in such fibers occur at very high temperatures where the specimens are completely dry. In the more hydrophobic fibers, having glass transition temperatures below 100° C., the moisture contents in the laboratory air are normally so low as to have negligible influence on the observed transition behavior.

Experimental

All measurements were carried out in a room maintained at 76° F. and 50% relative humidity. The experimental procedure and apparatus in the air-dry measurements were similar to those described by Brown [2]. For the wet measurements, a beaker containing water, heater, thermoregulator, and stirrer was mounted in the cross-head of the Instron Tester. Temperature was controlled to ±0.5° C. in both the wet and dry measurements. Low-twist filament yarn specimens were employed, except for cotton and wool, for which spun yarns were used. Two-inch specimens were stretched just beyond 1% extension at a rate of 0.2 in./min., giving a load–elongation record as shown in Figure 1. The stiffness modulus was defined as 100 times the stress at 1% elongation, and percent resiliency was calculated from the linear recovery as $AB/BO \times 100$. Separate specimens were used for the wet and dry measurements, but

[1] Paper presented at the Spring meeting of The Fiber Society in Clemson, South Carolina, April 30, 1958.

successive tests at increasing temperatures employed a single specimen. The wet stiffness measurements were begun 4–6 min. after immersion of the specimen in water. Thus, strictly speaking, the measured quantities refer to specimens having a particular history of immersion, temperature, and stretching. The load–elongation curves of secondary cellulose acetate and cellulose triacetate have been shown by Farrow to stiffen with increasing time of immersion [6], so that the wet stiffness moduli measured on those fibers are somewhat arbitrary, and would be higher for longer soaking times. In experiments where the immersion time at room temperature was increased from 5 min. to 16 hr., the stiffness of wet cellulose acetate increased from 16 g./den. to 21.5 g./den. and the cellulose triacetate stiffened from 19 to 24 g./den. None of the other fibers tested showed an appreciable change of stiffness with increased immersion time.

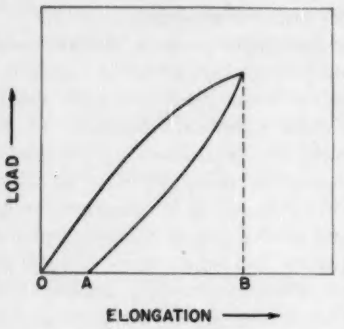

Fig. 1. Typical load–elongation cycle.

Results and Discussion

Acrylic Fibers

Figure 2 shows the stiffness–temperature and resiliency–temperature behavior of wet and air-dry polyacrylonitrile fiber. There is a pronounced decrease in modulus in the dry fiber between 60° and 140° C. as the fiber passes through the glass transition temperature region. The fact that the modulus decreases at lower temperatures in water indicates that the corresponding transition occurs at lower temperatures in the wet-plasticized fiber. In 100° C. air, the stiffness modulus of this fiber is still quite

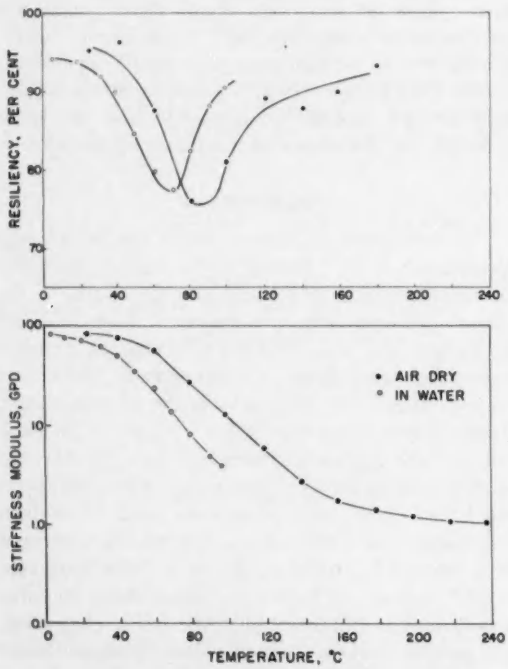

Fig. 2. Stiffness–temperature and resiliency–temperature behavior of wet and air-dry polyacrylonitrile fiber.

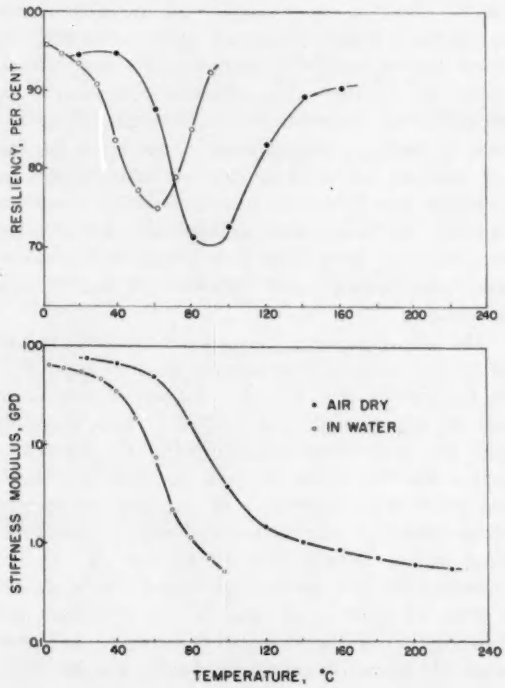

Fig. 3. Stiffness–temperature and resiliency–temperature behavior of wet and air-dry modified acrylic fiber.

high (around 11 or 12 g./den.) but in water at 100° C. the stiffness is reduced to about ⅓ of the dry value. More care must be taken in handling fabrics at the boil than in 100° C. air to prevent stretching and distortion, but the stiffness level is still high enough in polyacrylonitrile to prevent the problem from being a very serious one.

The stiffness–temperature curves present only a broad inflection over the glass transition region, and are not very suitable for estimating transition temperatures. Resiliency has been shown to pass through a more distinct minimum at the glass transition temperature, since at this temperature the maximum number of mechanisms have response times within the time scale of the stretching experiment [2]. Thus, the resiliency–temperature measurements are more suited for determining transition temperatures. The resiliency–temperature curves for wet and dry polyacrylonitrile fiber in Figure 2 show that the glass transition temperature is lowered by 15°–20° C. in water, from above 85° C. for the dry fiber to just below 70° C. for the wet. The shape of the resiliency curve is not appreciably altered in water, indicating that there is probably no major structural change in water, but mainly a uniform plasticization and speeding of molecular response.

Figure 3 shows the resiliency–temperature behavior of a modified acrylonitrile fiber, that is, one containing a minor amount of a polar component to improve dyeability. The transition temperature in the wet fiber is lowered by about 25° C., slightly more than for the polyacrylonitrile fiber.

There is a significant difference in the shape of the resiliency–temperature curves of the wet and dry fibers here illustrated. This effect is believed to result from a change in the degree of water-plasticization of the wet fiber with temperature. The effect appears to be rather minor in all cases, but it should be remembered that the wet fiber system does not necessarily remain at fixed composition as the temperature is varied.

The stiffness–temperature curves of the wet and dry modified acrylic fiber are also shown in Figure 3. In the dry fiber, the stiffness above the transition region is reduced below that found in the unmodified fiber, reflecting a somewhat lower degree of crystallinity. In the wet fiber, the lower crystallinity coupled with larger reduction in transition temperature leads to a very low stiffness in the 90–100° C. range, at which dyeing is frequently carried out.

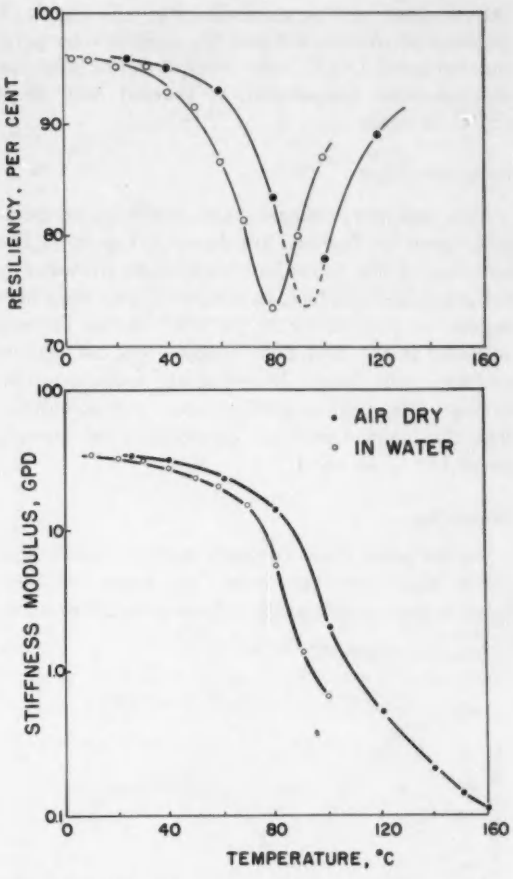

Fig. 4. Stiffness–temperature and resiliency–temperature behavior of wet and air-dry Dynel.

The low modulus under these conditions dictates that care be taken to avoid fabric stretching in piece dyeing or to prevent excessive matting and compression of fibers in stock dyeing. A knowledge of the modulus under the conditions of dyeing can serve as a guide in adjusting machine tensions to avoid excessive fabric distortion during dyeing.

Figure 4 shows the wet and dry stiffness–temperature behavior of Dynel. The fiber has a low degree of crystallinity, as shown by its low stiffness above the glass transition temperature, which is the result of its copolymer composition (60/40 vinyl chloride/acrylonitrile). However, the shift in transition temperature of the wet fiber is not as great as that found in fibers of higher acrylonitrile content, and as a result the hot wet stiffness is no lower than for

the modified polyacrylonitrile fiber of Figure 3. Figure 4 shows the wet and dry resiliency–temperature curves of Dynel, from which it can be seen that the transition temperature is lowered only about 15° C. in water.

Polyester Fiber

Wet and dry stiffness– and resiliency–temperature curves for Dacron [2] are shown in Figure 5. The lowering of the transition temperature by water is not great, and this fact, coupled with the rather high degree of crystallinity of the fiber, serves to keep stiffness at the boil high enough that no serious problems with fabric distortion are encountered in dyeing. The resiliency–temperature curves indicate that the glass transition temperature is lowered about 15° C. in water.

Polyolefins

To this point, fibers normally thought of as hydrophobic have been considered, yet water has been found to have a substantial influence on stiffness and resiliency. Figure 6 illustrates a completely hydrophobic fiber, polyethylene, for which both stiffness– and resiliency–temperature behavior is unaffected by water. Measurements must be extended to lower temperatures to determine the glass transition temperature of polyethylene; dilatometric [5] and dynamic mechanical [1] data show a transition at about −25° C., but there are indications that the glass transition occurs near −120° C. [10]. Polypropylene, with a transition temperature near −20° C., has also been found to be completely hydrophobic with regard to stiffness– and resiliency–temperature behavior.

Cellulose Acetate

Stiffness behavior of wet and air-dry secondary cellulose acetate is shown in Figure 7 along with that of cellulose triacetate (Arnel). The triacetate sample was heat-treated for about 30 sec. at 218° C. The dry stiffness curves are identical up to the transition region, where the lack of crystallinity in the secondary acetate causes it to lose stiffness more rapidly and virtually melt at about 190° C. The substantial reduction in stiffness when wet shows that these fibers are hydrophilic to a considerable degree. Cellulose triacetate is only about 20% stiffer than secondary acetate in water at room temperature, but drops off less rapidly with increasing temperature and is 350% stiffer than the secondary acetate in boiling water.

The resiliency–temperature data (Figure 7), as well as the stiffness curves, show that the wet yarns are entering a glass transition region near 100° C. Indications are that the transition temperature of both fibers is lowered some 75–80° C. by water.

[2] Du Pont trademark.

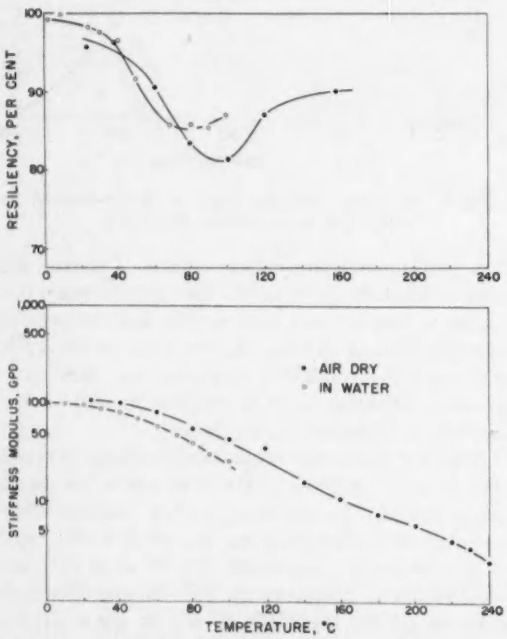

Fig. 5. Stiffness–temperature and resiliency–temperature behavior of wet and air-dry Dacron.

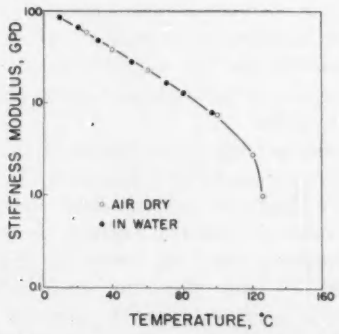

Fig. 6. Stiffness–temperature behavior of wet and air-dry polyethylene.

Nylon 66

Figure 8 shows the wet and dry stiffness– and resiliency–temperature curves of nylon 66. There is a pronounced lowering of stiffness in water, even at room temperature. The rise in stiffness at temperatures below 20° C. indicates that there is a glass transition in the wet fiber near 0° C.

The resiliency–temperature results also indicate a lowering of the transition temperature from about 60° C. in the air-dry fiber to near 0° C. in the wet. These values are in substantial agreement with the dynamic mechanical results of Woodward et al. [11] on unoriented nylon 66 samples tested as received and after conditioning at 100% relative humidity.

Natural and Regenerated Fibers

The wet and dry stiffness–temperature curves of textile viscose rayon, shown in Figure 9, indicate a drastic lowering of stiffness and of the glass transition temperature in water. The transition temperature is above 240° C. for the dry fiber, and appears to be near 0° C. for the wet fiber. In the temperature interval above 0° C., the wet fiber stiffness at first falls rapidly, then levels off and rises slowly above 60° C., due to the rubbery nature of the wet,

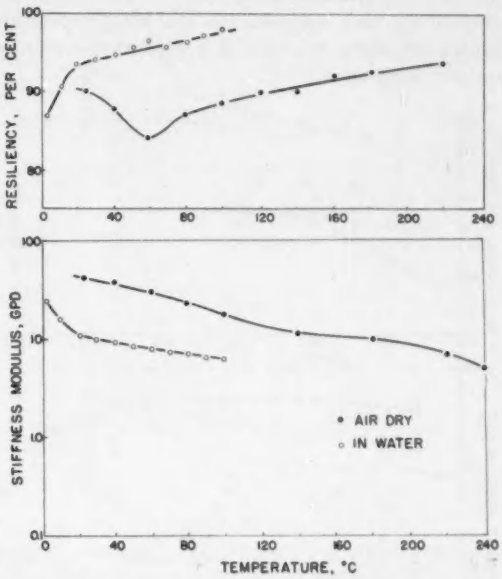

Fig. 8. Stiffness–temperature and resiliency–temperature behavior of wet and air-dry nylon 66.

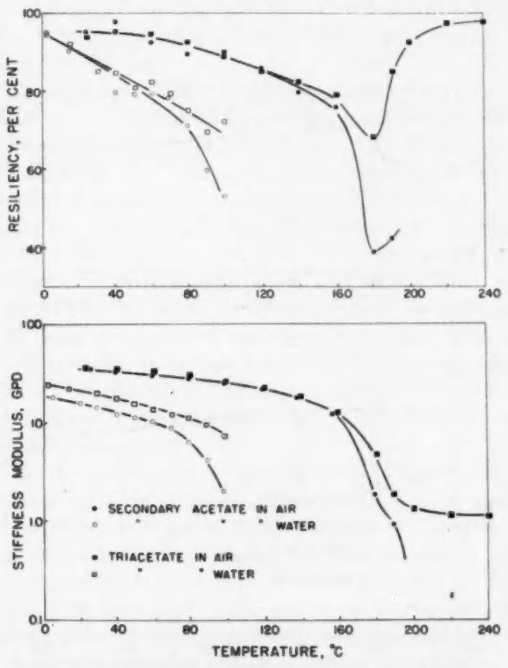

Fig. 7. Stiffness–temperature and resiliency–temperature behavior of wet and air-dry secondary cellulose acetate and cellulose triacetate.

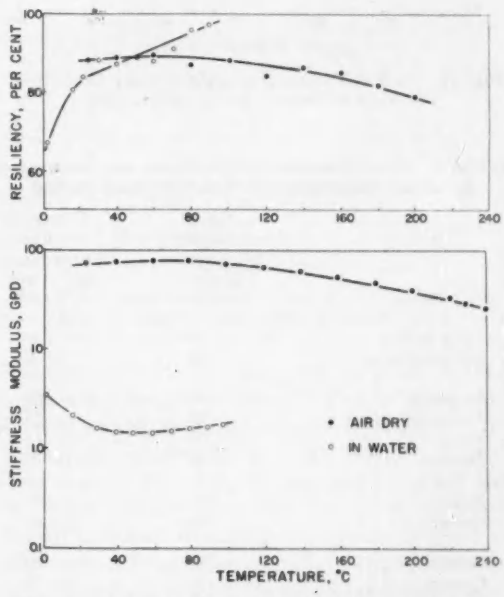

Fig. 9. Stiffness–temperature and resiliency–temperature behavior of wet and air-dry viscose rayon.

hot fiber. A slight maximum occurs in the dry stiffness curve near 60–80° C., which is due to the loss of moisture on heating the specimen. The resiliency–temperature data support the stiffness–temperature results and show evidence of a transition region of low resiliency near 0° C.

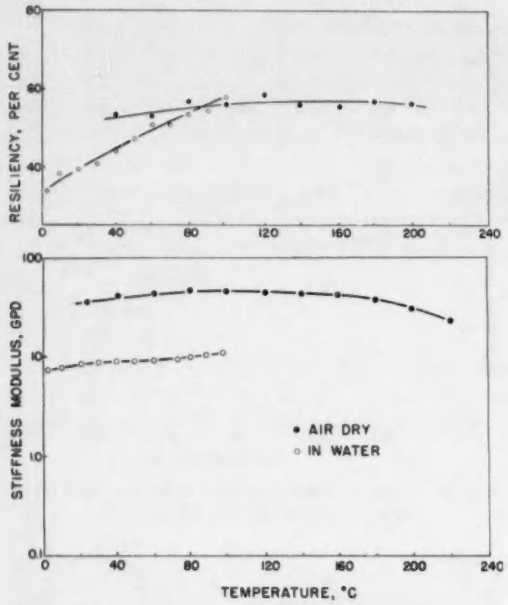

Fig. 10. Stiffness–temperature and resiliency–temperature behavior of wet and air-dry cotton yarn.

TABLE I. Glass Transition Temperatures and Lowering of Transition Temperatures in Water for Fibers Studied

Fiber	Glass transition temperature, air-dry, °C.	Change in transition temperature (dry − wet), °C.
Polyethylene	−25*	0
Polypropylene	−20	0
Nylon 66	60	60
Polyacrylonitrile	90	20
Dynel	90	15
Dacron	100	15–20
Arnel	180	75–80
Acetate	180	75–80
Wool	>200	>200
Cotton	>240	>240
Viscose	>240	>240

* A value of −120° C. has recently been suggested for polyethylene [10].

Although somewhat less satisfactory because of the need for working with spun yarns; the data for cotton and wool, Figures 10 and 11, show qualitative similarities to the viscose rayon results. In both of the natural fibers, the dry glass transition temperature is above 200° C., and decomposition begins before the transition temperature is reached. The transition temperature is greatly lowered in water, and the resiliency–temperature data show evidence of approaching glassy behavior below 0° C. The similar resiliency–temperature behavior of viscose rayon, cotton, wool, and nylon in water suggests that the same processes may be occurring just below 0° C., possibly an immobilization of polymer chains due to the "freezing out" of bound water.

Correlation of Transition Temperature and Moisture Sensitivity

Table I summarizes the transition temperature measurements on the wet and dry fibers. These fibers can be separated into four groups as follows: (1) the hydrophobic fibers, such as polyethylene and

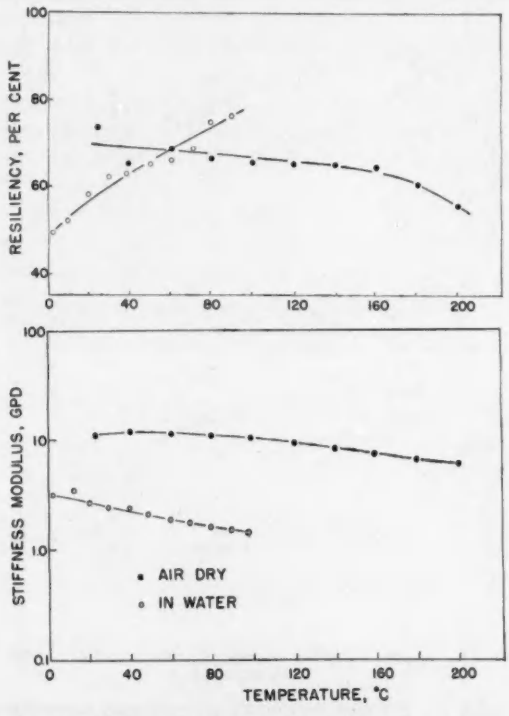

Fig. 11. Stiffness–temperature and resiliency–temperature behavior of wet and air-dry wool yarn.

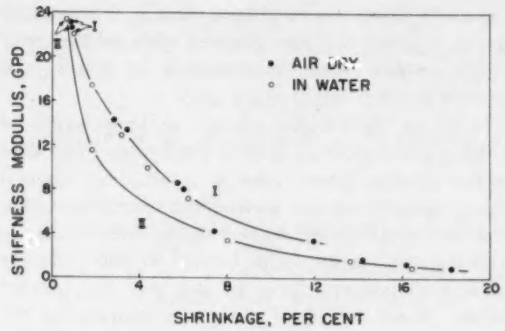

Fig. 12. Stiffness–shrinkage behavior of wet and air-dry polyethylene (Curve I) and special high-shrinkage acrylic yarn (Curve II).

polypropylene, which are unaffected by water and have a very low glass transition temperature; (2) moderately hydrophobic fibers, such as the acrylics, nylon, and Dacron, with a moderate transition temperature and a small lowering of transition temperature in water; (3) moderately hydrophilic fibers, e.g., acetate and Arnel, with a higher transition temperature and somewhat larger degree of softening by water; and (4) hydrophilic fibers, with a very high transition temperature and very high degree of plasticization by water.

These fibers, which include the most important classes of commercial fibers, show a close correlation between the magnitude of the glass transition temperature and the degree of plasticization by water. Such a correlation is not surprising, for the glass transition temperature can be thought of as the temperature to which the fiber must be heated to overcome interchain attractions and restrictions on free rotation so as to achieve molecular flexibility. The polar groups which give large interchain attractions and lead to a high transition temperature are also the groups which attract water, plasticizing the amorphous regions and lowering the transition temperature when wet.

Chain rigidity due to the presence of bulky side groups or rigid links in the molecular chain can exert an influence on the transition temperature without affecting the water uptake. Thus exceptions to the trend in Table I can be expected when chain rigidity is the major factor governing the transition temperature. This is the case to some extent in nylon, where the polar amide groups contribute to intermolecular attractions and water uptake, but the blocks of CH_2 groups give the chain considerable

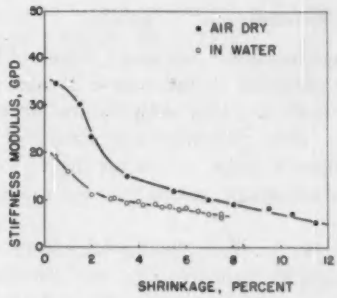

Fig. 13. Stiffness–shrinkage behavior of wet and air-dry nylon 66.

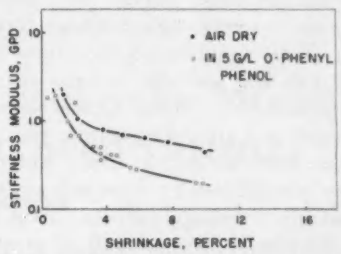

Fig. 14. Stiffness–shrinkage behavior of acrylic fiber in air and in 5 g./l. *o*-phenyl phenol solution, pH 5.

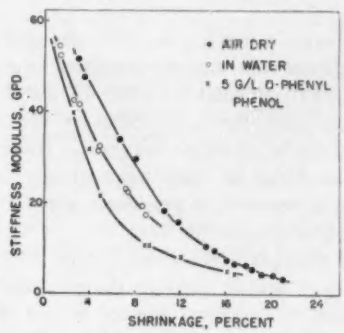

Fig. 15. Stiffness–shrinkage behavior of Dacron in air, water, and 5 g./l. *o*-phenyl phenol solution, pH 5.

flexibility and a lower transition temperature than would otherwise be expected. Other more pronounced exceptions to the correlation in Table I are to be expected wherever a rigid molecular chain is found in nonpolar polymers, (e.g., in polystyrene and the higher softening branched polyolefins) or when unusual flexibility is accompanied by the presence of water-attracting polar groups (e.g., polyethylene oxide). However, among the more important fibers, the correlation between transition temperature and water sensitivity is seen to be rather general.

Shrinkage Behavior

Shrinkage measurements as a function of temperature were recorded in the course of obtaining the stiffness– and resiliency–temperature data already presented. These permitted the plotting of wet and dry stiffness–shrinkage curves for the various fibers to see how shrinkages compare at the same stiffness level.

The number of fibers having shrinkage in water large enough to compare with the dry shrinkages over an appreciable range was limited to the less hydrophilic fibers. Figure 12 shows the wet and dry stiffness–shrinkage curves for polyethylene (Curve I) and a special high-shrinkage acrylic fiber (Curve II). As would be expected from the coincidence of the wet and dry stiffness–temperature curves of polyethylene (Figure 6), the same shrinkage is obtained at a given temperature, regardless of whether the fiber is wet or dry. Although the acrylic fiber is plasticized by water to a small extent, its wet and dry shrinkage–stiffness curves coincide also. In the acrylic fiber, as well as in all of the other examples which follow, the shrinkage at a given temperature was substantially greater for the wet fiber.

The previous examples, in which the wet and dry stiffness curves coincide, are for cases where water uptake is relatively small. Figure 13 shows the wet and dry stiffness–shrinkage behavior for wet and dry nylon, which has somewhat greater water uptake. In this case, it can be seen that a greater reduction in stiffness is required to produce a given shrinkage in the wet fiber than in the dry.

Another example is shown in Figure 14 for a normal shrinkage acrylic yarn in the presence of a 5 g./l. solution of *o*-phenyl phenol at pH 5. This solution produces a more drastic swelling of the acrylic fiber than water alone, giving a degree of swelling more comparable with the nylon–water case. The shrinkage–stiffness behavior is also comparable, in that the wet and dry curves no longer coincide and a greater degree of softening is required to produce a given degree of shrinkage in the wet swollen fiber.

The foregoing examples have indicated that the divergence between the wet and dry shrinkage versus stiffness curves becomes more pronounced as the degree of swelling becomes greater. This is also borne out in Figure 15, showing the shrinkage behavior of Dacron polyester fiber in air, water, and a swelling solution of *o*-phenyl phenol. The shrinkage at a given stiffness level is least in the most highly swollen state, intermediate in water, and greatest in air.

In all of the swollen fibers, the temperature at which a given stiffness level is reached is lower than in the air-dry fibers. As a result, less thermal energy is available for driving the oriented swollen fiber into a shortened, more random state. This is certainly one factor contributing to the different stiffness–shrinkage curves in the wet and air-dry fibers. Minor structural changes accompanying the swelling may also contribute to the altered stiffness–shrinkage characteristics.

Summary and Conclusions

1. Stiffness and resiliency measurements on wet and dry fibers as a function of temperature indicate that the swelling action of water results in a lowering of the glass transition temperature. The extent of lowering of the transition temperature in water can be used as a measure of water sensitivity.

2. Acrylic fibers are particularly susceptible to deformation in hot water, due to the combined effects of rather low degree of crystallinity and a lowering of their glass transition temperature by 15°–25° from the value of 85°–90° C. in the dry fiber. A modified acrylonitrile fiber, containing a minor portion of a polar monomer to promote dyeability, has substantially reduced stiffness in hot water compared to an unmodified polyacrylonitrile fiber, as a result of reduced crystallinity and greater plasticization by water.

3. Among the fibers examined, there is a correlation between the magnitude of the glass transition temperature of the dry fiber and the extent of lowering of the transition temperature in water, due to a common dependence on secondary bonding along the polymer chains. However, exceptions to this correlation are to be expected wherever inherent chain rigidity or flexibility is the dominant factor influencing the transition temperature.

4. Comparison of wet and dry stiffness–shrinkage curves indicates that, in general, a greater reduction in stiffness is necessary to produce a given amount of shrinkage in wet, swollen fibers than in the same fibers dry. As the degree of swelling is increased, the shrinkage at a given level of fiber stiffness is reduced. This effect may result from the lower temperature level at which a given shrinkage is reached

in the swollen fiber and/or from structural changes accompanying the swelling.

Literature Cited

1. Baccaredda, M. and Butta, E., *J. Polymer Sci.* **22**, 217 (1956).
2. Brown, A., TEXTILE RESEARCH JOURNAL **25**, 891 (1955).
3. Cheetham, R. C. and Edwards, H. D., *J. Soc. Dyers Colourists* **74**, 77 (1958).
4. Coplan, M. J., Wright Air Development Center Technical Report 53-21, March 1953.
5. Danusso, F., Moraglio, G., and Talamini, G., *J. Polymer Sci.* **21**, 139 (1956).
6. Farrow, B., *J. Textile Inst.* **47**, T58 (1956).
7. Guthrie, J. C., *J. Textile Inst.* **48**, T193 (1957).
8. Illingworth, J. W. and Kilby, W. F., TEXTILE RESEARCH JOURNAL **26**, 243 (1956).
9. Meldrum, K. and Ward, J. S., *J. Soc. Dyers Colourists* **74**, 140 (1958).
10. Willbourn, A. H., *Trans. Faraday Soc.* **54** 717 (1958).
11. Woodward, A. E., Sauer, J. A., Deeley, [illegible] Kline, D. E., *J. Colloid Sci.* **12**, 363 (195[illegible]

Manuscript received July 28, 1958.

Improved Instrument to Measure the Moisture Content of Lint Cotton, Seed Cotton, and Cottonseed

J. A. Reddick, S. C. Mayne, Jr., and Earl E. Berkley

Fiber and Spinning Laboratory, Anderson, Clayton & Co., Houston, Texas

Abstract

The cotton and cottonseed industries are modernizing technical methods and instruments along with suppliers of other raw materials. Described herein is an improved electrical conductivity instrument for measuring rapidly and accurately the moisture content of lint cotton, seed cotton, and cottonseed. Moisture contents in percentages, based on total weights of samples, are indicated on a direct reading dial. Accurate measurements of ± 1% in the 3.3–22% moisture range are obtainable with this instrument when compared with standard oven methods. A relatively large representative sample (35 g. lint cotton, 100 g. seed cotton and cottonseed), control of sample density (600 lb./sq. in. pressure), and a stable electrical system are the contributing factors for a successful instrument.

Background of Development

The industry has long recognized the need for a rapid and accurate method of determining the moisture content of cotton and cottonseed samples. As early as 1875 an international conference assembled in Switzerland to adopt standards for moisture regain in textile fibers and fabrics. Since then research has continuously provided a wealth of information on this subject; as a result, a number of useful instruments have been developed to measure moisture content.

Essentially all of the instruments developed to date that operate with speed and accuracy are of the electrical type, and these instruments can be divided into two general classes: the capacitance type, in which the dielectric constant is associated with moisture; and the conductivity type, in which the electrical resistance of the sample is correlated with the percentage of moisture. Of the two, the resistance method is the most popular.

Ed'efsen [2] summarized the potentials of the dielectric method for measuring the moisture content of textile materials; more recently, Hearle [3] has investigated the dielectric properties of fiber assemblies. Whitten and coworkers [4] concluded that the resistance method is the most practical for cottonseed.

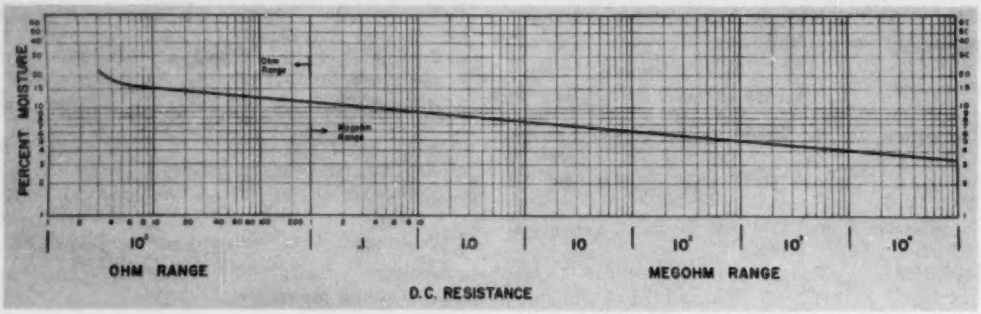

Fig. 1. Correlation of D.C. resistance and percent moisture content of sample.

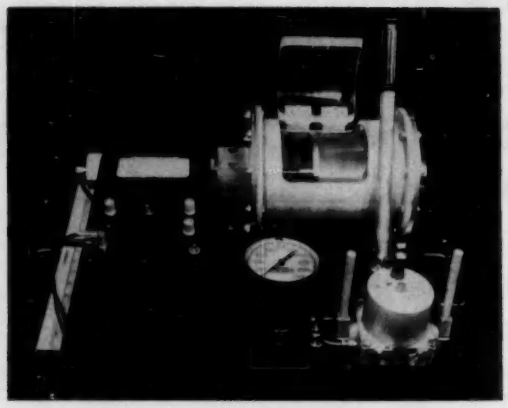

Fig. 2. Moisture testing instrument with test chamber in horizontal position.

The importance of having reliable information concerning the moisture content of cotton in the cotton industry is of paramount importance. With most cotton and cotton byproducts being traded on a weight basis, from a pecuniary standpoint alone the question of moisture—even differences of 1%—reach astronomical proportions when applied to the large volumes handled today. Efficient ginning and oil mill crushing operations depend upon an accurate knowledge and control of moisture. Berkley [1] recently pointed out that a bale of cotton grown and ginned in 1862 still retains its high spinning quality because it has been kept dry and free of weather damage.

The textile mill, in particular, has a problem of maintaining proper moisture control for efficient operations. In fact, all phases of the cotton industry now recognize the importance of moisture control in efficient operations as well as cost of raw materials. Measurement of the moisture content of cotton must be inexpensive; therefore, the ultimate goal of a simple, inexpensive, fast instrument which will produce results comparable to the oven test poses difficulties. It is not claimed that the instrument described herein fully satisfies all of these requirements; however, it is believed that it definitely is an improvement, from the standpoint of accuracy and versatility, over commercially available instruments. Problems of weight, maintenance, ease of operation, and accuracy are normal design criteria for any successful instrument; more important, if it is to have any commercial application, it must be marketed at a reasonable cost. As is often the case when an instrument is engineered for production, the manufacturer is forced to make certain embellishments in design to meet trade competition. More often accuracy is sacrificed in the interest of cost.

Method

This instrument utilizes the electrical conductivity method of measurement; i.e., correlating the D.C. electrical resistance of the sample with the percent moisture content (Figure 1). Percent moisture referred to in this paper is a ratio of the moisture content of the sample to the total weight, and may be calculated by the formula

$$\text{Percent Moisture} = \frac{100(a-b)}{a}$$

where a = total weight of sample (wet) and b = weight of dry sample. The term "oven method" referred to herein is a method commonly used by most laboratories, utilizing a drying time of 1½ hr. at 105–110° C. in a forced-draft oven.

By means of a direct reading dial, D.C. electrical resistance is converted to percent moisture content. This feature precludes the possibility of human er-

rors in referring to separate calibration curves. Figure 2 is a photograph of one version of the instrument with the test chamber in the horizontal position. The meter and electrical connections are on the left, and the hydraulic pump, gauge, and piping are in the right foreground. All components are mounted on a single base, and the instrument is complete with cover and carrying handles, which make it completely self contained and portable. The total weight is approximately 45 lb.

Figure 3 is a photograph of another version of the instrument, with the test chamber in the vertical position. This model utilizes the simplified hydraulic system. The basic difference between the two models is the cost. The vertical chamber model cost is approximately one-third that of the horizontal chamber model. In all other respects—sample size, compression rate, materials, electrical system, portability, and accuracy—the machines are identical. Carrying weight of this model is approximately 35 lb.

There are three contributing factors for a practical moisture testing instrument: sample size, control of sample density, and a reliable electrical system. Most commercially available instruments evaluated fell short of the desired results—not because of the principle employed, but because they failed to meet these three basic requirements.

Of the three basic requirements, suitable sample size is the most important. This is the one requirement that most instruments now on the market lack. It is fundamental to any testing procedure that the larger the sample the more representative the results. Samples of approximately 35 g. of lint cotton or 100 g. of seed cotton and cottonseed were found to be practical and adequate for reproducible results. These weights may be approximated by hand, thus eliminating a weighing procedure.

The sample must be kept under uniform compression during the test for good results. It was found during the course of the investigation that a surface force of 40 lb./sq. in. produced the best results (Figure 4). To produce and maintain the required compression force, hydraulic power was selected because of the excellent control possible and because it is relatively inexpensive.

The electrical system consists of a commercial type resistance meter with built-in voltage stabilizing features, connecting shielded cables, and two flat-plate electrodes. The electrodes are 5 in. in diameter, one movable and the other stationary. With the electrodes arranged in this manner, the current passes through the whole sample mass. It was found that this method produces much better results than an arrangement where the electrodes are on the same plane with the current flowing in a lateral direction. This method is an indication of surface moisture only, and is fairly representative of samples with uniform moisture content, e.g., well-conditioned samples measured under standard atmospheric conditions. However, most sampling is done under conditions that are other than ideal, and most of the sample surfaces will be either drier or wetter than the inside of the sample because of varying atmospheric conditions. Cotton fibers are hygroscopic; i.e., they tend to pick up or lose moisture from the air to maintain a state of

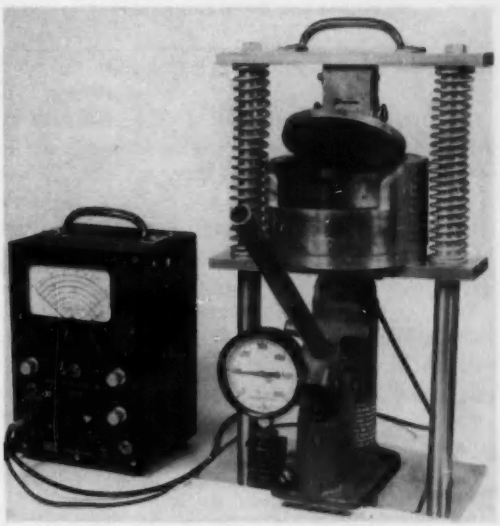

Fig. 3. Moisture testing instrument with test chamber in vertical position.

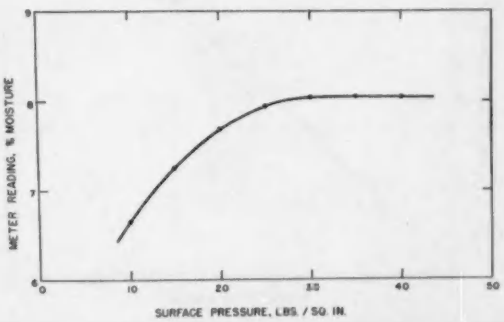

Fig. 4. The effect of sample pressure on meter readings.

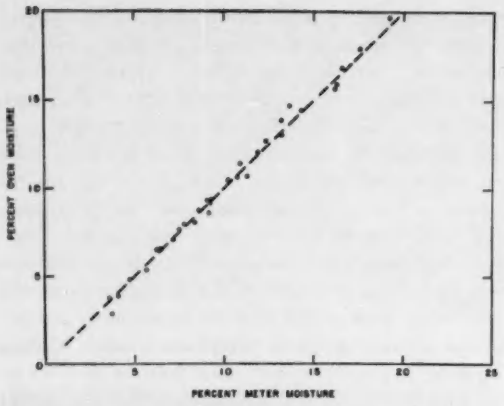

Fig. 5. Moisture relationship of lint cotton by the oven method and the moisture meter.

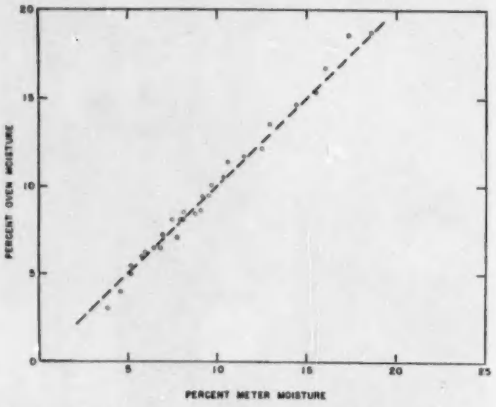

Fig. 6. Moisture relationship of seed cotton by the oven method and the moisture meter.

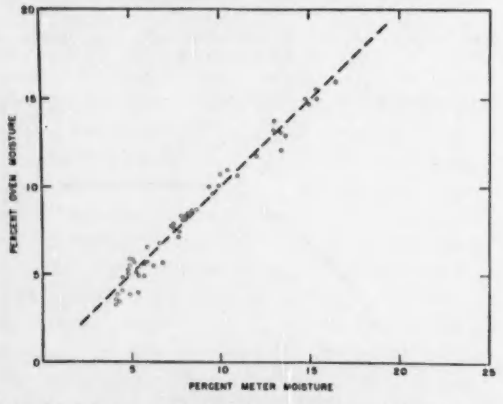

Fig. 7. Moisture relationship of cottonseed by the oven method and the moisture meter.

equilibrium with the surrounding atmosphere. The importance of a method of measuring the moisture content of the whole sample cannot be overemphasized.

With the sample compressed to the desired density, the reading may be taken immediately. The meter is equipped with a direct reading percent moisture dial to save time and to eliminate possible errors in reading separate curves. A single dial has been found satisfactory for all three materials without the need of a correction factor. Time for one complete cycle is approximately 1 min., including insertion and removal of the sample.

Results and Conclusions

Two models of an electrical moisture testing instrument have been designed, built, and tested under both controlled laboratory tests and under field conditions on lint cotton, seed cotton, and cottonseed. Accurate measurements with this meter are within ±1% of the oven moisture in the 3.3–22% moisture range, and ±0.6% in the 5–10% range (Figures 5, 6, and 7).

The testing apparatus is simple in operation, requiring no weighing of the sample. The method is fast, requiring approximately 1 min. for a determination. A direct reading percent moisture dial precludes operator bias on reading separate curves. The effect of temperature in the normal testing range of 70–90° F. was found to be inconsequential, and therefore no temperature compensation feature is provided.

Future tests will be conducted to determine possible application on other materials.

Acknowledgments

The assistance of ACCO laboratory personnel, particularly Edwin J. Jennings, Jr., in collecting the data reported here is gratefully acknowledged.

Literature Cited

1. Berkley, Earl E., TEXTILE RESEARCH JOURNAL **27**, 171–172 (1957).
2. Ed'efsen, N. E., *Agri. Eng.* **14**, 243–244 (Sept. 1933).
3. Hearle, J. W. S., TEXTILE RESEARCH JOURNAL **26**, 108–111 (1956).
4. Whitten, Marion E. and Holaday, Charles E., U. S. Dept. of Agriculture, Agricultural Marketing Service, Marketing Research Report 162 (April 1957).

Manuscript received December 2, 1958.

A Two-Phase Structure for Keratin Fibers

M. Feughelman

Wool Textile Research Laboratories, Commonwealth Scientific and Industrial Research Organization, 338 Blaxland Road, Ryde, N.S.W., Australia

Abstract

A two-phase structure is proposed for keratin fibers consisting of a water-absorbing matrix M, in which non-water-absorbing cylinders of phase C are embedded. The cylinders of phase C are parallel to the fiber direction. The main assumption made is that only the mechanical moduli of phase M are affected by moisture uptake as long as the fiber is not stretched. On this basis, using the longitudinal and radial swelling data available, quantitative relationships between the dry and wet Young's Moduli and rigidity moduli were obtained which agreed with experimental results. Further, other physical observations were shown to be compatible with this model.

Introduction

The work of Mercer, Rogers, Sikorski, and others [3, 7, 13, 16, 18] on the electron microscopy of developing keratin fibers indicates the presence of long microfibrils of the order of 60–80 Å diameter parallel to the fiber axis in a sulfur-rich matrix. These microfibrils are associated with the crystalline and the less water accessible regions of the wool fiber. Further, Fraser and MacRae [11] have shown by comparison of the low angle x-ray diffraction pattern with the high angle pattern for single wool fibers that the microfibrils have far lower water accessibility than the matrix, and that the intermicrofibrillar distance is of the order of 100 Å. Further, these two workers [10] have shown from the deuterium-hydrogen exchange for the (=N—H) amide group in wool fibers (from the change in the infrared absorption in the overtone region) that about 70% exchange can be obtained at room temperature. Nicholls and Speakman [17] have obtained a similar figure of about 70% water accessibility in wool fibers by calculation from the water adsorption isotherms. The purpose of this paper is to relate and explain some of the mechanical properties of wool fibers by means of a simplified two-phase structure suggested by the present picture of microfibrils embedded in a matrix.

Properties of the Two Phases

Consider a model fiber of circular section containing cylinders of phase C parallel to the fiber direction embedded in a matrix of phase M (see Figure 1). The following properties for phases M and C are proposed.

1. When the fiber is dry (at zero relative humidity) the mechanical properties of both phases are identical, and for small displacements (~1%) also isotropic.

2. Increase of relative humidity from 0 to 100% around the fiber progressively causes the phase M to swell isotropically. C unstrained does not swell with increase of relative humidity.

3. The increase of the relative humidity, and hence the moisture uptake of component M, reduces the mechanical moduli of this phase. Phase C remains unchanged.

4. The diametral dimensions of phase C are of molecular size.

5. When the fiber is being stretched, phase C becomes progressively accessible to moisture.

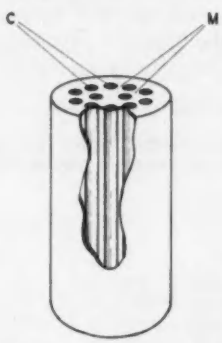

Fig. 1. Diagrammatic representation of the cylinders of phase C embedded in a matrix M inside a keratin fiber.

The above model will be used to explain observed physical properties of keratin fibers.

The Elastic Moduli and the Swelling of Keratin Fibers

The relationship between the modulus of rigidity and Young's Modulus for a homogeneous and isotropic material is given by

$$\text{Modulus of Rigidity} = \frac{\text{Young's Modulus}}{2(1+\sigma)}$$

where σ = Poisson's ratio. For keratin fibers [4, 8], the value of σ is quoted as between 0.35 and 0.5, which means that if a fiber is nearly homogeneous and isotropic the modulus of rigidity is approximately given by

$$\text{Modulus of Rigidity} = \frac{\text{Young's Modulus}}{3} \quad (1)$$

For dry wool fibers Speakman [19, 20] obtained a modulus of rigidity of 1.76×10^{10} dynes/cm.^{2} and a Young's Modulus of 4.76×10^{10} dynes/cm.^{2}. These two measurements agree within 10% with Equation 1. Further, for a number of dry keratinous solids Makinson [14] has shown that the elastic anisotropy is not very marked (about 20%) and that the anisotropy that does exist is to a large extent due to histological structure rather than molecular or near-molecular structure. The above, together with the compatibility of the rigidity and Young's Moduli of the dry wool fiber via Equation 1, indicates the relative isotropy and homogeneity of the mechanical properties of the dry fiber for small displacements. (The two moduli were measured for displacements in the Hookean region of the fiber in question.) This means that keratinous fibers conform with the first proposal. However, for wet wool the Young's Modulus is 1.81×10^{10} dynes/cm.^{2}, a drop by a factor of 2.6 compared with the dry fiber, while the rigidity is 1.1 to 1.2 $\times$ 10^9 dynes/cm.^{2}, a fall by a factor of 15, causing Equation 1 to become completely invalid for a wet fiber, indicating the high anisotropy of wet wool.

Consider now that the phase M is swollen by a volumetric fraction v due to water uptake. If the phase were free to swell unimpeded it would swell isotropically, resulting in a longitudinal and radial swelling x, given by

$$1 + v = (1 + x)^3 \quad (2)$$

However, due to restraint produced by phase C, the longitudinal swelling is reduced by the strain y (see Figure 4), and the radial swelling will be increased by a value of strain nearly equal to $y/2$, if the volume of the total fiber is to be the same as in the case of isotropic swellings. (The actual value of the radial strain for a wool fiber being swollen against the value of y is set out in Table I. The deviation of the radial strain from $y/2$ in practice is not great and introduces a difference of only 7% at full regain in the value of the strain.)

Let the Young's moduli of phases M and C be designated Y_M and Y_C respectively. Then at any fixed regain phase C is strained $(x - y)$, and phase M is strained $(-y)$ in the longitudinal direction (see Figure 4), so that

$$\frac{Y_M}{Y_C} = \gamma \frac{x - y}{y} \quad (3)$$

where γ is the ratio of the amount of phase C to phase M in the fiber.

By use of Speakman's data [19] for longitudinal and radial swelling in single wool fibers (see Figure 2) together with published volumetric swelling data [23], the values of unrestricted radial swelling of phase M (x), the longitudinal strain of phase M (i.e., y) and the longitudinal strain of phase C $(x - y)$ were calculated (Table I). A plot of

TABLE I. The Calculated Values [23] of Unrestricted Longitudinal and Radial Swelling of Phase M, Together with the Values of the Strains Produced by Restriction of Phase C on Phase M (See Figure 4)

Regain	5	10	15	20	25	30	33
Vol. swelling, %, v	4.24	9.07	14.25	20.00	26.21	32.80	36.78
Radial swelling, %	1.82	4.00	6.32	8.88	11.69	14.57	16.26
Unrestricted longitudinal and radial swelling, %, x of phase M	1.39	2.93	4.53	6.27	8.07	9.92	11.00
Radial strain $\left(\approx \frac{y}{2}\right)$	0.43	1.07	1.79	2.61	3.62	4.65	5.26
y	0.84	2.04	3.47	5.13	6.90	8.74	9.81
$(x - y)$	0.55	0.89	1.06	1.14	1.17	1.18	1.19

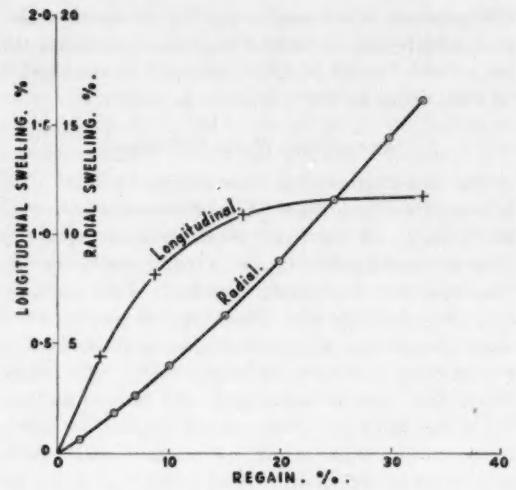

Fig. 2. The radial and longitudinal swelling of a single wool fiber plotted against regain (Speakman).

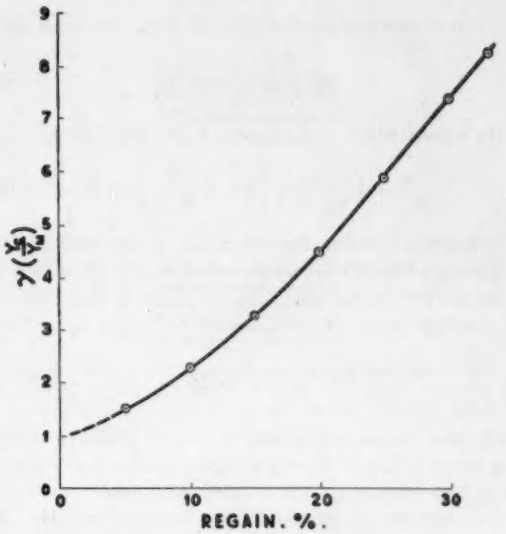

Fig. 3. The value $\gamma(Y_C/Y_M)$ is plotted against regain as calculated.

$\gamma(Y_C/Y_M)$ (from Equation 3) against regain (see Figure 3) shows a rapid decrease of Y_M relative to Y_C with increase of regain. Extrapolation of the curve in Figure 3 shows that $\gamma(Y_C/Y_M) \approx 1$, at zero regain. Since at this regain by the first proposal $Y_C = Y_M$ = Young's Modulus of the fiber, then $\gamma \approx 1$; i.e., the amount of phases M and C is equal in the dry state.

This value of γ is further confirmed in another but not independent manner from the swelling longitudinally and radially of the fiber at zero regain. Taking $Y_M = Y_C$ at zero regain, from Equation 3

$$x = \left(1 + \frac{1}{\gamma}\right) y$$

From Figure 4, the radial swelling is $(x + y/2)$ and the longitudinal swelling is $(x - y)$.

It follows that at zero regain

$$\frac{\text{Radial Swelling}}{\text{Longitudinal Swelling}} = \frac{x + \frac{y}{2}}{x - y}$$

$$= \frac{1.5 + \frac{1}{\gamma}}{\frac{1}{\gamma}}$$

$$= 1 + 1.5\gamma$$

From the curves in Figure 2 the value at zero regain = 2.7; i.e., $\gamma = 1.13$. For wet wool fibers the

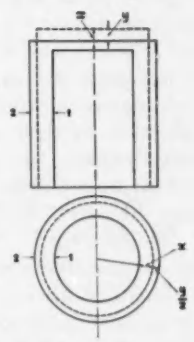

Fig. 4. 1: unswollen fiber; 2: swollen fiber. The dotted outline is the shape of the fiber if it were swollen isotropically.

volume swelling [23] of 36.8% is assumed to be taken up by phase M. If we call γ_W the volume ratio of phase C and M for the wet state, then taking $\gamma = 1.13$ for the dry state, and v as the swelling fraction of the whole fiber

$$\gamma_W = \frac{\gamma}{(1 + \gamma)(1 + v) - \gamma} = \frac{\gamma}{1 + v + v\gamma}$$
$$= 0.63$$

Consider now the longitudinal Young's Modulus Y_W of the wet fiber. It will be given by

$$Y_W = \left(\frac{\gamma_W}{\gamma_W + 1}\right) Y_C + \left(\frac{1}{\gamma_W + 1}\right) Y_M \quad (4)$$

From the curve of Figure 3, it can be seen that

$$\gamma_W \left(\frac{Y_C}{Y_M} \right) = 8.25 \qquad (5)$$

By substitution of Equation 5 in Equation 4,

$$\frac{Y_W}{Y_C} = \left(\frac{\gamma_W}{\gamma_W + 1} \right) \left(1 + \frac{1}{8.25} \right) = 0.43 \qquad (6)$$

Speakman's value for the ratio of the wet to dry Young's Moduli for wool = 1/2.6 = 0.39, which is in excellent agreement with the result of Equation 6.

At full regain from Equation 5, taking $\gamma_W = 0.63$

$$\frac{Y_M}{Y_C} = 0.076$$

i.e., the Young's Modulus of the M phase in water is about 0.076 × Young's Modulus of the dry fiber; i.e., has a value of 3.5×10^9 dynes/cm.^{2}.

It follows further that the torsional rigidity of the M phase (on the basis of Equation 1) would be about 1.2×10^9 dynes/cm.^{2}. In the wet state $\gamma_W = 0.63$; i.e., the M phase represents over 60% of the fiber, and its rigidity and Young's Modulus are 0.076 of the C phase. The whole fiber would therefore in the wet state act as a weak matrix containing parallel, almost unextensible cylindrical rods. These rods, due to their small diameter, would be relatively flexible. In torsion nearly all the shear deformation would occur in the M phase (see Figure 5), and the overall rigidity of the fiber would be $\sim 2 \times 10^9$ dynes/cm.^{2}. A more accurate attempt of estimation using methods similar to Cox [9] can hardly be justified when one considers the gross errors that may exist in the assumptions leading to the estimation of the value of the rigidity of the M phase. However, it is worth noting that this estimate of the overall rigidity of the wool fiber compares reasonably with Speakman's experimental values of 1.1 to 1.2×10^9 dynes/cm.^{2} for the rigidity of wool fibers at 100% relative humidity.

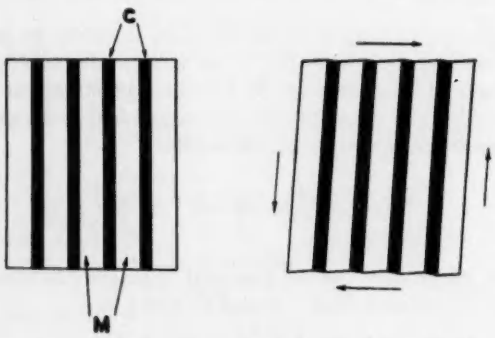

Fig. 5. A small component of the model unstrained and in shear.

Anisotropic Water Diffusion

The observations have been made by Haly [12] in wool fibers and Algie [2] in rhinoceros horn that the velocity of the front of water entering a dry fiber is considerably faster at right angles to the fiber direction than along the fiber. This phenomenon is compatible with the two-phase picture when one considers the state of the fiber as illustrated in Figure 6 for the two cases in question. At the top, where the front is entering in the fiber direction, the water must swell the matrix M, and in doing this, near the water front, the phase C will experience considerable longitudinal strain being forced to take up a sigmoid shape. Phase C, being of small diametral dimension, will bend but not extend. Phase C will react at the water front by creating a considerable compression stress opposing the swelling of phase M and hence tending to impede the movement of the front into the fiber. In the case of the water front entering at right angles (as in the bottom diagram), phase C does not suffer any severe strain with the swelling of phase M, and the water front enters the fiber with less impedance.

The Stretched Fiber

When a keratin fiber is stretched, Treloar [21] has shown that at a fixed relative humidity the equilibrium regain of the fiber is increased. Algie [1] has also shown that when a keratin fiber is stretched at a fixed relative humidity, its electrical conductivity is instantaneously decreased to a value far below the amount expected due to geometrical changes produced by the strain. However, the conductivity of the fiber rises again with uptake of moisture from its surroundings. Both these phenomena are explicable on the basis of the postulated properties of phases M and C. When the fiber is stretched, phase C becomes partially accessible to water and, being of small diametral dimensions, will rapidly come to moisture equilibrium with phase M. This implies that phase M loses water almost instantaneously to phase C, and itself is no longer in equilibrium with the atmosphere around the fiber. At this stage the electrical conductivity of the fiber will decrease rapidly, because the in-

crease in conductivity of phase C due to its uptake of moisture is far outweighed by the decrease of conductivity of phase M caused by its loss of moisture. (The electrical conductivity [15] of keratin is proportional to M^{15}, where M is the moisture concentration. If this relationship is considered to hold for the two phases, it follows that any alteration of the distribution of the moisture between the phases, with accompanying reduction of moisture concentration, must result in a decrease of conductivity, despite the fact that phase C would add its conductivity to phase M.) As phase M comes to equilibrium with the atmosphere, both the regain of the fiber and the conductivity will increase at a rate as shown by Algie [1] corresponding to the diffusion of moisture into the fiber. The author [6] with his colleagues has further shown that when a wool fiber is stretched to 40% the deuterium–hydrogen exchange at room temperature increases from 70% to a value greater than 90%. This result further reinforces the argument that, on stretching, the inaccessible phase C becomes progressively accessible to moisture.

Bendit's work [5] on the $\alpha \rightarrow \beta$ transformation in wool, based on x-ray diffractometer measurements, indicates the disappearance of α-keratin with increase of strain starting from approximately zero strain and not at about 20% as claimed by Woods [22]. The former would be the effect expected if the crystalline region in wool is associated with the C phase. Woods interprets the mechanical properties of keratin fibers as if the crystalline and noncrystalline regions essentially acted in series. However, Bendit's results favor a parallel system, which is in direct agreement with the parallel two-phase structure.

Remarks

Much progress has been made in recent years on understanding the molecular and near-molecular structure of keratin. However, no attempt appears to have been made to correlate these results with known physical properties of keratin. Some of these properties such as the change in torsional rigidity with regain and the longitudinal and radial swelling of single keratin fibers, although well-known phenomena, have had no overall structural explanation proposed. The two-phase structure proposed is obviously a first order approximation to the problem. No account is taken of the gradations that may exist between two such phases.

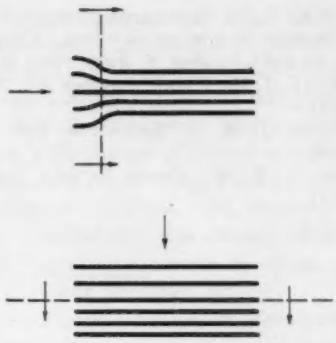

Fig. 6. The solid lines represent phase C, embedded in the matrix M. Top: the effect of a front of water entering a fiber in the longitudinal direction; bottom: a front entering the fiber radially.

However, simple as the structure proposed may be, it does give a satisfactory picture for a very wide range of mechanical and allied properties of keratin fibers.

Literature Cited

1. Algie, J., TEXTILE RESEARCH JOURNAL **29**, 1–6 (1959).
2. Algie, J. (private communication).
3. Andrews, M. W. and Sikorski, J., *Proc. Conference on Electron Microscopy*, Stockholm, 300–303 (1956).
4. Banky, E. C. and Slen, S. B., TEXTILE RESEARCH JOURNAL **26**, 204–210 (1956).
5. Bendit, E., *Nature* **179**, 535 (1957).
6. Bendit, E., Feughelman, M., Fraser, R. D. B., and MacRae, T. P., TEXTILE RESEARCH JOURNAL **29**, 284 (1959).
7. Birbeck, M. S. C. and Mercer, E. H., *J. Biophys. Biochem. Cytol.* **3**, 203–214 (1957).
8. Cassie, A. B. D., *Trans. Faraday Soc.* **41**, 458–464 (1945).
9. Cox, H. L., *Brit. J. Appl. Phys.* **3**, 72–79 (1952).
10. Fraser, R. D. B. and MacRae, T. P., *J. Chem. Phys.* **28**, 1120–1125 (1958).
11. Fraser, R. D. B. and MacRae, T. P. (private communication).
12. Haly, A. R. (private communication).
13. Jeffrey, G. M., Sikorski, J., and Woods, H. J., TEXTILE RESEARCH JOURNAL **25**, 714–722 (1955).
14. Makinson, K. Rachel, *Aust. J. Biol. Sci.* **7**, 336–347 (1954); **8**, 275–287 (1955).
15. Marsh, M. C. and Earp, Kathleen, *Trans. Faraday Soc.* **29**, 173 (1933).
16. Mercer, E. H. TEXTILE RESEARCH JOURNAL **27**, 860–866 (1957).
17. Nicholls, C. H. and Speakman, J. B., *J. Textile Inst.* **46**, T424–426 (1955).

18. Rogers, G. E., in "Summarised Proc. of Conference on Electron Microscopy of Fibres," Challice, C. E. and Sikorski, J., *Brit. J. Appl. Phys.* **8**, 1 (1957).
19. Speakman, J. B., *Trans. Faraday Soc.* **25**, 92–103 (1929).
20. Speakman, J. B., *J. Soc. Chem. Ind.* **49**, 209T (1930).
21. Treloar, L. R. W., *Trans. Faraday Soc.* **48**, 567 (1952).
22. Woods, H. J., *Proc. Leeds Phil. Lit. Soc.*, Scientific Section **3**, 577–583 (1940).
23. Wool Industries Research Association, Torridon, Headingly, Leeds, "Wool Research, Vol. 2, Physical Properties of Wool Fibres and Fabrics" 13 (1955).

Manuscript received August 25, 1958.

Density Changes in Cellulose Treated With Urea-Formaldehyde Resins

Richard Steele and Raymond P. Schiwall[1]

Textile Research Laboratories, Rohm & Haas Company, Philadelphia 37, Pa.

Abstract

Density changes produced in cotton and rayon fabrics by treatment with four thermosetting resin precondensates have been determined in density gradient columns. With the assumption that the density of resin cured *in vitro* corresponds to its density in the fiber, the results indicate that the predominant effect is fiber swelling, with very little resin being deposited in void spaces not previously accessible to the solvent mixture in the gradient column. Scouring the treated fabric to remove reaction residues lowers the density, indicating that the fiber structure does not collapse, presumably because it is stabilized by the reacted resin.

The effect of resin concentration on moisture regain was also determined with these samples. The results are consistent with the changes in mechanical properties observed for cross-linking and non-cross-linking resins on cotton and rayon.

TO PRODUCE crease resistance in cellulose fabrics with urea-formaldehyde resins, the precondensate must be able to diffuse into the fibers and react internally [3], and resin deposited on the surface of the fibers is not effective. Only part of the internal structure of cellulose fibers is accessible to chemical reagents, the degree of accessibility depending on both the cellulose structure and the size and shape of the diffusing molecule. The accessibility of cotton fibers is the order of 5–10% and that of rayon is considerably higher, about 30% [6]. This difference has been used to help account for the greater responsiveness of cotton to cross-linking materials [8] and for the various changes in physical properties produced in cotton and rayon by resins [9]. It also appears [8] that methylol ureas give chemically similar end-products when cured on either cotton or rayon.

However, there are still many unanswered questions about the location and mode of action of the deposited resin. It was believed that some of these questions could be answered by studying changes in the density of treated fibers, and the work described in this paper was undertaken for this purpose. The specific points the investigation sought to answer were (1) whether the resin swelled the fiber or was deposited in pre-existing void spaces, (2) whether rayon and cotton were alike with respect to the question of swelling or void-filling, and (3) whether different resins behaved alike in this regard, particularly whether monomethylol and dimethylol ureas (i.e., non-cross-linking and cross-linking materials) were alike.

[1] Present address: 418 Solly Avenue, Philadelphia 11, Pa.

The method used to determine the densities was the density gradient column of Linderstrøm-Lang [4], using the adaptations for textile purposes suggested by Preston and Nimkar [7]. This technique was first applied to fibers by Mark [11], and has been used by Stock and Scofield [10] to determine the pick-up of a colloidal melamine resin on wool and by Orr, Weiss, Moore, and Grant [5] to measure density changes of cotton modified by various chemical and physical means. In the present work, samples of rayon and cotton fabric were treated with various concentrations of monomethylol urea, dimethylol urea, dimethylol ethylene urea (Rhonite R-1), and Rhonite R-2, and then half of each sample was afterwashed. Density, resin content, and moisture regain at standard conditions were determined on both the original and washed fabrics.

Experimental Procedure

Fabric Treatment

Two fabrics were used, one an 80 × 80 bleached cotton printcloth weighing 4 oz./yd. and the other an 84 × 64 viscose rayon challis that was slightly lighter in weight, about 3.4 oz./yd. Four resin precondensates were applied to them at solution concentrations of 0, 5, 10, 15, and 20% solids. The four were monomethylol and dimethylol ureas, dimethylol ethylene urea, and Rhonite R-2. The first two were laboratory preparations made in the usual way and were applied promptly after their preparation. The dimethylol ethylene urea was the commercial product Rhonite R-1. Rhonite R-2 is a monomeric modified urea-formaldehyde precondensate. Ammonium chloride was used as a catalyst at a level of 0.2 mmol./g. of precondensate. The solutions were applied on a heavy laboratory pad using 2 dips and 2 nips, which gave a wet pickup of 80% for the cotton and 100% for the rayon. The wet samples were put on pin frames at their original dimensions, dried for 5 min. at 125° C., and cured for 10 min. at 150° C. Half of each sample was then scoured in the rinse cycle of a domestic washer, reframed, and dried.

Density Determinations

The technique used was that of Preston and Nimkar [7], using toluene and carbon tetrachloride in the columns. The solvents were C.P. grade materials and were not specially purified except by drying for several days over anhydrous calcium sulfate.

The columns were prepared in 250-ml. glass-stoppered graduates and kept in a constant temperature room at 22 ± 1° C. To avoid occasional difficulties with convection currents, the cylinders were surrounded with transparent plastic shields 3 in. in diameter. They were calibrated with floats which were hollow glass beads whose diameter was 1–2 mm. The densities of the floats were obtained by determining pycnometrically the density of a toluene–carbon tetrachloride mixture in which the bead would neither sink nor float.

Since the changes observed in preliminary experiments were quite small, it was necessary to make the density gradient rather shallow. A convenient gradient turned out to be a change of 0.004 g./cc. for each centimeter of column height. The columns were prepared by putting in five 50-ml. layers of solvent, each higher one containing 2.5% more toluene. For cotton the bottom layer was pure carbon tetrachloride. For rayon, it was 95% carbon tetrachloride, 5% toluene. A linear gradient was established overnight in columns prepared this way.

The test samples were pieces of yarn 2–4 mm. long which had been dissected out of the fabric. They were dried in an oven and boiled for a few minutes in toluene before being placed in the top of the column. At least 18 hr. was allowed for the samples to come to rest. All readings were made with the calibration floats in the column, and if the calibration line was not straight the column was discarded.

Five samples at a time were run in a column, those from a given fabric, resin, and aftertreatment being grouped together, and the density of each such group of five was determined twice in separate columns. The data from the duplicate tests plotted against resin concentration fell on smooth parallel curves, and the two determinations were averaged together. The vertical displacement of these curves represented the column-to-column variation of the procedure, and since the comparative changes in density were of interest, it was convenient to adjust the measurements to compensate for this. This was possible since each set of five measurements included an untreated control sample. To make the adjustment, the amount necessary to make the control sample density equal to the mean value of all the control samples was added or subtracted to each result in the set. After this adjustment, the density–resin concentration curves for each fabric all had a common origin. The mean density for untreated cotton

was 1.5498 with a standard deviation of 0.0003. For untreated rayon the mean was 1.5124 with a deviation of 0.0004.

Moisture Regain and Resin Content

Moisture regain was determined by taking samples that had been at standard testing conditions for a month and drying them to constant weight at 110° C. The moisture content was calculated on the basis of the cellulose alone, corrected for the resin content, which was determined by the acid extraction technique.

Resin Density

In order to interpret the changes in density produced by resin in the fibers, it is necessary to have some information on the density of the resin, which was obtained by determining the density of resin cured *in vitro*. Samples of each of the four resins were dried down with the normal amount of NH_4Cl catalyst (0.2 mmol./g. of precondensate) and with half and twice this amount. The catalyzed solutions were placed on watch glasses in an oven at 110° C. for 18 hr., then were ground to a fine powder in a mortar and returned to the oven for 3 hr. The densities of the 12 resulting samples were determined in separate columns; results are shown in Table I. All of the materials were spread over a range of densities, although in the case of dimethylol ethylene urea the range was remarkably narrow. In the case of the other materials, most of the material tended to be concentrated at the center of the range given. The average given in the last column is the density used in subsequent calculations.

TABLE I. Density of Resins Cured *in Vitro*

Precondensate	Density, g./cc. ½×normal cat.	Normal cat.	2×normal cat.	Av.
Monomethylol urea	1.352–1.385	1.351–1.380	1.399–1.410	1.38
Dimethylol urea	1.494–1.499	1.493–1.499	1.490–1.497	1.50
Dimethylol ethylene urea	1.395–1.400	1.399–1.403	1.396–1.401	1.40
Rhonite R-2	1.430–1.480	1.450–1.500	1.460–1.510	1.47

Results and Discussion

The results are recorded in Table II, and the density changes in the treated fibers are presented graphically in Figures 1 and 2. In every case the experimental results approach the line calculated for volume additivity of the resin and the cellulose by assuming that the values in Table I represent the densities of the resin in the fiber. This means that each of these materials acts essentially alike in swelling the fiber, with only small amounts of resin being deposited in pre-existing void spaces not accessible to the liquid of the gradient column. The percentage fraction of the added resin which was effective in swelling the fiber was calculated from the data in

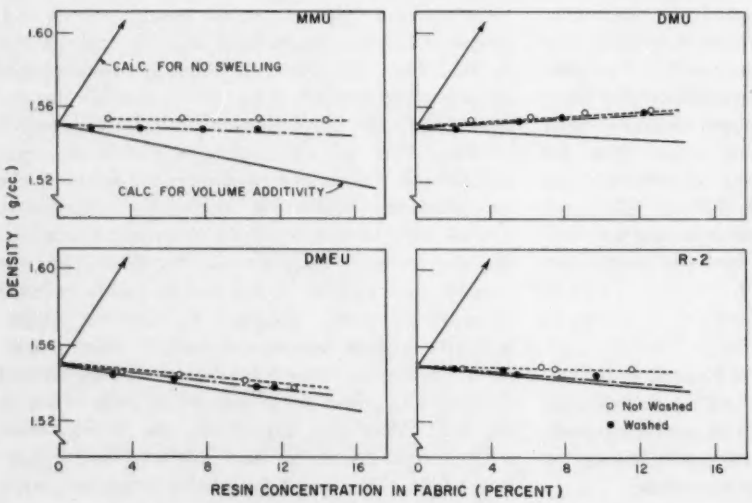

Fig. 1. Effect of monomethylol urea, dimethylol urea, dimethylol ethylene urea, and Rhonite R-2 on the density of cotton.

Tables I and II and is given in Table III. A three-factor analysis of variance was carried out on these data, leaving the effect of resin application level in the residual variance. The analysis is summarized in Table IV. The main effects were all significant at the 1% level, and the means showing the magnitude of these effects are as follows; the limits shown are two standard deviations of the mean.

Fabric effect:

Cotton	93.8% ± 1.1%
Rayon	96.7%

Aftertreatment effect:

Original	93.2% ± 1.1%
Washed	97.6%

TABLE II. Density of Resin-Treated Cellulose

Treatment	Cotton				Rayon			
	Resin conc., %	H_2O regain, %	Density, g./cc.		Resin conc., %	H_2O regain, %	Density, g./cc.	
			Raw	Adj.			Raw	Adj.
MMU—orig.	0	5.09	1.5487	1.5498	0	11.14	1.5101	1.5124
orig.	2.9	5.32	1.5523	1.5534	4.3	9.65	1.5136	1.5159
orig.	6.8	4.67	1.5525	1.5536	8.3	9.62	1.5152	1.5174
orig.	10.9	4.36	1.5524	1.5535	14.3	9.67	1.5152	1.5174
orig.	14.6	4.49	1.5519	1.5530	19.0	9.98	1.5160	1.5182
MMU—washed	0	5.39	1.5493	1.5498	0	10.56	1.5130	1.5124
washed	2.0	5.49	1.5484	1.5489	2.3	10.73	1.5118	1.5111
washed	4.6	5.26	1.5479	1.5484	5.3	10.83	1.5130	1.5124
washed	7.9	5.20	1.5470	1.5474	8.8	11.62	1.5125	1.5118
washed	10.7	5.30	1.5462	1.5467	12.7	11.30	1.5116	1.5109
DMU—orig.	0	5.60	1.5494	1.5498	0	12.22	1.5108	1.5124
orig.	3.1	5.34	1.5513	1.5517	3.8	10.98	1.5123	1.5138
orig.	6.2	4.61	1.5540	1.5544	8.0	11.48	1.5171	1.5186
orig.	9.1	4.11	1.5562	1.5566	11.6	9.41	1.5194	1.5210
orig.	12.7	4.07	1.5576	1.5580	17.1	8.89	1.5252	1.5267
DMU—washed	0	5.16	1.5504	1.5498	0	11.54	1.5134	1.5124
washed	2.3	5.95	1.5494	1.5488	3.0	11.66	1.5126	1.5116
washed	5.5	4.69	1.5532	1.5526	7.1	11.20	1.5130	1.5120
washed	8.0	4.08	1.5546	1.5541	10.9	10.96	1.5148	1.5138
washed	12.4	4.13	1.5572	1.5566	15.4	9.91	1.5188	1.5178
DMEU—orig.	0	5.04	1.5494	1.5498	0	11.84	1.5116	1.5124
orig.	3.5	5.17	1.5452	1.5456	4.4	10.72	1.5065	1.5073
orig.	6.6	—	1.5436	1.5440	8.4	—	1.5042	1.5050
orig.	10.0	4.91	1.5410	1.5414	12.1	11.90	1.5014	1.5022
orig.	12.8	4.74	1.5370	1.5374	16.5	12.24	1.5006	1.5014
DMEU—washed	0	4.98	1.5501	1.5498	0	11.20	1.5125	1.5124
washed	3.0	4.86	1.5451	1.5449	3.7	11.58	1.5066	1.5065
washed	6.3	4.84	1.5420	1.5418	5.6	11.19	1.5023	1.5022
washed	10.7	4.00	1.5376	1.5372	10.9	11.50	1.4978	1.4977
washed	11.6	3.90	1.5373	1.5370	14.4	11.48	1.4958	1.4957
R-2—orig.	0	5.36	1.5488	1.5498	0	11.60	1.5112	1.5124
orig.	2.5	5.34	1.5471	1.5481	3.0	11.84	1.5095	1.5107
orig.	6.7	4.33	1.5474	1.5485	5.4	11.74	1.5084	1.5096
orig.	7.4	4.06	1.5478	1.5480	6.9	11.38	1.5096	1.5108
orig.	11.6	4.30	1.5458	1.5468	10.0	11.64	1.5071	1.5083
R-2—washed	0	5.80	1.5492	1.5498	0	10.68	1.5139	1.5124
washed	2.0	5.84	1.5470	1.5475	2.1	11.32	1.5110	1.5095
washed	4.6	5.02	1.5462	1.5468	4.8	11.94	1.5088	1.5073
washed	5.5	4.88	1.5444	1.5449	6.1	10.77	1.5076	1.5061
washed	9.5	5.25	1.5412	1.5418	9.9	10.92	1.5038	1.5023

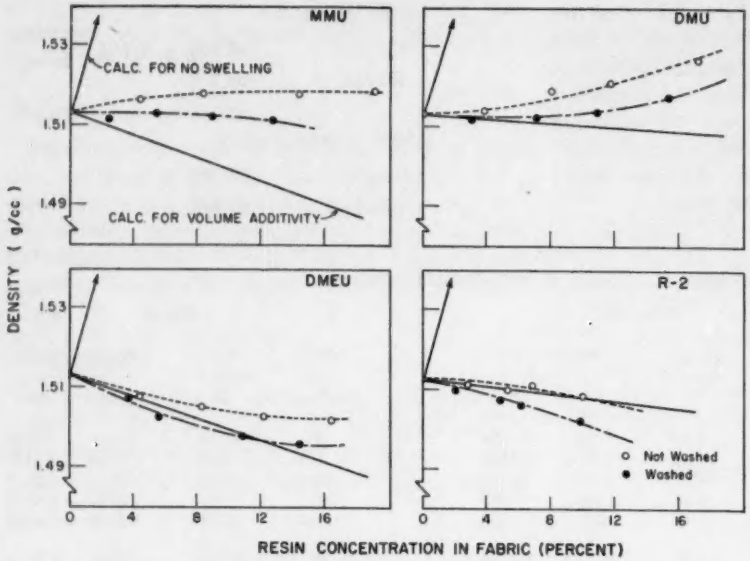

Fig. 2. Effect of monomethylol urea, dimethylol urea, dimethylol ethylene urea, and Rhonite R-2 on the density of rayon.

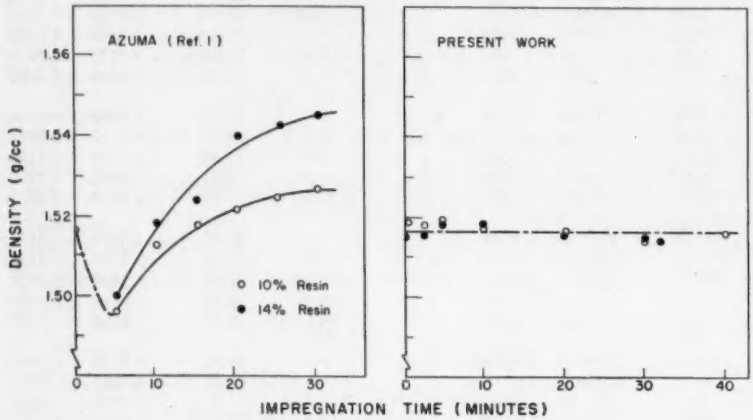

Fig. 3. Effect of impregnation time on the density of rayon treated with urea formaldehyde resin.

Resin effect:

MMU	89.1% ± 1.5%
DMU	95.1%
DMEU	97.0%
R-2	100.0%

While the difference in swelling effectiveness on cotton and rayon is highly significant in the sense that it is not likely to be due to chance, its magnitude is not very great. The difference is in the direction which might be expected from the fact that cotton has larger pores than rayon. Afterwashing, which removes unreacted resin and any reaction byproducts, does not result in a collapse of the space occupied by these materials, probably because the structure of the fiber has been stabilized by the reacted portion of the resin.

The means for the resin effect were compared by Duncan's multiple range test [2], using a 5% probability level. This comparison indicated significant differences between the monomethylol urea, Rhonite R-2, and the other pair of materials. The low value for monomethylol urea is consistent with the hypothesis that this material produces little or no cross-linking. The grafted side-chains which it forms [8] are more able to accommodate themselves to whatever open space is available than cross-linking mate-

rials are. The greater swelling effectiveness of Rhonite R-2 is probably due to the higher molecular weight of this precondensate. There was evidence in comparing fabric resin contents with treatment concentrations that rayon picked up proportionately less R-2 than cotton. This was not observed with the other materials.

Azuma, Tonami, and Yokota [1] have reported some density changes on rayon treated with urea-formaldehyde resin using a conventional displacement technique. They found, among other things, that the density of the treated fibers depended on the length of time they were allowed to stand in the precondensate solution. We have attempted to check their result, using dimethylol urea and rayon challis. The application was done in the manner described above, except that the samples were allowed to steep in the treatment solution for various lengths of time before being put through the padder. We were unable to confirm the result of the earlier work, and our experiment showed no effect of impregnation time. The data are plotted in Figure 3 in comparison with those of the Japanese workers. The composition of their resin was not entirely clear to us and may have had a lower formaldehyde-to-urea ratio than dimethylol urea, but it seems unlikely that this could account for the difference observed.

The moisture regain data are plotted in Figure 4 on a relative basis, using the untreated fabric as a reference, so that the two fibers may be compared. The results are in general consistent with other property changes observed in these two fibers [8, 9]. Reacted (washfast) monomethylol urea does not reduce the regain of either fiber, while cross-linking materials reduce the regain of cotton to a greater degree than that of rayon. Dimethylol ethylene urea and Rhonite R-2 do not reduce the regain of rayon up to 15% and 12% resin concentrations, respectively, but dimethylol urea shows some effectiveness in the 10–15% concentration range. On both fabrics the reaction residue from monomethylol urea treatment reduces the regain. This effect is not apparent with the other resins, where the amount of residue is considerably less. The percentage of fixed resin was 66% for monomethylol urea, 89% for dimethylol urea, 87% for dimethylol ethylene urea, and 81% for Rhonite R-2.

Conclusions

With the four resin precondensates studied, the treatment of cotton and rayon with thermosetting resin results in fiber swelling, with very little of the added material being deposited in any pre-existing void space in the fiber. Monomethylol urea appears to be slightly less effective in swelling than the cross-linking resins, while Rhonite R-2 is possibly a little more effective than dimethylol urea and dimethylol ethylene urea.

With each resin and each fabric, removing the unreacted material by scouring does not result in a collapse of the volume occupied by the material removed, presumably because the fiber structure is stabilized by the reacted resin.

The effects of resin treatment on the moisture regain of resin-treated fabric show similar differ-

TABLE III. Effectiveness of Urea-Formaldehyde Resins in Swelling Cellulose Fibers, %

	Cotton		Rayon	
Precondensate	Orig.	Wash	Orig.	Wash
Monomethylol urea	81.7	91.8	86.5	94.6
	79.5	90.7	92.5	91.3
	87.1	90.7	89.1	91.6
	87.8	90.7	89.4	91.9
Dimethylol urea	92.9	99.5	96.7	100.8
	92.1	93.6	94.1	99.6
	92.1	93.4	94.3	98.3
	92.7	93.4	93.8	94.2
Dimethylol ethylene urea	97.4	100.0	99.7	102.3
	95.5	97.8	98.0	103.8
	95.2	97.2	97.8	101.0
	87.4	96.8	80.8	99.6
Rhonite R-2	98.9	101.7	100.9	106.2
	96.1	98.6	99.2	103.9
	96.1	99.8	98.7	103.9
	96.4	99.5	99.8	104.0

TABLE IV. Analysis of Variance for Data on Swelling Effectiveness

Source of variance	Sum of squares	Degrees of freedom	Mean squares
Fabric (F)	138.65	1	138.65*
Resin (R)	1029.26	3	343.09*
Aftertreatment (A)	315.06	1	315.06*
F × R	6.90	3	2.30
F × A	1.38	1	1.38
A × R	18.07	3	6.02
Residual	493.40	51	9.67
Total	2002.70	63	
Recalculated residual		58	8.96
Standard deviation			2.99

* Significant at 1% level.

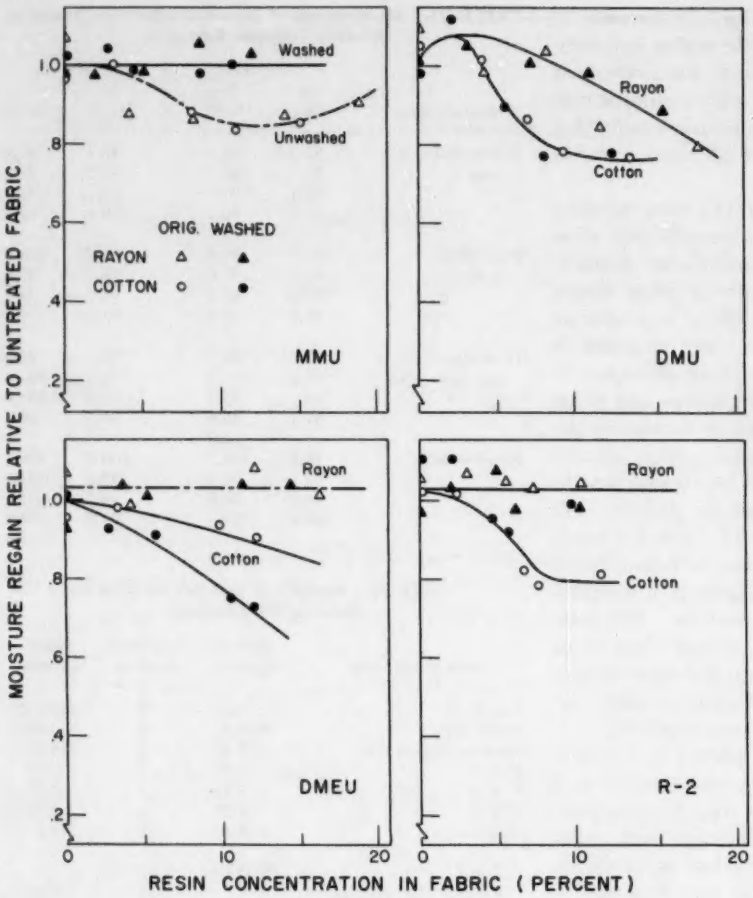

Fig. 4. Effect of monomethylol urea, dimethylol urea, dimethylol ethylene urea, and Rhonite R-2 on the moisture regain of cotton and rayon.

ences between cross-linking and non-cross-linking materials on cotton and rayon as are observed in changes in mechanical properties.

Literature Cited

1. Azuma, N., Tonami, H., and Yokota, D., *J. Soc. Textile Cellulose Ind. (Japan)* **10**, 310–313 (1954).
2. Duncan, D. B., *Biometrics* **11**, 1–42 (1955).
3. Gagliardi, D. D. and Gruntfest, I. J., TEXTILE RESEARCH JOURNAL **20**, 180–188 (1950).
4. Linderstrøm-Lang, K., *Nature* **139**, 713–714 (1937).
5. Orr, R. S., Weiss, L. C., Moore, H. B., and Grant, J. N., TEXTILE RESEARCH JOURNAL **25**, 592–600 (1955).
6. Ott, E., Spurlin, H. M., and Graffin, M. W., eds., "Cellulose and Cellulose Derivatives," New York, Interscience, 264 ff. (1954).
7. Preston, J. M. and Nimkar, M. V., *J. Textile Inst.* **41**, T446–T454 (1950).
8. Steele, R. and Giddings, L. E., Jr., *Ind. Eng. Chem.* **48**, 110–114 (1956).
9. Steele, R. and Giddings, L. E., Jr., TEXTILE RESEARCH JOURNAL **26**, 116–123 (1956).
10. Stock, C. R. and Scofield, E. R., TEXTILE RESEARCH JOURNAL **21**, 521–526 (1951).
11. Tessler, S., Woodberry, N. T., and Mark, H., *J. Polymer Sci.* **1**, 437–439 (1946).

Manuscript received August 10, 1958.

A Study of the Relationship Between Breaking Time and Breaking Load for Fabrics Tested on CRE and CRT Machines[1]

Audrey S. Tweedie, Margaret T. Mitton, and J. Margaret Fry

Textile Research Section, National Research Council, Ottawa, Canada

Abstract

A study has been made of the relation between breaking time and breaking load for six different fabrics, using 1-in. ravelled strips with 3-in. initial clamp separation, tested on a constant-rate-of-specimen-extension (CRE) machine operated at a number of rates of extension, i.e., cross-head speed. The fabrics used were cotton nainsook, heavy cotton duck, acetate/viscose gabardine, viscose crepe, and nylon taffeta, so as to cover a range of extensibilities and breaking loads. In general these fabrics showed a decrease in breaking load with increase in breaking time, as has also been reported in the literature for studies on fibers and yarns.

Tests were also carried out on constant-rate-of-traverse (CRT) pendulum machines at two or three different speeds for each fabric. Good agreement was obtained between the breaking loads measured on the CRE and CRT machines when compared at equal breaking times.

To put the measurement of breaking load of fabrics on a constant-breaking-time basis appears to offer the best means of obtaining comparable results with different types and capacities of testing machines. A breaking time of 20 ± 3 sec. has recently been proposed by ISO/TC 38 for single-strand testing of yarns on CRE, CRT, and CRL (constant-rate-of-loading) machines. The data obtained in this study on fabrics suggest that a breaking time of 20 ± 3 sec. will also be suitable for the measurement of the breaking load of fabrics on different types and capacities of machines. No evidence was obtained in favor of a longer breaking time such as the 60 ± 10 sec. commonly used with CRL machines abroad.

Introduction

There is much interest at the present time in obtaining general agreement on precise methods for measuring the breaking load (in tension) of fabrics. The interest in this subject has arisen in two ways. First, it stemmed from the relatively recent development and growing use on the North American continent of constant-rate-of-specimen-extension (CRE) machines, in contrast to machines of the pendulum constant-rate-of-traverse (CRT) type, which was for many years the only type of machine available here for testing fabrics over a wide range of breaking loads. This development has made it important to know whether it is possible to so define the conditions of use for each of these types of machine that the same breaking load value for any given fabric may be obtained with both types of machine. Second, the creation in 1946 of the International Organization for Standardization (ISO) and of its Technical Committee 38 on Textiles has resulted in active work, on the part of most countries participating in international trade, toward standardizing textile test methods. This work has revealed the wide differences in machines and procedures now used in the various countries for measuring the breaking strength of fabrics, including the use of a third basic type of machine, the constant-rate-of-loading type.

The work covered by this paper had its origin in the need, which arose during the course of revision of the Canadian Government Specification Board's "Schedule of Methods of Testing Textiles" [17], for information as to the most suitable operating procedures for CRT and CRE machines in fabric

[1] Presented at a meeting of The Institute of Textile Science, Montreal, Canada, September 8, 1958.

testing in order to be able to obtain good agreement between breaking load values obtained on these two types of machine. It is believed, however, that the findings may have a bearing on the wider problem of standardization of test methods for measuring breaking load.

The major factors which can affect the actual values obtained for the breaking load of a given fabric under standard atmospheric conditions are:

1. The type of test, e.g.:
   1-in. ravelled strip test with 3-in. initial separation of clamps
   2-in. ravelled strip test with 8-in. initial separation of clamps
   1-in. grab test with 3-in. initial separation of clamps.
2. The type of tensile testing machine and the operating conditions (e.g., speed and capacity) used, the machine types being classified as:
   CRT—constant-rate-of-traverse of the driven clamp, with the non-driven clamp having appreciable movement under load
   CRE—Constant-rate-of-extension of specimen
   CRL—Constant-rate-of-loading of specimen.

With respect to the type of breaking strength test, the 1-in. grab test is the most widely used test in the U.S.A. and Canada, but the 1-in. ravelled strip test with 3-in. initial clamp separation is also recognized, and is preferred in some laboratories since it requires less fabric, is easier to grip securely in the case of strong fabrics, and is more convenient for measuring the effect of different treatments on a given fabric, although it requires a somewhat longer time for specimen preparation. The 2-in. ravelled strip, usually with 8-in. initial clamp separation, is the standard test in Britain and a number of other countries.

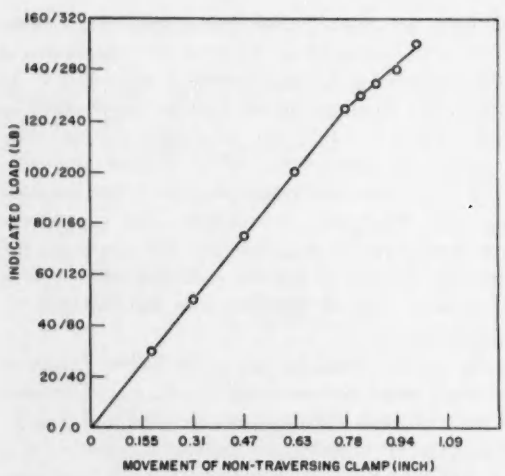

Fig. 1. Movement of non-traversing clamp under load in a 150/300 lb. capacity CRT pendulum machine.

Several investigations have been carried out in an attempt to find a universal relation between the breaking strength values obtained by the grab and ravelled strip tests [6, 12, 13]. To date no such relation has been found. There does not even appear to be a universal relation governing the breaking strength per unit width obtained with ravelled strip tests using specimens of different widths [2, 6, 10].

It is well known that differences in machines, e.g., type, method of operation, and capacity (particularly of pendulum-type machines), can result in different breaking load values being obtained for a given fabric in different laboratories, even though the same type of test and the same atmospheric conditions are used. Differences in the resultant breaking times appear likely to be the major factor responsible for these differences in breaking load values. There have been indications that similar breaking-load values can be obtained on CRT, CRE, and CRL machines provided that the breaking times are the same. Cryer [4], using the 1-in. grab test on a 10.5 oz./sq. yd. cotton duck, found that for a breaking time of approximately 60 sec. there was no significant difference in the breaking-load values obtained on the three types of machines. In that work, the CRT machine used was a Tinius Olsen Universal, a machine which utilizes a pendulum-balance weighing system.

The dependence of breaking load or apparent strength of textile materials on the duration of the test or, conversely, on the rate of loading, was referred to by Peirce [16] in 1927 as "well known." Most of the published work showing this relationship has been based on the testing of yarns and fibers. It shows a general decrease in breaking load with increase in breaking time. Barr [1] in 1920 showed that this effect was obtained with a linen fabric. The limited quantity of data published for other fabrics since then shows the same effect (see for example [5, 6]). However, it is only relatively recently that the importance of breaking time in the measurement of breaking load of fabrics and yarns

has been generally recognized (see for example [18]).

The characteristics of CRT, CRE, and CRL machines and of the operating conditions under which they have been commonly used up to the present time are discussed below.

CRT Machines

The constant-rate-of-traverse (CRT) machines are the type most widely used in all countries for tensile testing of fabric strength and elongation. Their relative simplicity of design, use and maintenance, and their compactness and moderate cost are in their favor. In CRT machines, one of the clamps holding the specimen is driven at a constant rate of traverse; the other clamp is attached to a load-indicating system of a type which gives increasing displacement of this non-driven clamp with increasing load on the specimen (see Figure 1), and thus the rate of specimen extension is not constant. The most commonly used load-indicating system is undoubtedly the pendulum balance, although spring-loading machines are also used.

The characteristics of pendulum-balance weighing systems which might result in errors in the apparent breaking load were recognized quite early [5, 11, 15]. Some of these were overcome by modifications of machine design and by limitation of the maximum permissible angle of inclination of the pendulum to the vertical. The possible effects of pendulum inertia were considered. Pendulum inertia might lead to overrun of the pendulum when a specimen breaks and thus give an indicated breaking load which would be too high; it was considered unlikely that this would be an important factor in most textile testing, since the pendulum is normally in steady motion at low velocity as the breaking load is approached. Conversely, too low an indicated breaking load might result from part of the tension on the fabric having to be used to accelerate the pendulum during the last part of a test, rather than merely balancing its movement. For a given breaking load, error of this kind would increase with increasing heaviness of the pendulum (i.e., with increasing load capacity of the machine) and very short breaking times. Essentially, this is an error resulting from the breaking time being less than the response time of the load-indicating mechanism.

However, for a given fabric tested at a single constant rate of traverse, higher capacity machines normally give higher instead of lower breaking-load values. It was recognized that this is due chiefly to the higher rate of loading applied to the specimen by the higher capacity machines and the resultant shorter time required to stretch the sample to its breaking point. Attempts were made to control the rate of loading of specimens on CRT machines of different capacities by specifying that the machine capacity used in testing a given fabric should be such that the indicated breaking load of the fabric would be between 10% and 90% of the capacity. However, for any given rate of traverse and initial clamp separation, this still permits a wide variation in rate of loading of the specimen; e.g., a fabric specimen having a nominal breaking load of approximately 60 lb. could be tested on a 500-lb. capacity machine (having 0.5-in. movement of the non-traversing clamp for an indicated load of 215 lb.) as well as on a 110-lb. capacity machine (having 0.5-in. movement of the non-traversing clamp for an indicated load of only 70 lb.). The much smaller movement per unit load of the non-traversing clamp on the 500-lb. capacity machine will result in a more rapid rate of loading of the specimen and thus in a shorter breaking time and a higher breaking-load value. Even where the same capacity of a single CRT machine can be correctly used for testing two fabrics having the same breaking elongation, a difference in their breaking strengths can cause a considerable difference in their breaking times when both are tested at the same rate of traverse. For example, with three different CRT machines operated at 4 in./min., the times required for the traversing clamp to take up the movement, under load, of the clamp attached to the weighing mechanism are 6, 7, and 9 sec. greater, respectively, for loads equal to 80% of either capacity of the individual machines than for loads equal to 30% of their respective capacities. These time differences are large in relation to the short breaking times obtained under certain testing conditions.

There has as yet been no general agreement on the most suitable rate(s) of traverse for CRT machines when used for testing fabrics. A rate of $12 \pm \frac{1}{2}$ in./min. has for many years been standard for CRT machines of U.S.A. manufacture, whereas both lower and higher rates, e.g., 4.5 and 18 in./min., have been used elsewhere. These rates, however, must be considered in relation to the initial clamp separations with which they are normally used; e.g., for a given fabric tested on a single CRT machine,

an 18 in./min. rate of traverse with 8-in. initial clamp separation produces a much slower rate of stretching of the specimen than does a 12 in./min. rate of traverse with a 3-in. initial clamp separation. Many CRT machines were originally designed to operate at a single speed, but some have multiple-speed drives, and existing single-speed machines can be modified to provide additional speeds without too much difficulty and expense.

The ISO Draft Proposal of April 1957 for "Determination of Breaking Load and Extension of Strips of Woven Textile Fabric" permits the use of CRL, CRE, and CRT machines. It specifies the use of 8-in. initial clamp separation and a rate of traverse of 4 ± 0.5 in./min. for CRT machines. Some experimental data and comments concerning the suitability of this requirement are presented elsewhere in this paper.

CRE Machines

The constant-rate-of-specimen-extension (CRE) machines are relatively new. Like the CRT machines, they have one clamp which is driven at a constant rate of traverse, but they differ in that their load-indicating systems cause negligible displacement of the non-driven clamp throughout the full range of loads. Each machine has a wide range of operating speeds, varying from a fraction of an inch to approximately twenty inches per minute. Machines of this type, like those of the constant-rate-of-loading (CRL) type, are large, expensive, and require a somewhat higher level of technical skill in their use and particularly in their maintenance than do CRT machines. There is as yet no generally agreed-upon procedure for testing fabrics with this type of machine.

The ISO Draft Proposal of April 1957 for "Determination of Breaking Load and Extension of Strips of Woven Textile Fabric" specifies the use of 8-in. initial clamp separation and a rate of extension of 2 ± 0.25 in./min. for CRE machines.

Standard D76-53 of the ASTM Standards on Textile Materials specifies a different rate of crosshead travel (specimen extension) on CRE machines for each of three ranges of breaking elongation of fabric specimens. However, revision of this 1953 standard is currently under consideration, and it is understood that present thinking favors the adoption of a constant-breaking-time basis for CRE testing of fabrics.

CRL Machines

The constant-rate-of-specimen-loading (CRL) machines are preferred to CRT machines by testing authorities in the United Kingdom and in some other countries, the rate of loading for each set of specimens being so chosen as to give the same average breaking time with all fabrics. Among the users of CRL machines for fabric testing, there appears to be fairly general agreement on a 60-sec. breaking time.

The concept of testing the breaking strength of fabrics, as well as fibers and yarns, under conditions of constant-rate-of-specimen-loading (CRL) appears to be of early origin. In England, the Avery shot-loading machine for testing fabrics under CRL conditions was developed during the 1914–18 war as an improvement over existing CRL machines and was used by the National Physical Laboratory in its studies on aircraft fabrics in order to obtain breaking strength data for different fabrics which would be truly comparative; i.e., which would not involve machine characteristics such as those which complicated the comparison of data obtained on CRT machines for different light-weight fabrics of relatively low extensibility [11]. This and other early British CRL machines were apparently not free from operational difficulties—notably those associated with the rapid changes necessary in the rate of specimen elongation during the latter part of a test in order to keep the weighing beam in constant equilibrium and the rate of loading therefore constant. Failure to achieve this could result in serious errors.

In the U.S.A., the Scott Inclined Plane Tester, which became available in 1921 [19], has been the

TABLE I. Description of Fabrics Used

Fabric	Weight, oz./sq. yd.	Yarns/in. Warp	Yarns/in. Weft	Yarns
Cotton nainsook, white	2.7	98	102	Singles
#4 Cotton duck, unbleached	24.5	30	22	4-ply
Acetate/viscose gabardine, white (scoured state, not resin-finished)	7.9	78	51	Spun, 2-ply
Viscose crepe (weft crepe), white	3.2	127	77	Filament, singles
Nylon taffeta, white	2.6	165	89	Filament, singles

only CRL machine used to any extent for testing yarns and fabrics. Its novel principle gave automatic take-up of the specimen extension as the load increased at a constant rate, and thus made it free of the major sources of error possible with the British CRL machines of the same period. Mechanical considerations, however, limited the maximum capacity of this type of machine so that, although it could be used for testing some fabrics, its chief use has been in the field of yarn testing.

Various constant rates of loading appear to have been used for fabric testing with CRL machines in the early years; e.g., Barr [1] at the National Physical Laboratory used a machine of this type to study "The Effect of Rate of Loading on the Apparent Strength of Cotton Balloon Fabrics." The First Report of the Fabrics Co-Ordinating Research Committee (Britain) in 1925 gave the results of some tests on cotton duck carried out on an Avery machine at two rates of loading such that the breaking times were 85 sec. and approximately 12 sec. respectively, the shorter breaking time being used for closer comparison with the results obtained in approximately the same breaking time on a pendulum machine. Midgley [15] stated in 1923 that a successful break of fabric specimens on the Avery CRL machine could seldom be obtained in less than 30 sec. He also stated that the lack, at that time, of a standard rate of loading militated very seriously against the use of the CRL type of machine for routine testing of yarns. The National Physical Laboratory, which was responsible for the testing of aeronautical fabrics (at that time chiefly light-weight linen and cotton fabrics) in Britain during the 1914–18 war, appears to have settled on the practice of choosing different constant-rates-of-loading for different test fabrics so as to obtain a constant breaking time of approximately 60 sec. in all tests. In 1930 that laboratory reported the use of the 60-sec. breaking time for CRL tests with the Avery machine in a study of the effect of test-piece dimensions on the tensile strength of several heavier linen and cotton fabrics and two wool fabrics, this work being done for the Fabrics Co-Ordinating Research Committee [2].

This 60-sec. breaking time chosen by the National Physical Laboratory for CRL tests appears to have been adopted by other users of CRL machines in Britain, although the number of these, judged by references in the literature, appears to have always been small in relation to the number of CRT machines in use in that country. In 1945, Bayes [3] referred to "the usual constant rate of load test in which the specimen is broken in one minute."

In 1944, the Textile Institute published Tentative Textile Standard No. 10, 1944—"Standard Testing Methods for Narrow Fabrics" [7]. For testing these fabrics, it specified a 7-in. initial clamp separation and *either* a CRL machine adjusted to give a breaking time of 1 min. *or* a CRT machine operating at 12 in./min.

Tentative Textile Specification No. 14, 1949, covered "Determination of Breaking Load and Extension of Strips of Woven Textile Fabric (By Means of Constant Rate of Load Testing Machines)" [8], and this subsequently formed the basis for British Standard 2576, 1955. It specified a breaking time of 60 ± 10 sec. and an initial clamp separation of 8 in.

In 1957, T. T. Standard No. 46, covering "Breaking Load and Extension of Strips of Woven Textile Fabric," was published [9]. It superseded T.T.S. No. 14 and forms the basis for the current revision of British Standard 2576, 1955; its requirements are identical with those of the April 1957 ISO Draft Proposal for "Determination of Breaking Load and Extension of Strips of Woven Textile Fabric." It covers, in addition to CRL machines, procedures for the use of CRE machines and of CRT machines of the pendulum type. An initial clamp separation of

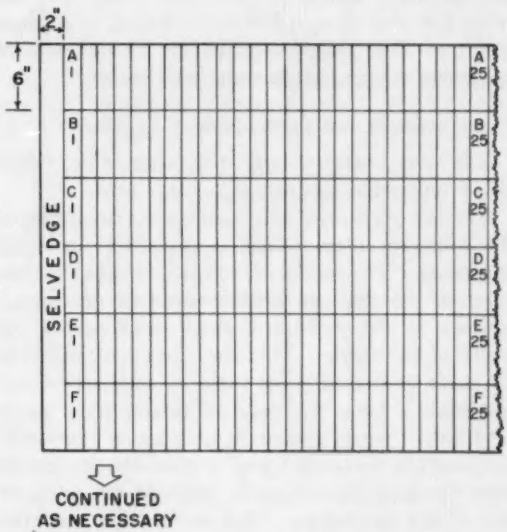

Fig. 2. Plan for layout of specimens on fabric.

8 in. is specified with all types of machine. The procedure for CRL machines specifies a constant breaking time of 60 ± 10 sec.

In order to reach a sound decision as to the most suitable operating conditions for CRE machines in fabric testing, it appeared necessary to obtain some experimental data to show the relation, for this type of machine, between breaking load, rate of specimen extension (i.e., speed of pulling clamp), and breaking time for a number of fabrics covering a range of extensibilities. It also appeared desirable to obtain some similar though less extensive data for the same fabrics, using CRT pendulum machines operated at a few different rates of traverse, in order to see what correlation might be possible between CRE and CRT machines. Preliminary work in this laboratory had indicated good agreement between the breaking load values obtained with CRT pendulum machines operated at 12 in./min. and the values obtained with a CRE machine operated at speeds which gave approximately the same average breaking time for a given fabric.

Plan of Work

Fabrics

The fabrics used in these tests are described in Table I. They provided a range of extensibilities from low to high and a range of breaking strengths from 45 to 270 lb. for 1-in. ravelled strips. Except for the duck, which was a wider fabric, only the warp direction of each fabric was tested, as a single width of these would not provide enough sets of specimens containing the same weft yarns.

Randomization and Preparation of Specimens

The 1-in. ravelled-strip test with 3-in. initial clamp separation was chosen for this work.

The test specimens were randomized according to the following plan, which is described for warp specimens. The randomization was planned to balance out the effect of possible variations in characteristics of the individual warp yarns across the width of the fabric. This was done by employing the same groups of warp yarns in each set of test specimens. Thus, if a band of weaker warp yarns occurred, it would appear in each set of specimens and could be recognized and, if desirable, eliminated from the data for the whole series of ten or more sets of test specimens. This would leave only the variations lengthwise of the fabric to be considered; i.e., variations in strength of individual warp yarns throughout their length, and any effect on warp breaking strength of the fabric which might result from possible variations in weft yarns or in weftwise tension throughout the length of the piece of fabric being tested. Any effects which these two variants might have on the warp breaking strength of the fabric as measured at different positions lengthwise of the fabric were minimized by randomizing the test specimens within each warpwise strip containing a given group of warp yarns.

This procedure required an estimate of the number of sets of test specimens likely to be required for each fabric. Preliminary work had indicated that 20 specimens per set would likely provide a reasonable level of accuracy of the means, so 25 specimens per set were normally prepared, in order to provide replacements for any that might show slippage in the clamps during test or require elimination for other reasons. The data reported for the final randomizations of three of the fabrics are the averages for 15 specimens instead of 20. This slightly increased the standard deviations and probable error of the means over those previously obtained with 20 specimens.

The layout of specimens in the fabric is shown in Figure 2, each specimen being 6 in. long and of the width necessary to provide a 1-in. ravelled strip after removal of a suitable number of yarns from its long edges. A typical set of test specimens from a fabric requiring a series of 10 sets of specimens was as follows: E1, A2, C3, H4, G5, A6, A7, D8, H9, E10 . . . D23, E24, H25.

With some of the fabrics, extension or modification of the testing originally planned made it necessary to prepare additional series of randomizations. However, except for the viscose crepe, and the weft direction of the cotton duck, the data reported in this paper are for a single randomization of each fabric.

Machines

All the tensile testing machines used were calibrated during the course of the work. The machines used were as follows.

CRE machine. This was a Tinius Olsen electromatic machine, classed as CRE, and having load capacities of 20, 50, 200, 500, 2000, and 5000 pounds, and variable rates of specimen extension obtained by cross-head speeds which could be varied from a fraction of an inch to approximately twenty inches

per minute. The clamps supplied with this machine had been modified in earlier work to provide higher and more uniform clamping pressure.

The normal method of operation for this machine required the motor to be shut off between tests and the machine left in gear. Hence the cross-head speed, and therefore the rate of specimen extension, at the beginning of a test was not constant but accelerated from zero to its nominal speed. The period of acceleration was not constant for all speeds, but depended on the nominal speed and on whether the "slow" or "fast" gear was used to attain the particular speed. The maximum acceleration times with the two gears were 2.5 sec. for the top speed of 2 in./min. available with the slow gear and 4.5 sec. for the top speed of 20 in./min. with the fast gear.

It is noted that these acceleration times would meet the requirement in the April 1957 ISO Draft Proposal for "Determination of Breaking Load and Extension of Strips of Woven Textile Fabric" that, for CRE machines, "The rate of increase in the distance between the clamps shall be uniform within ± 5% after the first 5 seconds of the test operation." In the present work, however, the acceleration periods made it difficult to obtain significant plots of rate of extension vs. breaking load, or of breaking time vs. breaking load, at high speeds and resultant very short breaking times approaching the acceleration time. It therefore became necessary to repeat some of the work, under conditions such that the rate of extension of the specimens was truly constant. This was done by positioning the specimen in the clamps set at 3 in. apart, then reducing the clamp separation to 1 or 2 in. before starting the test, thus providing time for the motor and cross-head to reach full speed before tension was applied to the specimen.

The response time of the load-indicating mechanism of this machine was approximately 4 sec. for full load in each capacity. Preliminary work showed the maximum rate of extension which could be used with a given machine capacity for each fabric so as to avoid obtaining falsely low indicated values of breaking load due to the breaking time being less than the response time of the load-indicating mechanism. False low values resulting from this cause are shown in the dotted portion of the curve in Figure 3. In order to be able to carry out the desired tests at very short breaking times on the nainsook, gabardine, and nylon taffeta, it was therefore necessary to use the next higher capacity of this CRE machine than the one which would have been chosen solely on the basis of the breaking load. The higher capacity was found to give slightly lower indicated breaking loads despite the calibrations (see Figure 4).

CRT machines. Three pendulum machines were used: two Scott machines having load capacities of 55/110 and 150/300 lb. respectively, and a Suter machine (horizontal model) with load capacities of 500/1000 lb.

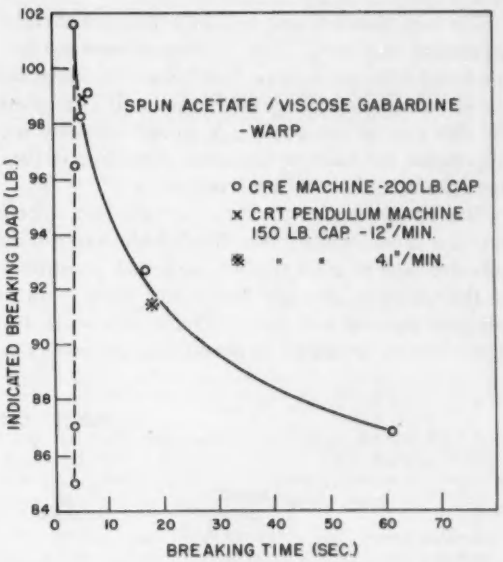

Fig. 3. Effect on indicated breaking load of the breaking time being less than the response time of the load-indicating mechanism. Dotted portion of curve shows false low values.

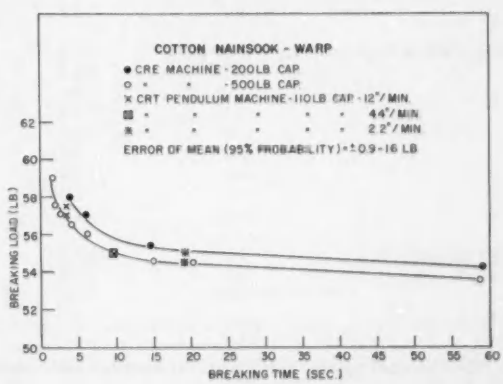

Fig. 4

These three pendulum machines are normally operated at 12 in./min. Reduced speeds were obtained by changing the pulleys and motors. The correct capacity of machine was used for each fabric. The breaking load values for the different fabrics actually fell within the range of 42–68% of the machine capacities used.

Test Procedures

The fabrics were conditioned and tested under standard atmospheric conditions of 70° F. and 65% RH.

The 1-in. ravelled strip test with 3-in. initial clamp separation was used. The specimens were not pretensioned with any specific load before clamping, but the same experienced operator was used throughout for this part of the work. A second operator was responsible for machine operation, recording of data, and special assistance in certain tests.

The clamps used with each machine had smooth flat jaw faces, which were lined with cotton-faced adhesive tape of good quality, such that penetration of the adhesive through the cotton surface under pressure was not excessive. Preliminary work had shown this to be helpful in preventing specimen slippage, especially with very smooth fabrics and with certain machine clamps where it was more difficult to apply the necessary clamping pressure. The tape was applied to the gripping surface of each jaw and extended onto both ends and side edges of the jaw. The lining was renewed as often as necessary, this being indicated by distortion, tearing or slippage of the tape on the metal surface, slippage of a specimen within a clamp, or excessive adhesion of specimens to the tape. In some cases, talcum powder was applied to the cotton surface of the adhesive tape in order to reduce the adhesion of specimens to the tape or of the tape surfaces of the two jaws to each other. Experience had shown this to be helpful with thin fabrics of high strength, such as the nylon taffeta, where considerable clamping pressure is necessary.

Lines were drawn on the specimens with a soft pencil at the proximal edges of the two clamps so that any oozing or flow of the specimen out of these edges of the clamps under load could be measured. Such flow was appreciable only with the two fabrics having high strength combined with high elongation; i.e., the warp direction of the cotton duck and the nylon taffeta. Its approximate amount was measured with calipers during the test.

TABLE II. Cotton Nainsook—Warp

Machine type and capacity	Speed of pulling clamp (C) in./min.	Breaking time, sec.	Breaking load: Av. for 15 specimens, lb.	Breaking load: Std. deviation, lb.	Breaking load: Error of mean at 95% probability, lb.	Elongation at break, %
CRE—200 lb. cap.	0.25	59.0	54.2	2.1	±1.2	
	1.0	14.6	55.4	2.2	1.3	
	2.5	6.0	57.0	2.6	1.5	
	4.0	3.8	58.0	2.2	1.3	
CRE—500 lb. cap.	0.25	58.4	53.5	1.8	1.0	
	0.75	20.3	54.5	1.9	1.1	5.3–6.3*
	1.0	15.0	54.5	1.7	1.0	
	2.5	6.1	56.0	2.0	1.1	
	4.0	4.0	56.5	1.8	1.0	
	4.0	4.0	56.5	2.1	1.2	
	6.0	2.6	57.0	2.1	1.2	
	8.0	2.0	57.5	2.5	1.4	
	10.0	1.6	59.0	2.5	1.4	
CRT (pendulum) 110 lb. cap.	2.2	19.3	55.0	1.5	0.9	
	2.2	19.2	54.5	2.8	1.6	
	4.4	9.4	55.0	1.9	1.1	5.3–7.0*
	12.0	3.7	57.0	2.6	1.5	
	12.0	3.6	57.5	2.2	1.3	

C—Constant speed. CRE machine operated with running start so cross-head was at full speed before any strain was placed on the specimens.

* Range of values obtained in two previous randomizations. Elongation not measured in above series.

Lines were also drawn on the specimens at the distal edges of the two clamps to facilitate the detection of any movement in the free ends of the specimen which would indicate any slippage of the specimen in the clamps. If any slippage occurred, the result was discarded and an additional specimen was tested.

For this work, a jaw break was defined as any break occurring within ¼ in. of the clamps, and a record was kept of all such breaks. In general, these were few in number. Such results were discarded only in those rare instances where they were appreciably lower than the lowest non-jaw break for the particular set of specimens being tested. In these cases an additional specimen was tested.

The elongation at break was measured for only the first five specimens of each set, as only an indication of the approximate elongation was required. The limited data obtained showed no significant relation between the elongation and breaking time.

Data

The data are given in Tables II–XIII and Figures 4–9.

Discussion of Data

All but one of the six series of tests on fabrics showed an increase in breaking load with decrease in breaking time, as has also been reported in the literature for studies on fibers and yarns and, to a more limited extent, for fabrics. This applied to the tests done on the CRE machine over a range of breaking times extending from approximately 4 sec. to 70 sec., and also to the tests done on the CRT pendulum machines operated at a few different rates of traverse.

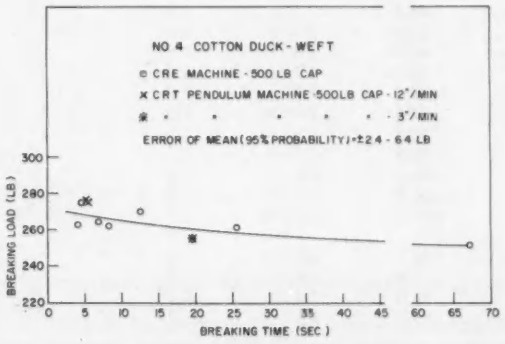
NO 4 COTTON DUCK - WEFT
CRE MACHINE - 500 LB CAP
CRT PENDULUM MACHINE 500LB CAP - 12"/MIN
" " " " " - 3"/MIN
ERROR OF MEAN (95% PROBABILITY) = ±2.4 - 6.4 LB
BREAKING LOAD (LB.)
BREAKING TIME (SEC.)

Fig. 5

Within the limits of accuracy involved, the warp direction of the #4 cotton duck showed no appreciable change in breaking load for breaking times extending over the wide range of 4–75 sec.

For the five series of tests which showed a change in breaking strength with change in breaking time, the rate of change was different for each fabric. For the warp direction of the nylon taffeta, the rate was essentially constant, but for the warp direction of the cotton nainsook, acetate/viscose gabardine, and viscose crepe, and for the weft direction of the

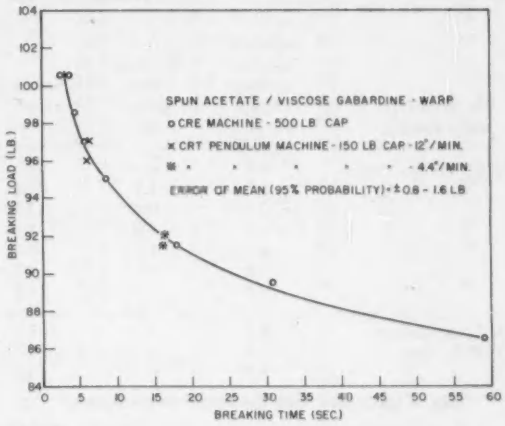
SPUN ACETATE / VISCOSE GABARDINE - WARP
CRE MACHINE - 500 LB CAP
CRT PENDULUM MACHINE - 150 LB CAP - 12"/MIN.
" " " " " - 4.4"/MIN.
ERROR OF MEAN (95% PROBABILITY) = ±0.8 - 1.6 LB
BREAKING LOAD (LB.)
BREAKING TIME (SEC.)

Fig. 6. Only the constant-speed data for the CRE machine are plotted. The curve for the CRE machine operated with the normal initial acceleration period is slightly displaced from this at the shorter breaking times.

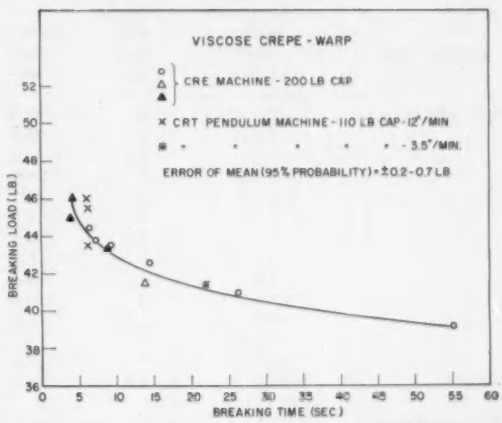
VISCOSE CREPE - WARP
CRE MACHINE - 200 LB CAP
CRT PENDULUM MACHINE - 110 LB CAP - 12"/MIN
" " " " " - 3.5"/MIN.
ERROR OF MEAN (95% PROBABILITY) = ±0.2 - 0.7 LB
BREAKING LOAD (LB.)
BREAKING TIME (SEC.)

Fig. 7. This graph includes values from three separate randomizations of specimens. The three CRT tests at 12 in./min. are from three randomizations. The CRE tests are from only two of these randomizations. ▲ = tests at constant speed.

#4 cotton duck, the rate of change decreased as the breaking time increased; see Table VIII.

The acetate/viscose gabardine and the viscose crepe showed the greatest sensitivity of breaking load to breaking time. Their respective breaking loads at 60-sec. breaking time were 14% and 17% less than those obtained at the respective minimum breaking times of 2.6 and 3.9 sec. achieved on the CRE machine at 14 in./min. rate of extension.

Good agreement was, in general, found between the breaking loads obtained on the CRE and the CRT pendulum machines when compared at equal breaking times.

Table IX shows the wide variation in breaking times which would be obtained for the fabrics used in this work if tested under some suggested operating conditions: on the CRT machines operated at 12 in./min. with 3-in. initial clamp separation; on the

TABLE III. No. 4 Cotton Duck—Weft

Machine type and capacity	Nominal speed of pulling clamp, in./min.	Acceleration time, sec.	Breaking time, sec.	Breaking load			Elongation at break, %
				Av. for 20 specimens, lb.	Std. deviation, lb.	Error of mean at 95% probability, lb.	
CRE—500 lb. cap.	0.4	0.9	67	251	8.6	±4.1	15
	1.0	1.7	25.6	261	13.4	6.4	14
	2.0	0.6	12.5	270	11.2	5.4	14
	3.0	1.0	8.3	262	7.9	3.8	12
	4.0	1.2	6.9	264	11.5	5.5	13
	6.0	1.7	4.7	274	11.6	5.6	13
	8.0	2.1	4.1	262	4.9	2.4	15
CRT (pendulum) 500 lb. cap.	12.0	—	5.5	275	9.6	4.6	12
	12.0	—	5.1	276*	12.5	6.0	13
	3.0	—	19.4	256*	9.0	4.3	12

* Sets of specimens from a second randomization.

TABLE IV. Spun Acetate/Viscose Gabardine—Warp

Machine type and capacity	Nominal speed of pulling clamp, in./min.	Acceleration time, sec.	Breaking time, sec.	Breaking load			Elongation at break, %
				Av. for 15 specimens, lb.	Std. deviation, lb.	Error of mean at 95% probability, lb.	
CRE—500 lb. cap.	0.6 (C)	0	58.9	86.5	1.5	±0.9	19
	1.2 (C)	0	30.6	89.5	2.3	1.3	—
	1.2	0.4	30.4	89.0	2.5	1.4	—
	2.0 (C)	0	17.9	91.5	2.3	1.3	18
	2.0	0.6	19.1	91.5	1.4	0.8	20
	4.0 (C)	0	8.5	95.0	1.8	1.0	19
	4.0	1.2	9.5	95.5	1.7	1.0	20
	6.0 (C)	0	5.8	97.0	1.7	1.0	19
	6.0	1.7	6.4	97.0	1.8	1.0	20
	8.0 (C)	0	4.5	98.5	2.3	1.3	17
	8.0	2.1	5.3	98.0	2.7	1.5	17
	10.0 (C)	0	3.7	100.5	1.9	1.1	19
	14.0 (C)	0	2.6	100.5	1.7	1.0	19
	14.0	3.3	3.8	101.5	2.2	1.3	17
CRT (pendulum) 150 lb. cap.	4.4	—	16.1	91.5	2.8	1.6	—
	4.4	—	16.3	92.0	1.8	1.0	—
	12.0	—	5.9	96.0	2.4	1.4	17
	12.0	—	5.9	97.0	1.8	1.0	17

C—Constant speed. CRE machine operated with running start so cross-head was at full speed before any strain was placed on the specimens.

CRT machines operated at 4 in./min. with 8-in. initial clamp separation, as specified in British T.T.S. No. 46, 1957 (draft revision of British Standard 2576); and also when tested on the CRE machine operated at 2 in./min. speed with 8-in. initial clamp separation as specified in T.T.S. No. 46, 1957, as

TABLE V. Viscose Crepe—Warp *

Machine type and capacity	Nominal speed of pulling clamp, in./min.	Acceleration time, sec.	Breaking time, sec.	Breaking load: Av. for 20 specimens, lb.	Breaking load: Std. deviation, lb.	Breaking load: Error of mean at 95% probability, lb.	Elongation at break, %
CRE—200 lb. cap.	1.0	1.7	55	39.1	0.5	±0.2	29
	2.0	0.6	26.2	40.9	0.5	0.2	29
	4.0	1.2	14.4	42.5	0.8	0.4	29
	4.0	1.2	13.9	41.5	1.3	0.6	—
	6.0	1.7	9.2	43.5	0.8	0.4	28
	6.0 (C)	0	8.8	43.4	0.7	0.3	—
	8.0	2.1	7.4	43.7	1.2	0.6	30
	10.0	2.5	6.5	44.4	0.8	0.4	29
	11.0 (C)	0	4.8	46.0	1.1	0.5	—
	14.0 (C)	0	3.9	45.0	1.0	0.5	28
CRT (pendulum) 110 lb. cap.	3.5	—	21.9	41.4	0.9	0.4	31
	12	—	6.2	46.0	1.1	0.5	28
	12	—	6.4	45.5	—	—	—
	12	—	6.3	43.5	1.4	0.7	30

C—Constant speed. CRE machine operated with running start so cross-head was at full speed before any strain was placed on the specimens.

* This table includes values for three separate randomizations of specimens.

TABLE VI. Nylon Taffeta—Warp

Machine type and capacity	Speed of pulling clamp (C) in./min.	Breaking time, sec.	Breaking load: Av. for 15 specimens, lb.	Breaking load: Std. deviation, lb.	Breaking load: Error of mean at 95% probability, lb.	Elongation at break, %
CRE—500 lb. cap.	1.1	57.2	127	1.2	±0.7	↑
	1.1	63.3	126	1.4	0.8	
	1.4	47.3	127.5	1.1	0.6	
	2.0	31.7	128	2.1	1.2	
	2.6	26.1	129.5	1.5	0.9	
	3.0	22.3	132	1.2	0.7	
	4.0	17.0	132.5	1.9	1.1	28–35*
	4.0	16.7	131	1.3	0.7	
	6.0	11.1	132	1.9	1.1	
	8.0	8.4	132.5	1.3	0.7	
	10.0	7.0	132	1.8	1.0	
	14.0	4.6	132	2.0	1.1	
	18.7	3.7	133	1.1	0.6	↓
CRT (pendulum) 300 lb. cap.	4.4	20.8	128	1.5	0.9	↑
	4.4	20.8	129	1.7	1.0	28–30*
	12.0	7.6	132	0.9	0.5	
	12.0	7.5	131	1.4	0.8	↓

C—Constant speed. CRE machine operated with running start so cross-head was at full speed before any strain was placed on the specimens.

* Range of values obtained in two previous randomizations. Elongation not measured in above series. The values were calculated from the actual clamp separation during each test minus the length of originally clamped fabric which flowed out of the proximal ends of the two clamps during the test, which was approximately 0.15 in.

TABLE VII. No. 4 Cotton Duck—Warp

Machine type and capacity	Nominal speed of pulling clamp, in./min.	Acceleration time, sec.	Breaking time, sec.	Breaking load: Av. for 20 specimens, lb.	Breaking load: Std. deviation, lb.	Breaking load: Error of mean at 95% probability, lb.	Elongation at break,* %
CRE—500 lb. cap.	1.0	1.7	75	236	8.8	±4.2	26
	5.0	1.4	14.1	235	9.6	4.6	25
	5.0 (C)	0	14.5	239	7.5	3.6	25
	8.0	2.1	9.6	237	10.9	5.2	24
	10.0	2.5	8.3	238	12.9	6.2	24
	14.0 (C)	0	5.0	237	12.6	6.0	27
	18.0	4.5	5.7	235	11.8	5.7	24
	18.2 (C)	0	4.1	238	11.7	5.6	27
CRT (pendulum) 500 lb. cap.	12.0	—	7.9	238	12.4	6.0	29†

C—Constant speed. CRE machine operated with running start so cross-head was at full speed before any strain was placed on the specimens.

* Calculated from the actual clamp separation during each test minus the length of originally clamped fabric which flowed out of the proximal ends of the two clamps during the test, which was approximately 0.36–0.48 in. with the CRE machine and 0.16 in. with the CRT machine.

† This increase in elongation as compared with tests on the CRE machine is due to approximately 0.1-in. "give" remaining in the clamped specimens on this pendulum machine of horizontal type, where no strain can be readily applied to the specimens during mounting.

TABLE VIII. Rate of Decrease in Breaking Load with Increase in Breaking Time

Br. time interval, sec.	Nainsook—warp		A/V gabardine—warp		Viscose crepe—warp		#4 Duck—weft		Nylon taffeta—warp		#4 Duck—warp	
	lb./sec.	%/sec.*	lb./sec.	%/sec.	lb./sec.	%/sec.	lb./sec.	%/sec.	lb./sec.	%/sec.	lb./sec.	%/sec.
1.6– 3.0	1.36	2.4	—	—	—	—	—	—	—	—	—	—
3 – 5	0.47	0.83	1.6	1.6	—	—	—	—	↑	↑	↑	↑
5 – 7.5	0.30	0.54	0.72	0.75	0.70	1.6	0.6	0.22				
7.5–10	0.16	0.29	0.52	0.55	0.36	0.83						
10 –15	0.08	0.15	0.38	0.41	0.20	0.47	0.5	0.19	0.11	0.08	0	0
15 –20	0.03	0.06	0.26	0.28	0.12	0.29	0.4	0.15				
20 –25	0.025	0.05	0.20	0.22	0.09	0.22						
25 –30	0.025	0.05	0.16	0.18	0.08	0.20	0.3	0.12				
50 –60	0.025	0.05	0.08	0.09	0.045	0.12	0.1	0.04	↓	↓	↓	↓

* Calculated as percentage of the breaking load for the midpoint of time interval.

TABLE IX. Variation of Breaking Time on CRE and CRT Machines Under Some Suggested Operating Conditions

	Breaking time, sec.				
	3-in. Initial clamp separation			8-in. Initial clamp separation*	
	CRT machines		CRE machine	CRT	CRE
	12 in./min.	4 in./min.	2 in./min.	4 in./min.	2 in./min.
Cotton nainsook—warp	3.6	10	8	27	20
#4 Cotton duck—weft	5.3	15	12	40	32
A/V gabardine—warp	5.9	18	18	48	48
Viscose crepe—warp	6.3	19	26	51	70
Nylon taffeta—warp	7.6	23	32	61	85
#4 Cotton duck—warp	7.9	24	36	64	96

* Calculated from data for 3-in. initial clamp separation.

well as at the same speed but with 3-in. initial clamp separation.

Although the slower speeds and/or greater initial clamp separation increase the breaking time, they still result in a wide range of breaking times, and therefore of rates of stretching, for fabric specimens of different elongations. This applies both to the CRE and to the CRT machines.

For those fabrics which showed the greatest change in breaking load with breaking time, the breaking loads obtained on the CRT pendulum machines operated at 12 in./min. and 3-in. initial clamp separa-

TABLE X. Variation of Average Breaking Loads with a CRE Machine over Suggested Breaking Time Limits of 20 ± 3 Sec. and 60 ± 10 Sec.
(Values taken from breaking load vs. breaking time curves)

	Av. br. load, lb.		Difference 17 sec. − 23 sec.		Av. br. load, lb.		Difference 50 sec. − 70 sec.	
	At 17 sec.	At 23 sec.	lb.	%	At 50 sec.	At 70 sec.	lb.	%
Cotton nainsook	54.5	54.4	0.1	0.2	53.7	53.2	0.5	0.9
#4 Cotton duck—weft	262	259	3	1.2	252	250	2	0.8
A/V gabardine	91.8	90.5	1.3	1.4	87.2	85.6	1.6	1.9
Viscose crepe	41.6	41.0	0.6	1.5	39.3	38.4	0.9	2.3
Nylon taffeta	131	130	1.0	0.8	127	125.5	1.5	1.2
#4 Cotton duck—warp	237	237	0	0	237	237	0	0

TABLE XI. Variation of Breaking Times Within Sets of 20 Specimens Tested at Constant Speed Per Set on CRE and CRT Machines

	Breaking time, sec.					
	Approx. 20 sec.				Approx. 60 sec.	
	CRT		CRE		CRE	
	Av.	Range	Av.	Range	Av.	Range
Cotton nainsook—warp	19.2 19.3	18.0–20.4 19.0–19.8	20.3	18.0–22.2	59	55–64
#4 Cotton duck—weft	19.4	18.3–20.5	25.6	23.0–27.0	67	62–72
A/V gabardine—warp	16.1 16.3	15.6–16.9 16.0–16.5	17.9	17.2–19.0	59	56–62
Viscose crepe—warp	21.9	21.1–22.9	26.2	25.4–27.2	55	52–57
Nylon taffeta—warp	20.8 20.8	18.7–22.4 19.2–21.7	22.3 17.0	19.4–23.4 14.8–18.4	57 63	50–63 58–66
#4 Cotton duck—warp	—	—	14.5	13.2–16.1	75	65–81

TABLE XII. Speeds of Pulling Clamp Required to Produce Breaking Times of Approximately 20 Sec. and 60 Sec. for the Fabrics Studied, with 1-in. Ravelled Strips and 3-in. Initial Clamp Separation

		CRE machine		CRT pendulum machines*	
	Av. elongation at break, %	Approx. speed, in./min.		Approx. speed, in./min.	
		For 20-sec. br. time	For 60-sec. br. time	For 20-sec. br. time	For 60-sec. br. time
Cotton nainsook—warp	5–6	0.75	0.25	2.1	0.7
#4 Cotton duck—weft	12–15	1.2	0.4	3.0	1.0
A/V gabardine—warp	17–20	1.8	0.6	3.6	1.2
Viscose crepe—warp	28–31	2.6	0.9	3.8	1.3
Nylon taffeta—warp	28–35	3.3	1.1	4.6	1.5
#4 Cotton duck—warp	24–29	3.6	1.2	4.7	1.6

* The speeds shown for the CRT machines apply to the particular machines and capacities used in this work, since the breaking time at a given speed depends partly on the distance the non-traversing clamp moves for the resultant breaking load.

tion lie on the steepest portion of the breaking load vs. breaking time curves. For these fabrics, the rate of change of breaking load with breaking time is much less for breaking times exceeding 15 sec.; see Table VIII. This evidence supports the oft-suggested idea of reducing the speed of CRT machines below 12 in./min., insofar as it provides one means of securing greater reproducibility of results in different laboratories.

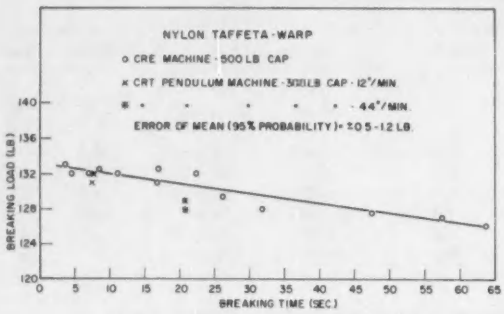

Fig. 8

Table X shows the difference between the average breaking loads which would have been obtained with the CRE machine if the breaking times used were at the outer limits specified for the two constant breaking times presently being considered for fabric testing: 20 ± 3 sec. and 60 ± 10 sec. (see Conclusions).

The maximum percentage difference in the average breaking loads for the limiting breaking times of 17 sec. and 23 sec. was obtained with the viscose crepe and amounted to only 1.5%. The corresponding difference in the average breaking loads for the limiting breaking times of 50 sec. and 70 sec. was 2.3%. The limits set for both the 20-sec. and the 60-sec. breaking times thus appear to be satisfactory with respect to limitation of breaking load variation for all the fabrics tested on the CRE machine.

Table X also shows that, for all the fabrics tested, the rate of change of breaking load with breaking time had become small enough in the region of 20 sec. that no increase in precision would be obtained

TABLE XIII. A Selection of Speeds for CRE and CRT Machines Which Will Provide a 20 ± 3 Sec. Breaking Time with Fabric and Yarn Specimens Covering a Wide Range of Breaking Elongations and Loads

Speed, in./min.	Suitable change-gear ratios for Instron CRE machine	Distance moved by driven clamp in 20 ± 3 sec., in.			Speeds, in./min., required for 20 ± 3 sec. breaking time with breaking elongations of 4–35% *							
					CRE machine				CRT machines and loads 10–90% of capacity			
					Initial clamp separation				Initial clamp separation			
		17 sec.	20 sec.	23 sec.	3 in.	8 in.	10 in.	20 in.	3 in.	8 in.	10 in.†	20 in.†
0.40	5:2	0.11	0.13	0.15								
0.50	2:1‡	0.14	0.17	0.19								
0.60	5:3	0.17	0.20	0.23								
0.75	4:3	0.21	0.25	0.29								
1.0	1:1‡	0.28	0.33	0.38								
{1.2 or	1.2:1‡	{0.34	{0.40	{0.46								
{1.25	—	{0.35	{0.42	{0.48								
1.5	3:2	0.43	0.50	0.58								
2.0	2:1‡	0.57	0.67	0.77								
2.5	5:2	0.71	0.83	0.96								
3.0	3:1	0.85	1.00	1.15								
4.0	5:2	1.13	1.33	1.53								
5.0	2:1‡	1.42	1.67	1.92								
6.0	5:3	1.70	2.00	2.30								
7.5	4:3	2.13	2.50	2.88								
10	1:1‡	2.83	3.33	3.83								
12	1.2:1‡	3.40	4.00	4.60								
15	3:2	4.25	5.00	5.75								
20	2:1‡	5.67	6.67	7.67								

* Apparent elongation, including any flow of specimens from clamped area.
† Calculated for Scott 55/110 lb. machine.
‡ Change-gears presently supplied with Instron Model TT-C.

by going to 60-sec. breaking time on the CRE machine.

Table XI shows that for a given set of fabric specimens tested at a constant speed such as to give an average breaking time of approximately 20 sec., or of 60 sec., the breaking times for individual specimens also fell within the respective limits of ± 3 sec. and ± 10 sec. of the average breaking time for the set, although this is not a specified requirement.

Table XII shows the speeds of the pulling clamp of the CRE and CRT machines which would be necessary with 3-in. initial clamp separation to produce average breaking times of approximately 20 sec. and 60 sec. for the fabrics studied. For an initial clamp separation of 8 in. the CRE speeds would have to be multiplied by a factor of approximately 2.7, and the CRT speeds by somewhat smaller factors.

Conclusions

CRE Machines

Since the breaking load of fabrics is generally affected to greater or lesser degree by their rate of extension, and thus by their breaking time, and since CRE machines provide a readily obtainable wide range of testing speeds, it would seem unwise to set a single operating speed for CRE machines, as this would result in a wide range of breaking times for different fabrics. The adoption of two speeds for use with two respective ranges of specimen elongation would reduce the over-all range of breaking times, but would introduce inequalities in the testing of specimens having elongations close to that forming the limit between the two ranges of elongation. The use of a constant breaking time results in all specimens being stretched to their ultimate elongation (and resultant break) in the same time interval, regardless of differences in extensibility of the material being tested and regardless of the specimen length (as with the 3-in. and 8-in. initial clamp separations now in general use for fabric testing in different countries, or as with the 20-in. distance proposed by ISO for yarn testing). The 8-in. initial clamp separation may, in general, give breaking load values slightly lower than those obtained with the 3-in. separation, but this is not a matter of machine operation.

The adoption of a fixed breaking time for the determination of breaking load of fabrics on CRE machines appears to be logical and to present no operating difficulties.

It is understood that ISO Technical Committee 38 on Textiles is currently considering the proposal of its Sub-Committee on Yarn Testing that a constant breaking time of 20 ± 3 sec. be adopted for single-strand testing of yarns on CRL, CRE, and CRT machines. A 20 ± 3 sec. breaking time has recently been adopted by the Sub-Committee on Textile Test Methods of the Canadian Government Specifications Board as the preferred method for testing the strength of fabrics on CRE and CRT machines by both ravelled-strip and grab methods, and is presently favored by the ASTM for fabric testing. A 60 ± 10 sec. breaking time is specified in Britain for testing fabrics on CRL machines and has also been proposed by ISO/TC38 for testing fabrics on CRL machines.

The work covered by this paper suggests that a constant breaking time of 20 ± 3 sec. is a suitable basis for the measurement of breaking load and breaking elongation of fabrics on constant-rate-of-extension machines. No evidence favoring the much longer breaking time of 60 ± 10 sec. was obtained in this work.

CRT Machines

The adoption of a constant breaking time as the controlling factor when testing fabrics on CRT pendulum machines also appears desirable, since it offers the best means of obtaining reproducible results on different CRT machines and of providing good agreement between the breaking-load values obtained on CRE and CRT machines. A breaking time of 20 ± 3 sec. appears to be as suitable and practical for CRT machines as for CRE machines.

Speeds Required for Testing on 20 ± 3 sec. Breaking-Time Basis with CRE and CRT Machines

Table XIII gives a selection of speeds which will provide a 20 ± 3 sec. breaking time for specimens of different elongations when tested on CRE machines, and also on CRT pendulum machines having ranges of displacement under load of the non-driven clamp which are of the same order as those for the machines used in this work. The ranges of speed which would be necessary with four initial clamp separations commonly used in fabric and yarn testing are indicated in the table.

The only extra work involved in testing by the constant breaking time procedure on CRE machines is preliminary testing of a very few specimens in

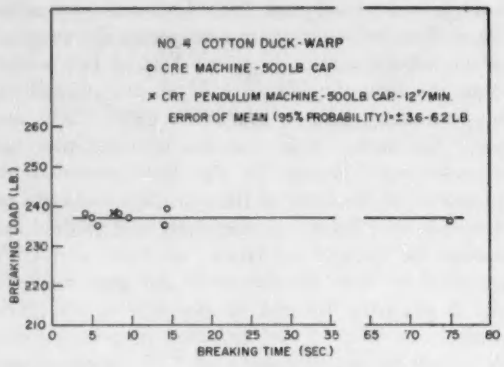

Fig. 9

order to obtain the approximate breaking elongation, if this is not already known. Alternatively, the breaking time can be measured for a few specimens tested at some known speed, and the speed required for 20 ± 3 sec. breaking time can then be calculated.

With CRT machines, the speed required to give a specified breaking time depends on the total movement of the driven clamp, which is the sum of the breaking elongation (inches) of the specimens and the displacement of the non-driven clamp at the breaking load. As with the CRE machines, preliminary testing of a very few specimens will enable easy calculation of the approximate speed required.

For laboratories testing a wide range of fabrics, and possibly of yarns also, on CRE machines which are not equipped with variable-speed cross-head drive, but which provide a number of fixed speeds through the use of readily interchangeable gears, a few extra pairs of change gears may be necessary in addition to those presently supplied with the machines. Some suitable gear ratios for Instron machines are given in Table XIII.

For laboratories testing a wide range of fabrics, and possibly of yarns also, on CRT pendulum machines, variable-speed drive will probably be necessary. Mereness [14] has recently pointed out the probable need for variable-speed drives on many machines used for testing yarns on the constant-breaking-time basis. Where the variety of materials normally tested requires fewer speeds per machine, these can probably be obtained with suitable pulleys and/or multiple-speed drives of the type which provide a limited number of fixed speeds.

CRL Machines

The work covered by this paper did not include the use of CRL machines. It is noted, however, that ISO has suggested the use of a 60-sec. breaking time for fabrics tested on CRL machines, and this is also specified in British Standard 2576, 1955, and in the current draft revision thereof. On the other hand, ISO/TC38 has proposed a 20-sec. breaking time for yarns tested on CRL, CRE, and CRT machines. The range of elongations to be coped with in fabric testing is not too different from that involved in yarn testing, which suggests that the 20-sec. breaking time proposed for yarn testing should be equally suitable for fabric testing with CRL machines. However, it is possible that the much longer breaking time of 60 sec. suggested for fabric testing is necessitated by the mechanics of the particular CRL machines now in use.

Acknowledgment

The authors are indebted to Miss H. Lacourciere for assistance in preparing the specimens for test, to Mr. C. H. Bayley for helpful discussions, and to Bruck Mills Ltd., Duplan of Canada Ltd., and the Empire Cotton Division of Wabasso Cotton Company Ltd., for supplying four of the fabrics used in this work.

Literature Cited

1. Barr, G., Aeronautical Research Committee (Britain), Report 757 (1920).
2. Barr, G., Second Report of the Fabrics Co-Ordinating Research Committee, Dept. of Scientific and Industrial Research (Britain), 140 (1930).
3. Bayes, A. W., *J. Textile Inst.* **36**, P182 (1945).
4. Cryer, N., "A Comparison of the Strip and Grab Methods of Determining the Tensile Strength of Woven Fabrics," Fifth Commonwealth Defence Conference on Clothing and General Stores, Canada (1956).
5. Fabrics Co-Ordinating Research Committee (Britain), First Report of, Appendix III, 29 (1925).
6. Goodings, A. C., "The Effect of Some Variable Factors on the Breaking Strength of Textile Fabrics," Third Commonwealth Conference on Development, Design and Inspection of Clothing and General Stores, United Kingdom (1950).
7. *J. Textile Inst.* **35**, S7 (1944).
8. *J. Textile Inst.* **40**, S1 (1949).
9. *J. Textile Inst.* **48**, P680 (1957).
10. Walen, E. D., *Proc. ASTM* **16**, I, 379 (1916).

11. Walen, E. D., *Proc. ASTM* **18**, I, 370 (1918).
12. Larose, P., *J. Textile Inst.* **32**, T167 (1941).
13. Lewis, W. S., *Proc. ASTM* **16**, I, 366 (1916).
14. Mereness, H. A., TEXTILE RESEARCH JOURNAL **28**, 351 (1958).
15. Midgley, E., *Shirley Inst. Memoirs* **2**, 137 (1923).
16. Peirce, F. T., *J. Textile Inst.* **18**, T481 (1927).
17. "Schedule 4-GP-2, Methods of Testing Textiles," Canadian Government Specifications Board, National Research Council, Ottawa, Canada.
18. Schwartz, E. R., ASTM Standards on Textile Materials, 485 (1948).
19. Scott, H. L., *Textile World* **60**, 3006 (1921).

Manuscript received July 29, 1958.

Rheological Interpretation of the Mechanism of Crease Recovery of Fiber[1]

Hiroshi Sobue and Kenkichi Murakami[2]

Faculty of Engineering, Tokyo University, Japan and
The Textile Research Institute of Japanese Government, Yokohama, Japan

Abstract

In an attempt to interpret the mechanism of creasing and the recovery therefrom, a theoretical study of the visco-elastic behavior of fibers and/or filaments has been made. The relationship between crease angle of fiber, temperature, and creasing time is discussed theoretically and experimentally.

Introduction

The problem of crease resistance is very important for fabrics, especially for cellulosic fabrics like rayon, cotton, and linen, and numerous types of aftertreatment are now being tested as a means of creaseproofing. The mechanism of crease recovery in fabrics has been studied by researchers such as Borghetty [1], Buck and McCord [2], Cooke [3], Gagliardi and Gruntfest [5], Hamburger [7], Nuessle [5], Steele [13], and others. However, a fundamental theoretical solution of the mechanism from a rheological standpoint has not been attained, and an attempt is made by the present writers to clarify this issue.

When the relation between fabric structure and its crease recovery is under consideration, obviously the three elements of fiber, yarn, and fabric should be separated from one another. A theoretical treatment of wrinkle recovery of yarn and fabric is difficult because the factors involved in them are many and complicated, although some of these have been studied by Hamburger and others [8], Ikeda and Okajima [9], Go and Suzuki [6], Steele [12], Jameson, Whittier, and Shiefer [10], and Krasny, Mallory, Phillips, and Sookne [11]. To simplify the situation as much as possible, the present theoretical study has been restricted to single filaments or multifilament yarns having no twist.

Discussion

Visco-Elastic Behavior of Filaments During Creasing

Two assumptions are made in this discussion. One is that the cross sections of all filaments are perfect circles; the other is that the filaments are uniform throughout.

In bending a filament through an angle of 180°, as shown in Figure 1, no change occurs at the central plane shown by the dotted line, but the portion outside of this plane is elongated while the inner portion is in compression. The effects of elongation and compression by such bending will be assumed to be confined only to the left parts of

[1] This paper is partially based upon a dissertation submitted by K. Murakami for the degree of Doctor of Engineering at Tokyo University.

[2] Present address: Department of Chemistry, Princeton University, Princeton, N. J.

the straight line $\overline{pp'}$. Then from a derivation which is to follow we obtain:

$$\frac{L_1}{L_0} = \frac{\frac{(8+\pi)}{16} \cdot \pi r}{\frac{\pi r}{2}} = \frac{8+\pi}{8} = 1.39 \qquad (1)$$

where the diameter of the filament is r, the length of the central plane, ABC, is L_0, and the average length of outer parts from this plane (from $x = r/2$ to r) is L_1. This equation is derived from Equations 3 and 5 below, assuming that the absolute value of elongation in one part of the outside is equal to that of compression of the inner side, where both parts are symmetrical with the central line ABC.

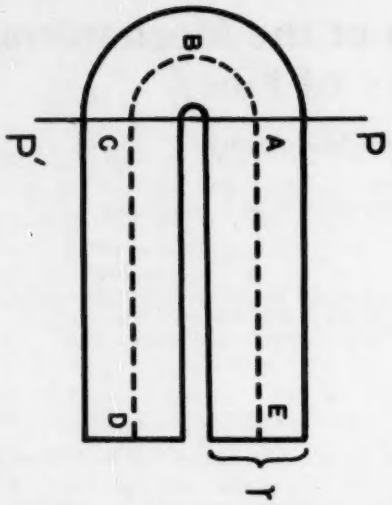

Fig. 1. Creased state of single filament bent to 180°.

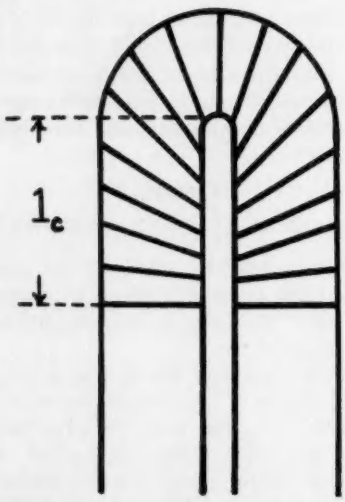

Fig. 2. The range of the effects of elongation and compression on single filament bent to 180°.

From Equation 1 it will be seen that the average percentage elongation of the outer parts of the filament is nearly 40%. However, it is clear that even non-resin treated rayon does not have as high an extensibility as 40%. This discrepancy is obviously due to the assumption that the effects of elongation and compression on a filament are limited only to the left side of $\overline{pp'}$. Naturally, the idea that similar effects may be seen for a certain extent at the right side of $\overline{pp'}$ follows, and this fact is confirmed by observing the double refraction of creased filament samples. The additional length influenced by elongation or compression is indicated as l_c in Figure 2. It was observed in this investigation that l_c was 80–100 μ for a 5-den. filament of viscose rayon. This value may not be reliable, however, in view of possible experimental errors arising from the difficult measurement involved. Besides, the value of l_c will vary with sample thickness, finishing treatment, and the nature of the fiber. Fortunately, as indicated below, a general formula for various kinds of fibers can be obtained in which l_c cancels out in the course of calculations. The part shown by a thick line of the letter U set upside down in Figure 3A is the central plane. Based upon the assumption previously mentioned, the compression of the inner parts from this plane being neglected, the average values of total elongated length of the outer parts from this plane in the state of Figure 3 are calculated. Naturally, these average values are to be regarded equal to those of the elongated filament in linear form. At first, calculations are made for the case of Figure 3A; the original length before elongation is expressed as l_0 and the length elongated to some extent in linear form is expressed as l_e. The ratio of elongation $\gamma_{t=0}$ may then be expressed by

$$\gamma_{t=0} = \frac{l_e}{l_0} - 1 \qquad (2)$$

It may be questioned what value shall be given to l_c in the case of filament bent to angle 180° as shown in Figure 3A. Here, the length of the central plane, E′A′B′C′D′ is assumed to be equal to l_0.

Then the resulting formula becomes

$$l_0 = 2l_c + \frac{r}{2}\pi \tag{3}$$

As the value equal to l_e is expressed by the integral average value of all elongated outer parts from the central plane in Figure 3A, calculations can be carried on as given below. The length of the outer side having the distance x from the central plane is as follows:

$$2l_c + \left(\frac{r}{2} + x\right)\pi$$

Hence

$$l = \int_0^{r/2} \left\{\left(\frac{r}{2} + x\right)\pi + 2l_c\right\} dx \Big/ \frac{r}{2} \tag{4}$$

The value of l corresponds to the average of all elongated outer parts at $y = 0$ along the x-axis as shown in Figure 3A, the cross section of the filament. Furthermore, when the total average value, l_e, is calculated from $y = -\gamma/2$ to $\gamma/2$, the following result is obtained:

$$\begin{aligned} l_e &= \int_{-r/2}^{r/2} \int_0^{\sqrt{(r/2)^2 - y^2}} l(x) \\ &= \int_{-r/2}^{r/2} \int_0^{\sqrt{(r/2)^2 - y^2}} \left[\left\{2l_c + \pi\left(\frac{r}{2} + x\right)\right\} \Big/ r\sqrt{\left(\frac{r}{2}\right)^2 - y^2}\right] dxdy \\ &= 2l_c + \frac{(8+\pi)}{16} \cdot \pi r \end{aligned} \tag{5}$$

Then, considering the elongation Δl_e, we obtain

$$\begin{aligned} \Delta l_e = l_e - l_0 &= \left\{2l_c + \frac{(8+\pi)}{16} \cdot \pi r\right\} - \left(2l_c + \frac{r}{2}\pi\right) \\ &= \frac{\pi^2}{16} \cdot r \end{aligned} \tag{6}$$

The calculations given below are made for the case of the angle becoming ψ as shown in Figure 3B. If the total average value of all elongated lengths in the state of Figure 3B is expressed as l_ψ, and calculated in the same way as already described, the following is obtained:

$$\begin{aligned} l_\psi &= \int_{-r/2}^{r/2} \int_0^{\sqrt{(r/2)^2 - y^2}} \left[\left\{2l_c + (\pi - \psi)\left(\frac{r}{2} + x\right)\right\} \Big/ r\sqrt{\left(\frac{r}{2}\right)^2 - y^2}\right] dxdy \\ &= 2l_c + \frac{(8+\pi)(\pi - \psi)}{16} r \end{aligned} \tag{7}$$

When the length elongated from the original state in this case is expressed as Δl_ψ, the result obtained may be expressed

$$\begin{aligned} \Delta l_\psi = l_\psi - l_\psi &= \left\{2l_c + \frac{(8+\pi)(\pi - \psi)}{16}\right\} - \left\{2l_c + \frac{r}{2}(\pi - \psi)\right\} \\ &= \frac{\pi(\pi - \psi)}{16} r \end{aligned} \tag{8}$$

Since l_ψ is the original length shown in Figure 3B

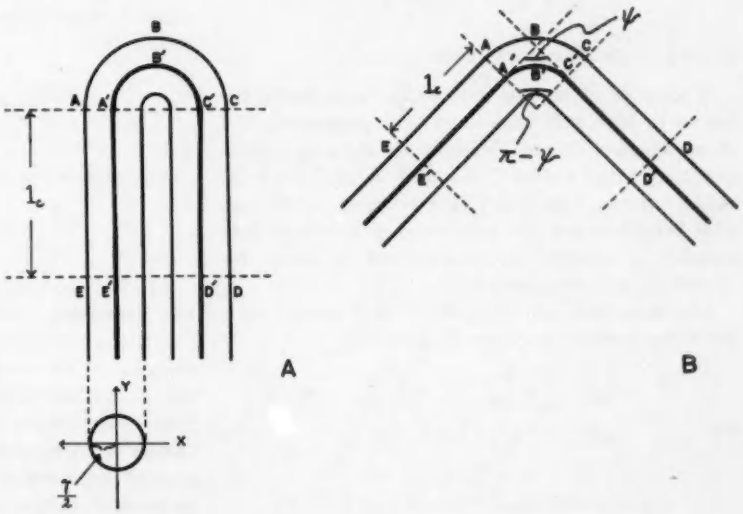

Fig. 3. Mechanical analysis of creased single filament.

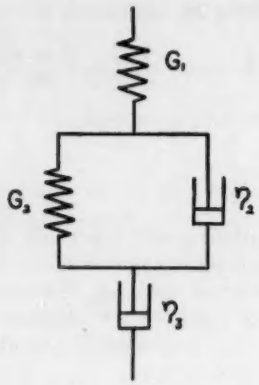

Fig. 4. Voigt's four-element model.

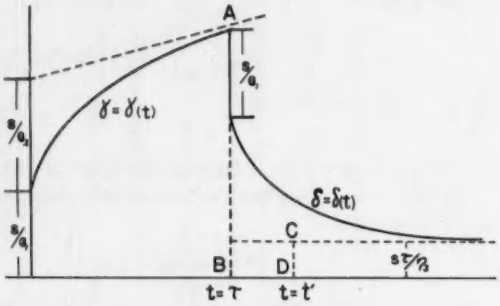

Fig. 5. Creep of a fiber and its recovery curve.

indicated by the curve E'A'B'C'D', it follows that

$$l_\psi = 2l_c + \frac{r}{2}(\pi - \psi)$$

Creep and Its Recovery in Fiber Creasing

A number of models indicating visco-elastic behavior of high polymers have been suggested. Of them, Maxwell's model is useful for showing relaxation and Voigt's model is found helpful for indicating creep. The Voigt four-element model was used here, because this was found to be simple and suitable in treating the mechanism of crease recovery as mentioned below.

The equations indicating the state of motion with the Voigt's model is generally given by

$$S = G_k\gamma_k + \eta_k\frac{d\gamma_k}{dt} \quad (k = 1, 2, \cdots n)$$

and

$$\gamma = \sum_{k=1}^{n}\gamma_k \tag{9}$$

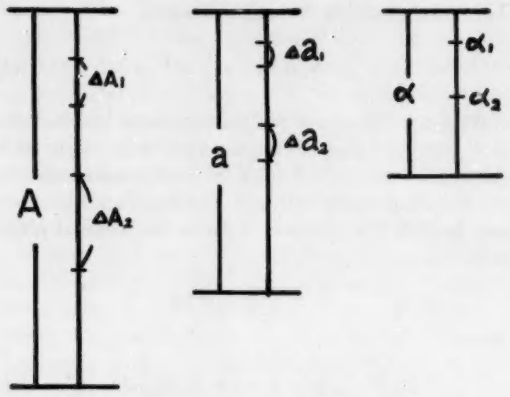

Fig. 6. The changes of the length by elongation of uniform single filament.

where S = load, γ = elongation, n = number of models, G = elastic constant, and η = viscous constant. In the model of Figure 4, $n = 3$, $\eta_1 = 0$, and $G_3 = 0$ are given. Therefore, differential equations are shown as follows:

$$\gamma = \gamma_1 + \gamma_2 + \gamma_3$$
$$S = G_1\gamma_1$$
$$S = G_2\gamma_2 + \eta_2\frac{d\gamma_2}{dt}$$
$$S = \eta_3\frac{d\gamma_3}{dt} \tag{10}$$

Differential equations can be solved by substituting $\gamma_1 = S/G_1$, $\gamma_2 = 0$, and $\gamma_3 = 0$ at the initial stage of the motion; thus Equation 11 below is obtained:

$$\gamma_{(t)} = S\left[\frac{1}{G_1} + \frac{1}{G_2}(1 - e^{-t/\lambda_2}) + \frac{t}{\eta_3}\right] \tag{11}$$

where $\lambda_2 = \eta_2/G_2$. When the fiber is unloaded after $t = \tau$ in Figure 5, Equation 11 becomes

$$\delta(t) = S\left[\frac{1}{G_2}(1 - e^{-\tau/\lambda_2})e^{-(t-\tau)/\lambda_2} + \frac{\tau}{\eta_3}\right] \tag{12}$$

Precisely speaking, Equation 11 in Figure 5 gives the increasing curve in the range of $0 \leqq t \leqq \tau$. On the other hand, Equation 12 represents the decrease in the range of $\tau \leqq t$. So it is clear that the elongation becomes S/G_1 right after loading, then creep occurs for $t = \tau$, and after unloading, elongation S/G_1 is at once recovered, followed by a gradual recovery approaching the constant $S\tau/\eta_3$. In general, in the case of an original uniform fiber

(Figure 6) when an original length a becomes A after elongation, or A becomes a after shrinking, given arbitrarily minute portions of α_1, α_2, then Δa_1, Δa_2 in the fiber shrunk to a and ΔA_1, ΔA_2 in those elongated to A are obtained respectively. These may be expressed as

$$\frac{\Delta a_1}{\Delta A_1} = \frac{\Delta a_2}{\Delta A_2} = \cdots = \frac{\Delta a_i}{\Delta A_i} = \cdots = \frac{\Delta a_n}{\Delta A_n} = \frac{a-\alpha}{A-\alpha} \quad (13)$$

This concept can be applied to the case of creasing fiber as mentioned before. The ratio of elongation in both cases of Figures 3A and 3B is here regarded as $\Delta l_\psi / \Delta l_e$. On the other hand, $\Delta a_i / \Delta A_i$ means the ratio arbitrarily taken in a uniform fiber. Then we naturally arrive at

$$\frac{\Delta l_\psi}{\Delta l_e} = \frac{\Delta a_i}{\Delta A_i} = \frac{a-\alpha}{A-\alpha}$$

When Equations 6 and 8 are substituted into the above equation, it becomes

$$\frac{\frac{\pi(\pi-\psi)r}{16}}{\frac{\pi^2 r}{16}} = \frac{a-\alpha}{A-\alpha}$$

$$\frac{\pi-\psi}{\pi} = \frac{a-\alpha}{A-\alpha} \quad (14)$$

Now, the total length after loading for $t = \tau$ shown in Figure 5 becomes $L\{1+\gamma(\tau)\}$, the original length being assumed L. Similarly, the length of fibers unloaded and after $t = t'$ is regarded as $L\{1+\delta(t')\}$. We obtain

$$\frac{\delta(t')}{\gamma(\tau)} = \frac{a-\alpha}{A-\alpha} = \frac{\pi-\psi_t}{\pi} \quad (15)$$

In the case of $t = \tau$, or right after unloading, we obtain

$$\frac{\gamma(\tau) - S/G_1}{\gamma(\tau)} = \frac{\delta(\tau)}{\gamma(\tau)} = \frac{\pi-\psi_0}{\pi} \quad (16)$$

In the case of equilibrium being attained, or $t = \infty$ after unloading, we obtain

$$\frac{S\tau/\eta_3}{\gamma(\tau)} = \frac{\pi-\psi_\infty}{\pi} \quad (17)$$

Crease angles ψ_0, ψ_t, and ψ_∞ which satisfy Equations 16, 15, and 17 respectively are indicated in Figure 7. When $\delta(t')/\gamma(\tau) = \sigma$ is given, where σ means the ratio of recovery length $\delta(t')$ to the maximum creep length $\gamma(\tau)$, Equation 18 is obtained. From Equation 15, it follows that

$$\frac{\pi-\psi_t}{\pi} = \frac{\delta(t)}{\gamma(\tau)} = \sigma \quad (18)$$

Here, $\delta(t')$ is altered to $\delta(t)$ for convenience in operations, which causes no trouble in the process of calculations hereafter. Then Equation 18 becomes

$$\pi - \psi = \sigma\pi$$
$$\therefore \quad \psi = \pi(1-\sigma) \quad (19)$$

Equation 19 indicates the relationship of mechanical properties between bending form and linear form of the same fiber. The creased state of a filament at some distance from the center point P in Figure 8 should naturally be taken into account in studying the crease of a fiber, because while the creased form of the fiber as shown in Figure 8 is regarded as a general case, the forms of Figures 3A and 3B are thought to be the special case of Figure 8; that is, the distance R from the point P is negligibly small in Figures 3A and 3B. Calculating for Figure 8A can be handled in the same way as that of Figure 3A for bending to 180°.

$$l_e = \int_{-r/2}^{r/2} \int_0^{\sqrt{(r/2)^2-y^2}} l(x)$$
$$= \int_{-r/2}^{r/2} \int_0^{\sqrt{(r/2)^2-y^2}} \left[\left\{ 2l_e + \pi\left(\frac{r}{2} + x + R\right) \right\} \Big/ r\sqrt{\left(\frac{r}{2}\right)^2 - y^2} \right] dxdy$$
$$= 2l_e + \frac{(8r + \pi r + 8R)}{16} \cdot \pi$$

Then the elongation Δl_e will be

$$\Delta l_e = l_e - l_0 = \left\{ 2l_e + \frac{(8r + \pi r + 8R)}{16} \cdot \pi \right\} - \left\{ 2l_e + \left(\frac{r}{2} + R\right)\pi \right\} = \frac{\pi r - 8R}{16} \cdot \pi$$

Fig. 7. Crease angles of single filament varied.

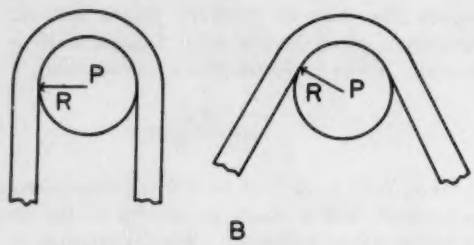

Fig. 8. Creased state of single filament at some distance from the point of center P.

Next, the case of Figure 8B becomes

$$l_\psi = \int_{-r/2}^{r/2} \int_0^{\sqrt{(r/2)^2-y^2}} \left[\left\{ 2l_c + (\pi - \psi) \times \left(\frac{r}{2} + x + R \right) \right\} \Big/ r\sqrt{\left(\frac{r}{2} \right)^2 - y^2} \right] dxdy$$

$$= 2l_c + \frac{(8r + \pi r + 8R)}{16} (\pi - \psi)$$

The elongation Δl_ψ becomes

$$\Delta l_\psi = \left\{ 2l_c + \frac{(8r + \pi r + 8R)}{16} (\pi - \psi) \right\} - \left\{ 2l_c + \left(\frac{r}{2} + R \right) (\pi - \psi) \right\}$$

$$= \frac{\pi r - 8R}{16} (\pi - \psi)$$

Therefore

$$\frac{\Delta l_\psi}{\Delta l_c} = \frac{\frac{(\pi r - 8R)}{16} (\pi - \psi)}{\frac{(\pi r - 8R)}{16} \pi} = \frac{\pi - \psi}{\pi} = \frac{\Delta a_i}{\Delta A_i}$$

$$= \frac{a - \alpha}{A - \alpha} = \sigma$$

This value is equal to that of Equation 14. In other words, Equation 19 can be applied in every case, independent of the distance R. When the value of $\delta(t)$ in Equation 12 and that of $\gamma(\tau)$ in Equation 11 are substituted into Equation 18, we have

$$\sigma(t, \tau) = \frac{\delta(t)}{\gamma(t)} = \frac{\frac{1}{G_2}(1 - e^{-\tau/\lambda_2})e^{-(t-\tau)/\lambda_2} + \tau/\eta_3}{\frac{1}{G_1} + \frac{1}{G_2}(1 - e^{-\tau/\lambda_2}) + \tau/\eta_3} \quad (20)$$

Accordingly, when Equation 19 is substituted by Equation 20, it follows that

$$\psi(t, \tau) = \pi \left\{ 1 - \frac{\frac{1}{G_2}(1 - e^{-\tau/\lambda_2})e^{-(t-\tau)/\lambda_2} + \tau/\eta_3}{\frac{1}{G_1} + \frac{1}{G_2}(1 - e^{-\tau/\lambda_2}) + \tau/\eta_3} \right\}$$

$$= \pi \cdot \frac{\frac{1}{G_1} + \frac{1}{G_2}\{1 - e^{-\tau/\lambda_2} - e^{\tau/\lambda_2}(1 - e^{-\tau/\lambda_2})\, e^{-t/\lambda_2}\}}{\frac{1}{G_1} + \frac{1}{G_2}(1 - e^{-\tau/\lambda_2}) + \tau/\eta_3} \quad (21)$$

The complicated Equation 21 can be simplified as follows:

$$\psi(t, \tau) = \pi(a - be^{-t/\lambda_2}) \quad (22)$$

where

$$a = \left\{ \frac{1}{G_1} + \frac{1}{G_2}(1 - e^{-\tau/\lambda_2}) \right\} \Big/ \left\{ \frac{1}{G_1} + \frac{1}{G_2}(1 - e^{-\tau/\lambda_2}) + \frac{\tau}{\eta_3} \right\}$$

$$b = \frac{1}{G_2} e^{\tau/\lambda_2}(1 - e^{-\tau/\lambda_2}) \Big/ \left\{ \frac{1}{G_1} + \frac{1}{G_2}(1 - e^{-\tau/\lambda_2}) + \frac{\tau}{\eta_3} \right\}$$

Both a and b are constants under given conditions. Generally speaking, crease angle ψ includes four variable factors of t (time), τ (creasing time), T (temperature), and humidity. Figure 9 is obtained when τ, T, and relative humidity are constants. From the foregoing it will be seen that the visco-elastic behavior of the crease of a fiber is theoretically established. It may be easily assumed that while the derivation of Equation 22 is based upon the Voigt four-element model, we shall have the same, or an equation approximate to Equation 22 when the model, which indicates the behavior of fiber creep more actually than those used in this report, is employed.

Relationship Between Fiber Creasing, Temperature, and Time

In this section, experimental results will be compared with the theoretical values obtained above. A sample of a continuous filament of viscose rayon was employed, and the crease measurement of E. Elöd and P. Etzkorn [4] was adopted.

A sample fiber previously relaxed on a plate in a desiccator under given relative humidity for 2 hr. was used. One end of the fiber was then fixed by adhesives to a point on a glass plate 0.7–0.8 mm. thick. After the fiber was conditioned, a given weight (here, 20 g./100 den. was used) was attached to one end of the fiber to provide tension. The fiber was then wound around the glass plate (1–2 mm. between coils) and the end secured with adhesives. After the fiber had been left in this condition for the required time, it was cut along the length of the plate glass to measure its crease angle. In the case of relative humidity, creasing time, and temperature T being constant, both a and b are constants, and Equation 22 becomes

$$\psi_{(t)} = \pi(a - be^{-t/\lambda}) \tag{23}$$

When $t = 0$

$$\psi_{(0)} = \pi(a - b) \tag{24}$$

and when $t = \infty$

$$\psi_{(\infty)} = \pi a \tag{25}$$

By actual measurement of the crease angle $\psi_{(0)}$ right after unloading, and $\psi_{(\infty)}$ in equilibrium, the values of a and b can be easily derived from Equations 24 and 25. On the other hand, Equation 23 may be modified to

$$\lambda = \frac{t}{2.303 \log \dfrac{\pi b}{\pi a - \psi}} \tag{26}$$

Then, λ is calculated by substituting ψ, t being experimentally known. Thus the effect of the factors τ and T on λ can be measured.

Experimental Results on the Sample of Viscose Rayon

When temperature T is constant (25° C.), and creasing time τ is variable, Table I can be obtained. From the results described, it will be seen that crease angle ψ is decreased as τ is increased, and conversely relaxation time λ is increased. When creasing time τ is constant and temperature T is variable, the results are as given in Table II.

It is also found that the increase of crease angle ψ at longer times grows remarkably while temperature becomes higher. In this case, the value of λ has the tendency of decreasing with increase of

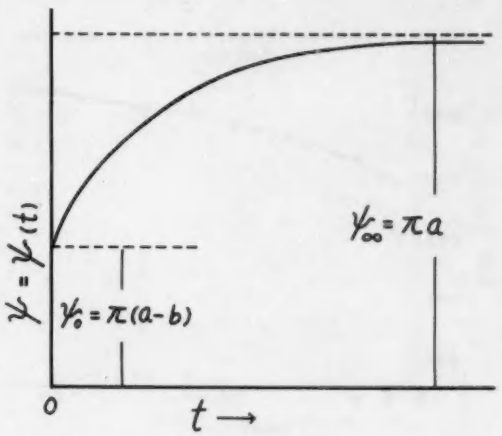

Fig. 9. Theoretical curves of $\psi(t) = \pi(a - be^{-t/\lambda})$.

TABLE I. Crease Angles of Rayon Fibers as a Function of Time at 25° C. and 65% Relative Humidity

Time, min.	(a) τ = 5 min. ψ, radians	λ	(b) τ = 10 min. ψ, radians	λ	(c) τ = 30 min. ψ, radians	λ	(d) τ = 60 min. ψ, radians	λ
0.5	0.95	3.17	0.86	3.18	0.73	2.75	0.64	3.18
1.0	1.01	3.33	0.93	3.10	0.78	2.97	0.74	(2.00)
1.5	1.08	2.99	0.98	3.28	0.83	2.89	0.75	2.70
2.0	1.13	2.97	1.04	3.07	0.87	2.88	0.77	3.11
2.5	1.18	2.85	1.13	2.40	0.89	3.15	0.79	3.34
3.0	1.22	2.78	1.14	2.73	0.93	2.91	0.83	3.07
4.0	1.30	(2.39)	1.18	2.97	0.96	3.20	0.87	3.11
5.0	1.34	(2.29)	1.22	2.97	0.99	3.25	0.89	3.35
6.0	1.37	(2.09)	1.24	3.14	1.01	3.35	0.92	3.16
10.0	1.39	2.53	1.30	3.03	1.06	3.28	0.96	3.34
πa =	1.40		1.32		1.08		0.98	
πb =	0.53		0.54		0.42		0.40	
Average λ		2.95		2.99		3.06		3.15

temperature. We know, however, that the value of λ calculated from Equation 26 by substituting t and ψ causes small deviations in some parts of Tables I and II. The causes of these deviations may be considered to be due to the following assumptions.

1. Elongation and compression in symmetrical portions by the central plane occur at the same ratio, though the direction is opposite.

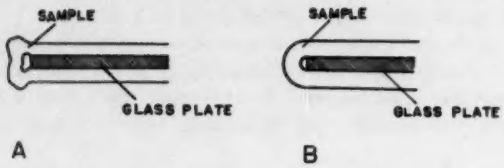

Fig. 10. Deformation in creasing. A: actual state; B: ideal state.

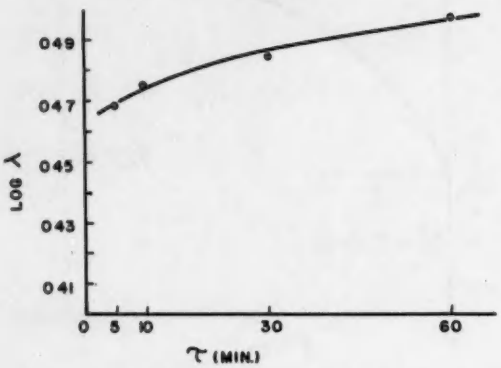

Fig. 11A. Relationship between creasing time τ and log λ.

2. Cross section of the filament is a perfect circle.

3. Deformation shown in Figure 10A occurs in creasing.

The relation of $\log \lambda \sim \tau$ and $\log \lambda \sim T$ is described in Figures 11A and 11B. The factor τ is apparently connected with E_{act} in the Arrhenius relationship $\lambda = Ae^{E_{act}/RT}$, since $\log \lambda$ increases with increasing τ and $\log \lambda \sim 1/T$ is linear in accord with the equation.

Comparison of Theoretical and Experimental Results

If Equation 23 is differentiated by $\log t$, we obtain

$$\psi'(\log t) = \frac{d\psi}{d \log t} = 2.303 \frac{\pi b}{\lambda} te^{-t/\lambda} \qquad (27)$$

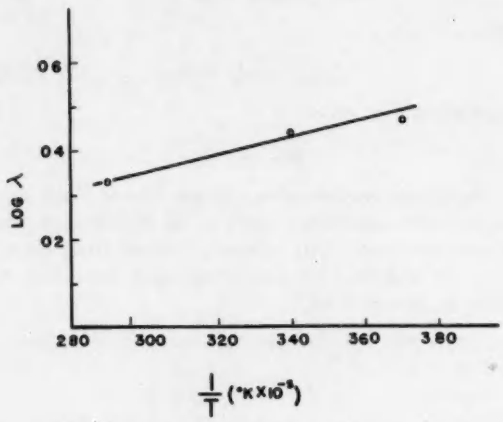

Fig. 11B. Relationship between temperature T and log λ.

TABLE II. Crease Angles of Rayon Fibers as a Function of Time at Creasing Time 5 Min. and 65% Relative Humidity

Time, min.	(a) T = 70° C. ψ, radians	(a) T = 70° C. λ	(b) T = 25° C. ψ, radians	(b) T = 25° C. λ	(c) T = 0° C. ψ, radians	(c) T = 0° C. λ
0.5	1.31	2.16	0.95	3.17	0.79	3.18
1.0	1.48	1.95	1.01	3.33	0.84	3.42
1.5	1.57	2.16	1.08	2.99	0.93	2.65
2.0	1.66	2.18	1.13	2.97	0.94	3.17
2.5	1.73	2.20	1.18	2.85	1.03	(2.43)
3.0	1.81	2.06	1.22	2.78	1.04	2.63
4.0	1.88	2.15	1.30	(2.39)	1.08	2.76
5.0	1.94	2.07	1.34	(2.29)	1.12	2.63
6.0	1.97	2.08	1.37	(2.09)	1.14	2.68
10.0	2.02	2.22	1.39	2.53	1.17	3.17
πa =	2.02		1.40		1.19	
πb =	0.90		0.53		0.47	
Average λ		2.12		2.95		2.96

Furthermore, upon differentiation of Equation 27 by log t we have

$$\psi''(\log t) = \frac{d^2\psi}{d(\log t)^2} = 5.304\frac{\pi b}{\lambda}t\left(1 - \frac{t}{\lambda}\right)e^{-t/\lambda} \quad (28)$$

Equations 27 and 28 help us to picture the curves of equations $\psi = \psi(\log t)$ and $\psi' = \psi'(\log t)$ shown in Figure 12. The degree of fit of experimental data to the theoretical curves is shown in Figures 13 and 14. Actual values of the constants a, b, and λ were substituted into Equations 23 and 27. The values of these constants were deduced from the experimental data of Tables Ia and Id. The points of Figure 13 are the experimental values of ψ in Table Ia and points in Figure 14 correspond to experimental values from Table Id.

It is easily understood from the above figures that the value of λ can be also obtained by picturing the relationship of $\psi' \sim \log t$ instead of using Equation 26.

Summary

The mechanism of crease recovery of a single fiber was discussed from a rheological standpoint. By use of several assumptions, Equation 22 was theoretically developed for expressing the value of crease angle as a function of time. The dependence of crease angle on creasing time and temperature T at constant humidity was followed experimentally.

By use of another relationship (Equation 26), values of the relaxation time λ were found. The effects of τ and T on λ became clear and were found to be connected with the Arrhenius relationship.

Finally, experimental data of crease angle were compared with theoretically developed equations relating crease angle with log t.

Literature Cited

1. Borghetty, H. C., *Am. Dyestuff Reptr.* **45**, 518 (1956); Borghetty, H. C. and Fornelli, D., *Textile World* **105**, 102 (December 1955).
2. Buck, Jr., G. S. and McCord, F. A., TEXTILE RESEARCH JOURNAL **19**, 216 (1949).
3. Cooke, T. F., Dusenbury, J. H., Kienle, R. H., and Lineken, E. E., TEXTILE RESEARCH JOURNAL **24**, 1015 (1954).
4. Elöd, E. and Etzkorn, P., *Angew. Chem.* **51**, 45 (1938).
5. Gagliardi, D. D. and Gruntfest, I. J., TEXTILE RESEARCH JOURNAL **20**, 180–8 (1950); Gruntfest, I. J. and Gagliardi, D. D., *Ind. Eng. Chem.* **41**, 760–4 (1949); Gagliardi, D. D. and Nuessle, A. C., *Am. Dyestuff Reptr.* **40**, 409 (1951); Gagliardi, D. D. and Nuessle, A. C., *Am. Dyestuff Reptr.* **39**, 12 (1950).
6. Go, Y. and Suzuki, M., *Chemistry of High Polymers (Japan)* **13**, 484–490 (1956); **13**, 507–518 (1956).
7. Hamburger, W. J., TEXTILE RESEARCH JOURNAL **15**, 169 (1945); **18**, 102 (1948).
8. Hamburger, W. J., Platt, M. M., and Morgan, H. M., TEXTILE RESEARCH JOURNAL **22**, 695–729 (1952).

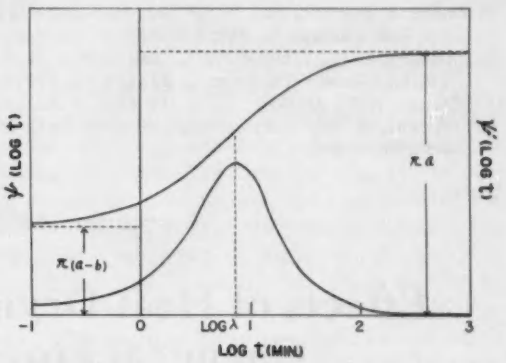

Fig. 12. Theoretical curves of $\psi(\log t)$ and $\psi'(\log t)$.

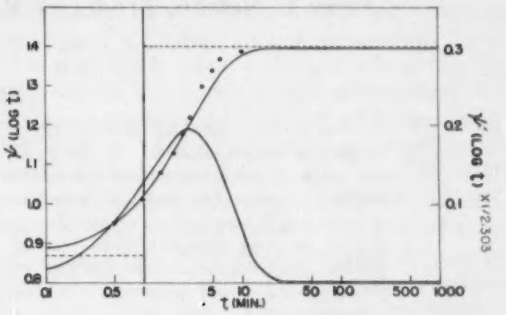

Fig. 13. Comparison of theoretical curve $\psi(\log t)$ with experimental data (A).

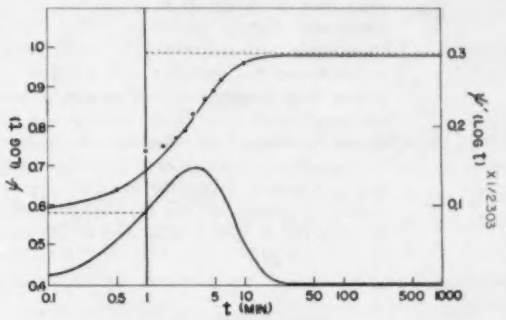

Fig. 14. Comparison of theoretical curve $\psi(\log t)$ with experimental data (B).

9. Ikeda, S. and Okajima, S., *J. Soc. Tex. and Cellulose Ind. (Japan)* **11**, 28–31 (1955).
10. Jameson, L. H., Whittier, B. L., and Shiefer, H. F., TEXTILE RESEARCH JOURNAL **22**, 599–608 (1952).
11 Krasny, J. F., Mallory, G. D., Phillips, J. K., and Sookne, A. M., TEXTILE RESEARCH JOURNAL **25**, 499–506 (1955).
12. Steele, R., TEXTILE RESEARCH JOURNAL **26**, 739–744 (1956).
13. Steele, R. and Browne, C. L., *Am. Dyestuff Reptr.* **45**, 525–8 (1956); Steele, R. and Giddings, Jr., L. E., *Ind. Eng. Chem.* **48**, 110–4 (1956).

Manuscript received April 26, 1958.

Effects of Heat-Drying on the Physical and Chemical Properties of Cottons

Mary L. Nelson, Frederick R. Andrews, and James N. Grant

Southern Regional Research Laboratory,[1] New Orleans, Louisiana

Abstract

The poor spinnability of some lots of gin-dried cotton has been attributed to overheating of the seed cotton. To determine what changes in the lint might be responsible, two series of gin-dried cottons and one series that was flash-heated in the laboratory were studied. Appropriate physical and chemical properties of the lint were measured, such as fiber length distribution, single-fiber and fiber-bundle strength and elongation, moisture regain, nepping potential, fiber friction, microscopical swelling, alkali swelling, wettability, fluorescence, copper number, carboxyl content, pH, infrared spectra, and wax properties. Limited spinning and weaving tests allowed yarn and fabric properties to be measured.

Nearly all tests showed no evidence of radical permanent changes in lint properties. The one significant finding was an altered fiber length distribution in some heated lots such that the proportion of shorter fibers was increased while the percentage of long fibers was slightly decreased. This change appeared to be correlated with poorer yarn appearance and uniformity, a slight reduction in yarn and fabric strength, and poorer resistance to flex-abrasion. A blend of unheated lint with enough short (cut) fibers to give a fiber-length distribution approximately the same as that of a gin-overheated lot produced yarns and fabric with properties in close agreement with the overheated lot whose fiber-length distribution was approximated by the blending.

Laboratory tests showed that fiber strength was lower when tested immediately after heating—that is, when the moisture regain was temporarily greatly reduced. From this finding it is deduced that the change in length distribution is the result of excessive fiber breakage when lint is subjected to mechanical agitation at too low a moisture content.

Introduction

As a consequence of the successful development and widespread use of the mechanical cotton picker, gins have had to handle not only peak loads of seed cotton but also much that was too moist to gin. This has required the installation of drying systems ahead of the ginstand. A further consequence of the use of mechanical pickers is the need for more drastic cleaning equipment to remove the greater quantity of trash picked up with the cotton.

The spinning industry has complained for several years of the poor spinnability of some lots which were allegedly overheated or overdried at the gin. Several studies have attempted to find out how gin-heating and gin-cleaning affected spinnability and other properties of interest to cotton mills. Gerdes et al. [4] in 1950 compared the effects of different

[1] One of the laboratories of the Southern Utilization Research and Development Division, Agricultural Research Service, U. S. Department of Agriculture.

drying conditions on green, damp, hand-picked cotton and damp, mid-season machine-picked cotton. For both types Gerdes et al. found that excessive heating decreased the moisture content, improved the grade, and decreased the fiber length and strength slightly. The National Cotton Council initiated a "17-mill test" in 1951 [10]. Their findings were similar: excessive heat gave (a) increased grade index, (b) decreased moisture content, (c) increased ends down in spinning, and (d) more neps in dyed cloth. Leitgeb and Wakeham [6] subjected hand-picked cotton to moderate and severe tower drying before ginning. Spinning tests showed more ends down, lower yarn strength and evenness, and poorer yarn appearance with increasing severity of tower drying. Tests on the raw lint cotton showed only minor changes in fiber properties: (a) more short and fewer long fibers, (b) slight increase in alkali-centrifuge values, (c) lower moisture content, (d) slightly redder color in the Goldthwait differential dye test, and (e) inconclusive differences in fluorescence. Hart et al. [5] in a similar study concentrated their testing on spinnability. Their findings were essentially the same as those of Leitgeb and Wakeham. Delany [2] has recently presented data on the combined effects of heat and different amounts of cleaning equipment on mill performance, in such a way that the effects of heat and equipment could be separately evaluated in the analysis of the data. It was obvious that by far the greatest source of spinning and weaving trouble was excessively severe cleaning. Heat before cleaning and ginning merely aggravated this effect.

The studies previously cited were aimed primarily at evaluating the effect of heat on mill performance. Several pertinent studies on the effect of heat under laboratory conditions on the properties of lint cotton should be noted. In these studies, temperature, time of exposure, and humidity of the atmosphere were varied to give a wide range of degradation. Wiegerink [11] established from yarn tests that breaking strength, elongation, and dyeability decreased with increasing temperature and time of exposure and that fluidity increased. Orr et al. [9] confirmed this and showed that breaking load and elongation of single fibers decreased linearly with time, and simultaneously, so that the secant modulus remained unchanged. Fluidity increased with time, and degradation was more severe in a moist atmosphere. Farquhar et al. [3] observed that changes in carboxyl and hydroxyl content, weight loss, and the formation of characteristic spirals in the Congo Red test were negligible except at high temperatures for long periods. The weight loss from enzymatic hydrolysis decreased with heat exposure.

The present study was undertaken to tie together and extend these previous findings. By making all appropriate chemical and physical tests on the raw lint as received from the gin, and then carrying the samples through normal mill processing to yarns and fabric, we hoped to find some change in a property or combination of properties of the lint by which poor spinnability and poor textile behavior could be predicted. Some new chemical tests were performed with the idea that definite chemical changes had occurred during heating. Some new types of physical tests were applied to see if such physical properties as surface friction had been altered. Thus, it was desirable to obtain such usual data on the lint as fiber length distribution, fiber-bundle strength and elongation, and moisture regain, to determine single-fiber strength, and to examine such properties as fiber friction, microscopical swelling behavior, alkali swelling, wettability, fluorescence in ultraviolet light, copper number, carboxyl content, pH, infrared spectra, and wax properties. Some or all of these properties have been reported to be susceptible to alteration by excessive heat. The question was whether gin-heating was sufficient to give a detectable change. Experiments were performed on cotton heated at the gin and also on lots heated under laboratory-controlled conditions.

Materials

Most of the data here reported were obtained on three series of cottons: the 1955 gin series, the 1956 gin series, and a laboratory flash-heated series. The 1955 series consisted of three varieties of hand-picked cotton (Stoneville 2B, Deltapine 15, and Bobshaw), grown at the Mississippi State Delta Experiment Station or bought on the open market in that vicinity, and ginned at the U. S. Cotton Ginning Research Laboratory at Stoneville, Mississippi. Three lots of each variety were processed (using the minimum of cleaning equipment) with the following drying-tower temperatures: (a) without heat (ambient temperature 80°–95° F.), (b) with moderate heat (160° F.), and (c) with high heat (240° F.).

The 1956 gin series was drawn from one lot of hand-picked Delfos variety, grown and ginned at the same places as the 1955 series. The main lot

was subdivided into five sublots which were ginned as follows: (a) naturally dry, no heat; (b) naturally dry plus moderate heat (200° F.) in two drying towers; (c) naturally dry plus excessive heat (365° F.) in drying towers; (d) premoistened and dried with moderate heat (200° F.); and (e) premoistened and dried with excessive heat (365° F.). The premoistening was accomplished by adding, the night before the cotton was to be ginned, sufficient water to bring the moisture regain of the lint to about 12%.

Cotton for the laboratory flash-heating was damp locks of Deltapine 15 variety picked at the Louisiana Agricultural Experiment Station just after the bolls had cracked. The heating was performed in an apparatus designed to circulate heated air at 1400 cu. ft./min. through a 12 × 12-in. screen on which the locks of cotton were spread. The locks were divided into three lots for different series. Series A was heated as soon as received; Series B was heated after air-drying in the sun for one day; and Series C was heated after thorough air-drying for about two weeks in the laboratory. In separate runs of each series, temperatures of the air stream were approximately 265° F. (130° C.), 320° F. (160° C.), and 428° F. (220° C.). Times of exposure were 15, 30, 60, 90, and 180 sec. After being heated, the lint was removed from the seeds in a laboratory-model roller-gin.

Results

Chemical and Physico-Chemical Tests

Copper number, carboxyl content (cation exchange capacity), and pH were measured on samples of all three series. No significant differences due to heating were detected. In a laboratory experiment it was found that the copper number decreased slightly when lint cotton was heated for 1 hr. at 329° F. (165° C.) but then slowly increased upon further heating. Cotton wax (chloroform extractable fraction) was examined. No significant differences between unheated and gin-heated lots were found in the quantity of wax, its melting point, hardness, infrared spectrum, or in qualitative spot tests for various reactive groups that might have been expected to appear or to be changed by heat. The infrared spectra of both gin-heated and oven-heated samples of lint were examined, but no differences were found between these and the spectrum of the unheated cotton. A distinctive odor (variously described as "chocolate-peanut" or "caramel") could easily be detected on severely overheated cotton when the previously heated lint was exposed to a moist atmosphere, but no test could be found to identify the odor.

Moisture regain at standard conditions (65% RH) (Tables I and II) was reduced 0.1–0.8% by excessive gin-drying; the difference appeared to decrease with time of storage so that after 1–2 yr. it disap-

TABLE I. Physical Properties of Gin-Heated Lint

Sample identification	Length, Fibrograph		Tenacity		Elongation, ⅛-in. gauge, %	Moisture regain	
	UHM,* in.	UR,* %	Zero gauge, g./tex	⅛-in. gauge, g./tex		After htg., %	Stand. cond., %
1955 Gin Series							
Stoneville, unheated	1.14	85	29.9	17.0	7.2	—	7.4
Stoneville, 240° F.	1.10	83	31.1	16.8	7.0	2.8	6.6
Deltapine, unheated	1.06	85	32.7	17.8	6.1	—	7.1
Deltapine, 240° F.	1.03	85	33.4	17.6	6.1	2.6	6.8
Bobshaw, unheated	1.11	86	30.8	19.1	9.3	—	7.3
Bobshaw, 240° F.	1.14	86	30.7	19.0	9.5	2.9	6.8
1956 Gin Series							
Delfos, unheated	1.05	86	33.2	17.4	9.3	7.4	7.7
Delfos, dry; 200° F.	1.03	86	32.5	17.7	9.5	4.6	7.7
Delfos, moist; 200° F.	1.07	85	34.6	17.1	8.7	4.4	7.6
Delfos, dry; 365° F.	1.02	84	32.5	17.2	9.3	2.1	7.5
Delfos, moist; 365° F.	1.02	81	32.6	17.2	8.3	3.0	7.4

* UHM = upper-half mean; UR = uniformity ratio.

peared. Crystallinity index (as determined by x-ray diffraction) was not affected by gin-drying; the x-ray 50% angle (orientation angle) apparently decreased very slightly. The density (as determined in density-gradient columns) increased slightly (about 3 parts in 1500) after gin-heating. Fluidity showed a slight increase (about 6%, which is within the error of measurement) after excessive gin heat. A larger increase (from 1.42 rhes to 2.08 rhes) occurred after severe laboratory flash-heating (1 min. at 428° F.).

Various tests that measure accessibility and swellability showed only small differences due to gin-heating. The premoistened lot of Delfos cotton that was dried at 365° F. dyed to a slightly lighter shade with a direct blue dye, and dyed somewhat redder in the Goldthwait differential (red-green) dye test. The lots of cotton heated when dry and the premoistened lot heated at 200° F. failed to show this difference. Iodine sorption showed a very slight decrease after severe gin-heating, but the difference was within the error of measurement. The alkali-centrifuge swelling test showed a slight increase with severe laboratory flash-heating but no increase after gin-overheating. Partial and complete mercerization failed to show any differences related to gin-heating. Yarns that had been spun from the various gin lots were treated with a series of caustic solutions ranging from 6% to 22% NaOH (by weight). Moisture regain, x-ray crystallinity and extent of conversion to mercerized cotton, and the differential dye test all failed to show any difference in swellability that could be related to previous history of heating.

Wettability was measured on fabrics and yarns. Previous gin-heating of the lint had no effect, but severe oven-heating (392° F. for 1 min. or more) of yarn or fabric increased the wettability very slightly.

Visual observations under ultraviolet light indicated very little, if any, detectable difference in brightness or color of fluorescence except in those samples that had been so severely heated that a yellowish or tan color could be detected in ordinary

TABLE II. Physical Properties of Lint of Deltapine Variety Flash-Heated in a Laboratory Apparatus

Sample identification	Length, Fibrograph		Tenacity, ⅛-in. gauge, g./tex	Elongation, ⅛-in. gauge, %	Moisture regain	
	UHM,* in.	UR,* %			After htg., %	Stand. cond., %
Series A: Wet						
Unheated	1.05	83	18.9	8.2	—	—
322° F./60 sec.	1.05	81	18.8	7.6	—	—
428° F./30 sec.	1.06	79	18.6	8.0	—	—
428° F./60 sec.	1.05	80	17.5	7.8	—	—
Series B: Partly dry						
Unheated	1.06	82	18.0	7.7	9.1	7.1
266° F./180 sec.	1.05	82	18.2	7.5	2.1	7.2
322° F./60 sec.	1.07	79	18.2	7.6	2.8	6.9
428° F./15 sec.	1.05	81	18.0	7.7	2.8	6.8
428° F./30 sec.	1.02	80	17.3	7.6	2.3	—
428° F./60 sec.	0.97	81	17.4	7.2	2.2	6.7
Series C: Well air-dried						
Unheated	1.02	81	18.0	7.5	5.7	7.1
266° F./180 sec.	1.02	80	18.2	8.1	0.7	6.9
322° F./30 sec.	1.02	80	17.6	7.8	1.0	6.9
322° F./60 sec.	1.00	78	18.0	8.0	0.5	7.0
428° F./15 sec.	0.98	76	17.6	7.5	0.7	6.8
428° F./60 sec.	0.94	80	17.5	7.0	0.5	6.6

* UHM = upper-half mean; UR = uniformity ratio.

light. Attempts to make some quantitative measurement of fluorescence (such as by photographing a group of samples under ultraviolet light using an appropriate filter over the camera lens) failed to reveal any appreciable differences.

Physical Tests

Lint. Fiber surfaces were examined with the electron microscope by a replica technique. No differences were found between gin-heated and unheated samples. In lint that had been severely oven-heated (446° F. for 2 min. or 320° F. for 48 hr.) there seemed to be a slightly more frequent occurrence of transverse ridges or bulges on the fiber surface than in unheated lint.

Under the light microscope the Clegg test did not show any differences due to heating. Staining with ruthenium red, methylene blue, or Nile blue sulfate gave small but distinguishable differences on samples that had been severely heated in the laboratory oven. The most sensitive microscopic test was a combination of staining with Nile blue sulfate and controlled swelling in cupriethylenediamine hydroxide. This test could differentiate unheated lint, moderately overheated lint, and severely heat-damaged lint. In Figure 1, it is seen that the typical "balloons" or "beads" which develop when unheated fibers (Figure 1A) and undamaged heated fibers (upper fiber in Figure 1B) are swollen by the reagent, tend to become elongated into sausages in slightly damaged fibers (middle fiber in Figure 1B), and disappear altogether to give uniform swelling in severely damaged fibers (Figure 1C). In the 1955 gin series, no heat damage was detected by this test. In the 1956 gin series, all of the gin-heated lots (both moderate and high heat, dry and moist) showed slightly more uniform swelling than did the unheated lot. In the laboratory flash-heated series, at 265° F. no damage was detectable; at 320° F. for 60 sec. the appearance was suspicious but not definite; while at 428° F. there were some damaged fibers in the lint exposed for 15 and 30 sec. and definite, severe damage after 60 sec. It should be noted that these latter samples were visibly browned by the heating.

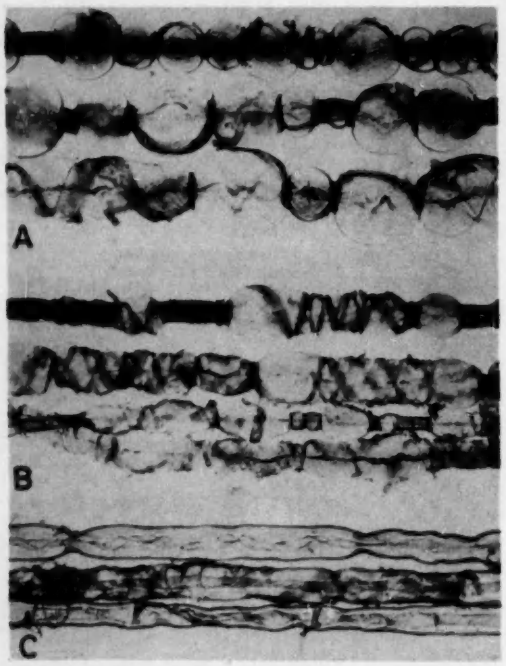

Fig. 1. Photomicrographs of cotton fibers stained with Nile blue sulfate and swollen in dilute cupriethylenediamine solution. (A) Normal unheated fibers. (B) Fibers from lint ginned after moistening and drying at 365° F. (C) Fibers from lint flash-heated 60 sec. at 428° F. (120×).

Fiber length was measured with the Fibrograph [2] and the Suter-Webb [2] sorter. The Fibrograph data (Table I) indicated small decreases (about 3%) in upper-half mean length for most of the gin-heated lots and slightly greater decreases in mean length in some cases. The uniformity ratio (ratio of mean to upper-half mean) decreased for the Delfos and the Stoneville varieties heated at high temperatures. In the laboratory flash-heated series (Table II), significant changes in length and length-uniformity ratio occurred only at the highest temperature (428° F.) and not uniformly even there. This might be attributed to the fact that the seed cotton had cooled and regained some of its moisture content before being roller-ginned.

Suter-Webb arrays gave a similar pattern for the 1955 and 1956 gin series. When length distributions were plotted (Figure 2), no differences could be found between several of the pairs of heated and control samples, but an increase in the proportion of shorter fibers did appear in the overheated Stoneville cotton (not shown) and in the Delfos cotton subjected to high heat when moist.

Fiber strength was determined on flat bundles with the Stelometer [2] at zero and at $\frac{1}{8}$-in. gauge lengths.

[2] The mention of trade names does not imply their endorsement by the Department of Agriculture over similar products not mentioned.

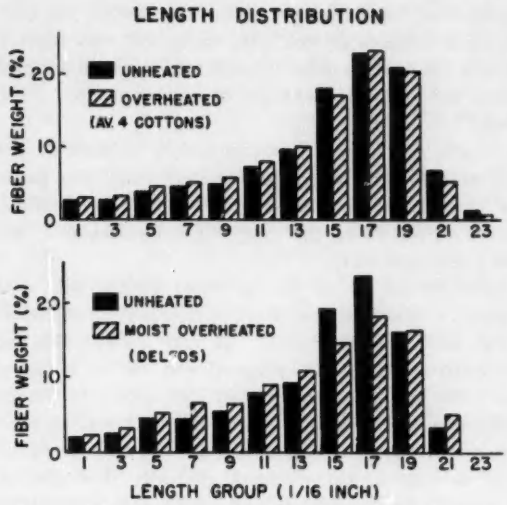

Fig. 2. Length distribution data from Suter-Webb fiber length arrays. Upper bar diagram, averages of paired lots of four varieties; lower bar diagram, Delfos variety (1956 series).

Data are given in Tables I and II. There were no significant differences in strength due to heat except in the severely overheated flash-heated samples, and these were of borderline significance. One interesting and possibly significant difference in elongation at break should be noted in the 1956 gin series (Delfos variety). The fiber-bundle elongation of the two premoistened lots was reduced by about 10% as compared to the unheated control or to the two lots that were heated when dry. This pattern of reduced elongation tended to persist into the tensile behavior of the yarns.

Single-fiber strength tests were made with an Instron [2] tester on the Delfos gin-dried series and, in addition, on fibers heated at 320° F. for 15 sec. and tested immediately. The data in Table III show that gin heating caused permanent damage only when moist lint was heated at 365° F., whereas fibers tested dry (that is, immediately after oven-drying) were 20% weaker than the control fibers.

Micronaire [2] fineness was unchanged by gin-heating. Maturity (determined by the sodium hydroxide method on separate Suter-Webb length groups) appeared to show a very slight increase in the middle length groups of the premoistened heated lots of Delfos cotton and a corresponding decrease in the shortest length groups.

TABLE III. Tensile Data on Single Fibers of Various Lots of Delfos Variety. Values Are Means of 100 Measurements

Treatment	Breaking load		Elongation	
	Mean, g.	Std. error, g.	Mean, %	Std. error, %
Unheated control	4.8	0.3	8.7	0.3
Heated dry; 200° F.	5.2	0.3	9.8	0.3
Heated moist; 200° F.	4.4	0.2	9.5	0.4
Heated dry; 365° F.	4.7	0.3	10.0	0.3
Heated moist; 365° F.	4.0	0.2	8.4	0.3
Unheated	4.3	0.2	7.8	—
Oven-dried (320° F., 15 sec.) and tested immediately	3.5	0.2	5.9	—

TABLE IV. Nepping Potential of Cottons as Measured with the Nepotometer

Sample identification	Nep-potential grades
1955 Gin Series	
Stoneville, unheated	2.8
Stoneville, 240° F.	3.4
Deltapine, 160° F.	1.6
Deltapine, 240° F.	2.0
Bobshaw, unheated	3.3
Bobshaw, 240° F.	3.3
1956 Gin Series	
Delfos, unheated	2.4
Delfos, dry: 200° F.	2.8
Delfos, moist: 200° F.	3.3
Delfos, dry: 365° F.	2.4
Delfos, moist: 365° F.	3.0

The nepping potential of samples in the two gin series was measured with the Nepotometer.[2] The ratings given in Table IV show increases in nep-potential grade for the overdried Stoneville sample and the premoistened lots of Delfos. Small increases were also observed for overdried Deltapine cotton and for the dry, moderately heated Delfos.

Three methods were used to detect changes in fiber friction. Sliver tenacity was measured but the tests were inconclusive due to the many uncontrollable factors which affect this test (*cf.* Mereness [8]). The "drafting recovery" of roving was measured in a special apparatus [1] which consisted of three pairs of drafting rolls with adjustable drafting

ratio between the first and second pairs and with the third pair operated at the same speed as the second pair. If a measured amount of slack is introduced into the roving between the second and third pairs of rolls, the slack will gradually be taken up. The time required for the take-up depends on some property or properties of the roving, all other variables being constant. It was found that the recovery rate was very sensitive to the drafting ratio. Maximum recovery occurred at a drafting ratio of 1.12, with a sharp decrease on either side of this ratio. Unheated and overheated Delfos rovings reversed their relative positions at low and high draft ratios. At a ratio of 3, the gin-overheated lots had a higher recovery rate than the unheated control. It appears that a difference in interfiber friction due to heating is not the only controlling factor, since roving made from a blend of the unheated lot with sufficient short fibers to make the fiber length distribution match that of the moist, overheated lot had about the same recovery rate as the overheated sample.

The friction between sets of fiber fringes was measured by the method of Lord [7]. It was established that this method could detect frictional differences between raw and solvent-extracted lint and between raw and oven over-heated lint. When fiber fringes of the Delfos gin series were tested, the friction in samples ginned after high heat was slightly lower than in the unheated control, but the difference was not quite statistically significant at the 95% level.

Yarn properties. Six-pound lots of each of the samples in the two gin series were spun into yarns of several twist multipliers. Short lengths of fabric were woven using the experimental yarns as filling in a common warp.

A blended lot of the unheated Delfos was also spun to determine the effect of fiber length distribution on yarn properties. It had been noted, in measuring the physical properties of the lint samples, that the moist, overheated lot had about 8% more fibers in the short and intermediate length groups than the control and normally heated lots, probably due to fiber breakage during ginning. Portions of unheated Delfos cotton were cut in a special cotton cutter to nominal lengths of $\frac{1}{2}$, $\frac{1}{4}$, and $\frac{1}{2}$ in., and sufficient amounts of each length were added to lint at the finisher lap to bring the fiber length distribution in the sliver to a good approximation of that found in the moist, overheated Delfos sample. The blended lot was carded and spun exactly like the other lots.

TABLE V. Physical Test Data on Yarns of the 1955 and 1956 Gin Series

Material	Tenacity Mean g./tex	Tenacity S.E.	Elongation, %	Impact strength, in.-lb.	Flex-abrasion Mean cycles	Flex-abrasion S.E.	Uster uniformity, % C.V.*
1955 Series (16s/3, 4.1 T.M.)							
Stoneville, unheated	15.7	0.2	11.7	44	1881	91	7.8
Stoneville, 240° F.	15.3	0.2	11.9	43	1687	77	8.2
Deltapine, 160° F.	16.6	0.2	10.2	42	1572	37	8.1
Deltapine, 240° F.	16.7	0.2	10.6	40	1601	71	8.0
Bobshaw, unheated	17.0	0.3	12.2	50	1807	60	7.8
Bobshaw, 240° F.	16.5	0.3	12.1	50	1782	91	8.0
1956 Series (Delfos) (16s/2, 4.75 T.M.)							
Unheated	16.2	0.3	9.9	102	1820	44	13.8
Heated dry; 200° F.	15.0	0.2	9.7	93	1573	48	14.3
Heated moist; 200° F.	15.8	0.2	9.7	89	1759	51	14.9
Heated dry; 365° F.	15.4	0.2	9.9	98	1756	73	14.6
Heated moist; 365° F.	14.7	0.3	8.9	86	1543	55	14.8
Unheated; blended short fibers	14.8	0.3	9.7	91	1622	96	15.3

* 1955 series, 2-ply yarns; 1956 series, singles yarns.

The yarns were spun with several twist multipliers to see if there was a relation between gin heating and the twist for maximum strength, but none was found. The physical properties of the yarns given in Table V are, therefore, those of yarns spun to approximately the optimum twist multiplier.

Yarn appearance was judged by several observers. In general, yarns from gin-heated cotton rated slightly poorer than the controls. Yarn uniformity, as determined for short-period variation with the Uster [2] tester (see Table V) rated the various yarns in approximately the same order as observation of yarn-appearance boards. With respect to mill performance (spinnability, waste, ends down), no appreciable differences between lots were observed. The small size of the lots would make such discrimination difficult.

Yarn tenacities for the 1955 series (Table V) were apparently not detectably affected by gin-heating. In the 1956 series (Delfos cotton), yarn tenacities of all of the heated lots were slightly below the control, but the differences were rather small. The moist, high-heat lot, which had been matched in fiber length distribution in preparing the blended lot, had the greatest reduction in tenacity (9%). The tenacity of the blended lot was reduced by the same amount.

Yarn elongation at break followed the pattern of fiber-bundle elongation; that is, it was about equal for all lots except the moist, overheated lot, which was definitely lower. Tensile tests were also made on portions of these yarns that had been (a) washed, (b) washed and scoured, and (c) slack-mercerized. Wet specimens of the scoured and of the mercerized yarns were also tested. The pattern of relative tenacities and elongations was the same for each group of processed yarns and for the groups tested wet as for the group of raw yarns. These are shown as bar diagrams in Figure 3.

Impact strength was somewhat reduced in yarns of the Delfos series by gin-heating and by blending in short fibers.

Flex-abrasion resistance appeared to be slightly reduced in the heated Stoneville yarn but not in the case of the Deltapine and Bobshaw lots. In the Delfos series, both the heated lots and the blend of short fibers with unheated lint produced yarns with slightly reduced flex-abrasion. For yarns with normal (near optimum) twist, data for which are given in Table V, the reduction is too small to be significant. When, however, low-twist yarns (3.0 and 3.25 T.M.) were tested, the differences between control and heated lots were substantially greater. For Stoneville yarn, the cycles withstood were decreased by 25% in the gin-heated lot; for the Delfos series, decreases ranged from 40% to 60%. For the blended lot containing added short fibers, the decrease was 50%. This poor resistance to flex-abrasion most likely is related to the somewhat greater non-uniformity of yarns made from heated cotton and from the blend.

Fabric properties. The fabrics were sateen weave, with fillings of the experimental yarns in a common warp. Breaking strength and tongue-tear strength were measured in the filling direction. Flex- and flat-abrasion tests were done on the filling face of the sateen weave.

From the data in Table VI, it is seen that fabric breaking strength was decreased slightly by gin-heating of Stoneville variety, but fabrics made from overheated Deltapine and Bobshaw varieties were

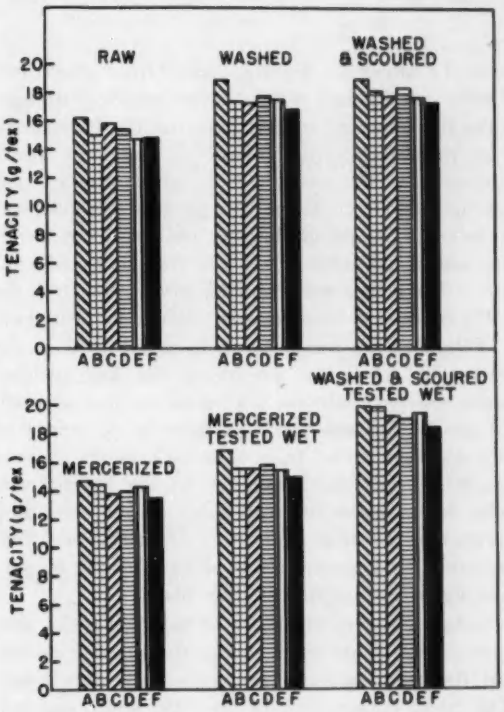

Fig. 3. Tenacities of processed yarns of the Delfos gin series. (A) Unheated. (B–E) Heated:—(B) dry, 200° F.; (C) moist, 200° F.; (D) dry, 365° F.; (E) moist, 365° F. (F) blend (unheated plus short fibers).

TABLE VI. Physical Test Data on Fabrics Woven from Experimental Yarns

Material	Breaking strength, lb.	Elongation, %	Tongue tear, lb.	Flex abrasion, cycles
1955 Series				
Stoneville, unheated	99.8	10.0	—	2239
Stoneville, 240° F.	88.0	9.9	—	1931
Deltapine, 160° F.	94.4	8.3	—	1740
Deltapine, 240° F.	94.6	8.5	—	1710
Bobshaw, unheated	104.6	11.9	—	1978
Bobshaw, 240° F.	102.6	11.9	—	1934
1956 Series (Delfos)				
Unheated	88.8	14.2	14.6	1483
Heated dry, 200° F.	80.9	14.1	13.7	1351
Heated moist, 200° F.	85.6	14.2	13.9	1387
Heated dry, 365° F.	84.2	14.5	13.6	1286
Heated moist, 365° F.	82.4	14.2	13.7	1387
Unheated, blended short fibers	82.6	14.1	13.3	1158

scarcely affected. Fabrics made from gin-heated Delfos variety had 4–9% lower breaking strength than the unheated control, whereas the blended lot was reduced by 7%. Fabric elongation at break appeared to be unaffected by gin-heating. Tear strength of Delfos fabric (tongue-tear method) was reduced by 7% by gin-heating and by 9% by blending additional short fibers with the unheated control. The construction of the fabrics made from the 1955 series of cottons was not suitable for tear tests.

Flex-abrasion was reduced by about 14% in the Stoneville fabric by gin-drying the lint; neither Deltapine nor Bobshaw cotton fabric was affected. In the Delfos series, the decrease in resistance to flex-abrasion varied from 6 to 13% in the various gin-heated lots and was 22% in the blended lot. The flex-abrasion tests on fabrics show the same trends as the tests on yarns. Flat-abrasion was measured, and appeared to be affected neither by gin-heating nor by addition of short fibers.

Crease recovery of fabrics of the 1955 series was very slightly lower in all fabrics from heated cotton, but the difference was not statistically significant. The fabric construction of the 1956 series was not suitable for making crease recovery measurements.

Experiments on fabric weight loss and changes in air permeability after exposure to the action of the Accelerotor [2] showed no relation of these quantities to previous history of heating.

There appeared to be very slight visually detectable differences in color or brightness of the Delfos fabrics; therefore, quantitative data were obtained with the Hunter Reflectometer.[2] Neither yellowness (Y values) nor difference in total color as compared to the unheated fabric (ΔE values) was found to show any significant differences due to heating.

It is of interest to compare the relative strengths of gin-heated and control samples of Delfos cotton at different stages of processing. Figure 4 shows flat-bundle strength of the lint, single-end strength of yarn, and strip breaking strength of fabric of each of the gin-heated lots as well as the blended lot, expressed as a percentage of the unheated control. There is less relative strength loss in the fiber samples than in the yarns and fabrics made from these lots. Thus, fiber strength would not necessarily indicate lowered yarn or fabric strength due to gin-heating and certainly would not predict the lowered strength of the blended sample made from the unheated lint.

Discussion

Nearly all of the physical measurements and chemical tests made on gin-heated seed cottons have yielded negative evidence of radical permanent alteration of any properties of the lint by exposure to heat at the gin. The one significant finding is a change in fiber length distribution, along with a very slight decrease in mean fiber length. The alteration in length distribution can be detected by a decrease in uniformity ratio (ratio of mean to upper-half mean) from Fibrograph data, or by careful comparison of the length distribution curves obtained from length-array data. Since a change in length distribution strongly indicates fiber breakage, it is appropriate to examine reasons why certain samples dried with heat before ginning should show a greater tendency toward fiber breakage at the ginstand or during cleaning. Single fibers have less strength and lower elongation when tested immediately after oven-drying; that is, when the moisture regain is very low. Lint cotton that has been heat-dried excessively, either by too high a temperature in the drying tower or because it was already well air-dried, undoubtedly reaches the ginstand in a temporarily weakened condition due to its very low moisture content. Once fiber breakage has occurred, subsequent recovery of

a nearly normal regain will not repair the physical damage. The presence of the greater proportion of short fibers in such lots of cotton might be responsible for the slightly greater nep potential, the poorer yarn appearance and uniformity, the slight reductions in yarn and fabric strength, and the poorer resistance to flex abrasion. The performance of the yarn and fabric made from the blended lot, in which this excess of short fibers was artificially produced, was in very close agreement with that of the moist, overheated lot whose fiber-length distribution was approximated by the blending.

One other interesting observation merits brief comment: the reduction in elongation at break noted in the Delfos lint that had been brought to a high moisture content before passing through the drying towers. This reduced elongation apparently was quite permanent, being found not only in the raw yarns spun from that lot of lint but also in the yarns tested after washing, scouring, and even after mercerizing. It is conceivable that if lots of moist and dry cotton were dried and ginned consecutively so that they became mixed in the bale, or if bales of such initially moist and initially dry lots were mixed at the mill, the resulting yarns would be weaker than normal because of the difference in extensibility of the fibers.

Acknowledgments

Appreciation is expressed to the several groups without whose assistance this study could not have been made: to the U. S. Cotton Ginning Research Laboratory, Stoneville, Mississippi, for procuring and ginning the samples of the 1955 and 1956 gin series; to the Louisiana Agricultural Experiment Station, Baton Rouge, Louisiana, for furnishing the damp cotton locks for the laboratory experiments; and to the several units in the Southern Utilization Research and Development Division for numerous physical and chemical tests and for the spinning and weaving of experimental yarns and fabrics.

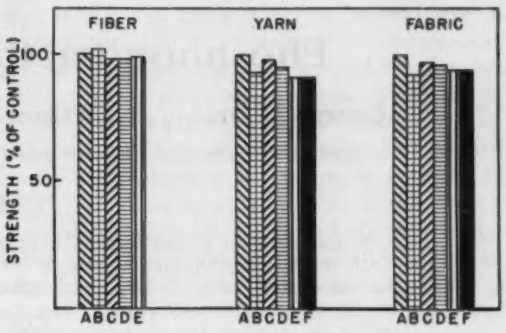

Fig. 4. Relative strengths of experimental samples of Delfos cotton at different stages of processing. (A) Unheated. (B–E) Heated:—(B) dry, 200° F.; (C) moist, 200° F.; (D) dry, 365° F.; (E) moist, 365° F. (F) blend (unheated plus short fibers).

Literature Cited

1. Barnes, J. C., private communciation.
2. Delany, J. L., TEXTILE RESEARCH JOURNAL **27**, 175–176 (1957) and *Textile Ind.* **121**, No. 2, 136–138 (1957).
3. Farquhar, R. L. W., Pesant, D., and McLaren, B. A., *Can. Textile J.* **73**, No. 3, 51–56 (1956).
4. Gerdes, F. L., *Cotton Ginners' J.* **18**, 26–27 (March 1950).
5. Hart, W. J., Bailey, T. L. W., Jr., Keyser, W. R., Jr., and Compton, J., TEXTILE RESEARCH JOURNAL **25**, 415–421 (1955).
6. Leitgeb, D. J. and Wakeham, H., TEXTILE RESEARCH JOURNAL **24**, 1047–1057 (1954).
7. Lord, E., *J. Textile Inst.* **46**, P41–P55 (1955).
8. Mereness, H. A., TEXTILE RESEARCH JOURNAL **25**, 363–372 (1955).
9. Orr, R. S., Weiss, L. C., Humphreys, G. C., Mares, T., and Grant, J. N., TEXTILE RESEARCH JOURNAL **24**, 399–406 (1954).
10. Regnery, W., *Ann. Cotton Merchandising Clinic Proc.* **5**, 5–10 (1952); *Proc. Am. Cotton Cong.* **13**, 46–58 (1952).
11. Wiegerink, J. G., TEXTILE RESEARCH **10**, 493–509 (1940).

Manuscript received October 10, 1958.

Phosphonomethylation of Cotton

George L. Drake, Jr., Wilson A. Reeves, and John D. Guthrie

Southern Utilization Research and Development Division,[1] New Orleans, La.

Abstract

A new phosphorus-containing ether of cellulose was prepared by the reaction of cotton with chloromethylphosphonic acid in the presence of sodium hydroxide. Phosphorus contents from 0.2% to 4.0% were obtained. By proper control of the phosphonomethylation reaction, derivatives were made which ranged from water soluble to fibrous materials in which the physical properties of the untreated cotton were substantially unaltered. Phosphonomethyl cotton was flame resistant in the ammonium salt form and had a cation exchange capacity equivalent to some of the cation exchange resins.

THE USE of several phosphorus-containing chemicals to introduce new physical and chemical properties into cellulose through chemical modification has been reported in the literature. Ford and Hall [5] and others [3, 11] produced phosphorylated cotton by curing cotton with a mixture of phosphoric acid and urea. Chance, Warren, and Guthrie [2] produced phosphatoethyl cotton by heating cotton with a mixture of sodium 2-chloroethylphosphate and sodium hydroxide. The purpose of the present paper is to describe the preparation and properties of a new phosphorus-containing ether of cotton cellulose, phosphonomethyl cotton. This partial ether of cellulose was prepared by the reaction of cotton with chloromethylphosphonic dichloride, or chloromethylphosphonic acid, and sodium hydroxide. Reaction conditions and concentration of reagents govern the degree of substitution. The reaction takes place as follows:

$$\text{CellOH} + \text{ClCH}_2\overset{\overset{\text{O}}{\|}}{\text{P}}\text{—(OH)}_2 + 3\,\text{NaOH} \rightarrow \text{CellOCH}_2\overset{\overset{\text{O}}{\|}}{\text{P}}\text{—(ONa)}_2 + \text{NaCl} + 3\,\text{H}_2\text{O}$$

By comparison of the structures shown below for phosphorylated cellulose, phosphatoethyl cellulose, and phosphonomethyl cellulose, it can be seen that the phosphonomethyl cellulose is the only one of the group in which the phosphorus atom is attached directly to a carbon atom, not through an oxygen atom as in the other cellulose modifications. The carbon-to-phosphorus bond is a more stable linkage.

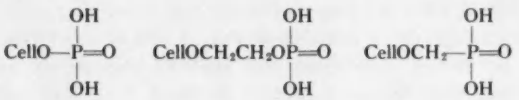

Phosphorylated Cotton | Phosphatoethyl Cotton | Phosphonomethyl Cotton

By proper control of the phosphonomethylation reaction, derivatives may be made ranging from water soluble to fibrous materials which have a permanently starched effect or to those which substantially retain the original physical properties of the untreated cotton.

Phosphonomethyl cotton fabric exhibits cation exchange properties which can be equivalent to some of the ion exchange resins. On conversion of the phosphonic acid group to the ammonium salt, flame resistance is obtained.

Although it has been stated in the literature [8, 13] that the reactivity of the halogen atom on the chloromethylphosphonic acid and its derivatives is very low, even with alkalies, it has been found that chloromethylphosphonic acid will react readily with the hydroxyls of cellulose in the presence of sodium hydroxide.

Experimental

Materials and Methods

The fabric used was a standard type 4.5-oz. 48×48 cotton sheeting which had been boiled off, desized, scoured, and peroxide bleached in a continuous range with a caustic pretreatment.

[1] One of the laboratories of the Southern Utilization Research and Development Division, Agricultural Research Service, U. S. Department of Agriculture.

The chloromethylphosphonic dichloride, chloromethylphosphonic acid, and the sodium hydroxide were commercial grade materials. The tearing strengths reported are the Elmendorf tears as described in ASTM [1].

Phosphorus was determined by the colorimetric reduced molybdate method after digestion with sulfuric acid and hydrogen peroxide [9].

Nitrogen was determined by the Kjeldahl method, using a mercury catalyst.

An electrically heated forced air type oven was used to dry and cure fabric for all of the treatments.

The degree of flame resistance of the fabrics was determined by the strip test method ([10], p. 529). By this method, the end of a strip of fabric 1 cm. in width is ignited with the fabric surface vertical, and the angular position at which it must be held for the flame to go out is determined. For example, if the strip did not burn in the vertical position when ignited at the bottom, it passed the 180° flame test and had a high degree of flame resistance. If the flame went out when it was held with the long edge of the strip horizontal and the fabric surface vertical, it passed the 90° flame test and was moderately flame resistant. Strips of the cloth prior to the treatment would burn continuously even when held vertically and ignited at the top. Samples passing approximately the 135° angle would pass the standard vertical flame test [10, 12]. Samples passing the 180° angle test represent the highest degree of flame resistance.

Preparation of the Treating Solution

Both chloromethylphosphonic dichloride and chloromethylphosphonic acid were used in this study. Since the reaction with cotton was carried out in aqueous alkali solutions, the actual compound reacting with the cotton was the same regardless of the starting reagent; that is, disodium chloromethylphosphonate. The use of both starting materials is reported because in one case large quantities of sodium chloride were present in the treating solutions due to the use of the acid chloride, and also because the end results were somewhat different in a number of instances.

Method I: The use of chloromethylphosphonic dichloride. Chloromethylphosphonic dichloride was reacted with the stoichiometric quantity of sodium hydroxide in water to form disodium chloromethylphosphonate. This reaction was carried out at 15° C. The sodium salt was not isolated but was used in solution along with the sodium chloride formed in the above reaction. This aqueous solution of disodium chloromethylphosphonate was mixed with various concentrations of sodium hydroxide and used to treat cotton fabric.

Method II: The use of chloromethylphosphonic acid. Chloromethylphosphonic acid, with m.p. of 88–95° C., was dissolved in the stoichiometric quantity of aqueous sodium hydroxide to form the disodium salt. The temperature of the solution was maintained below 30° C. to prevent hydrolysis of the halogen of the chloromethyl group. This aqueous solution of disodium chloromethylphosphonate was mixed with various concentrations of sodium hydroxide and used to treat cotton fabric.

A Typical Phosphonomethylation Procedure

A sample of 48×48 cotton sheeting was padded, using 2 dips and 2 nips and a light squeeze roll pressure, with a solution consisting of 15 parts disodium chloromethylphosphonate and 25 parts sodium hydroxide. The wet pickup was 143%. The wet fabric was heated for 30 min. at 110° C. in a forced draft oven, washed with water, and dried.

Salt Forms

The resulting fabric contained 1.99% P and had an ion exchange capacity of 1.18 meq./g. A strip of this fabric in the sodium salt form would pass the 90° angle flame test with a slight afterglow. The conversion of this phosphonomethyl cellulose sodium salt to the corresponding ammonium salt was made by soaking a sample of the cloth for 15 min. in 5% hydrochloric acid, washing free of the acid with distilled water, and then soaking in 5% ammonium hydroxide solution. The fabric was washed with distilled water and dried. It now contained 1.95% phosphorus and 0.78% nitrogen, and passed the standard vertical flame test [12] and the 180° angle strip flame test without an afterglow.

Phosphonomethylation Using Chloromethylphosphonic Dichloride As a Starting Material

Small pieces of 48×48 cotton sheeting were padded through each of the solutions prepared by Method I and listed in Table I using 2 dips and 2 nips with a light squeeze roll pressure. The weight percent of free sodium hydroxide in solution was varied from 10% to 25%, and the disodium

chloromethylphosphonate from 5% to 30%. The cure time of the wetted sample was varied from 5 min. to 24 hr. and the cure temperature from room temperature to 140° C. Phosphorus analyses and cation exchange capacities were obtained. Data for these experiments are reported in Table I.

According to the results shown in Table I, the solution consisting of 25% NaOH and 15% O ‖ $ClCH_2P—(ONa)_2$ was the best solution concentration and gave the highest degree of reaction, especially at a temperature of 140° C. for 5 min. With the above conditions and solution concentration, a fabric was produced which contained 1.99% P and had a cation exchange capacity of 1.28 meq./g.; it passed the 180° strip angle flame test in the ammonium salt form (see Table I below, line 22).

Variation of $ClCH_2P—(ONa)_2$ at constant caustic concentration also showed that the best degree of substitution was obtained by using 25% NaOH and 15% $ClCH_2P—(ONa)_2$, employing a 5-min. cure at 140° C.

The Elmendorf tear strength and strip breaking strength were determined on the samples containing 0.75% P and 1.57% P listed in Table I. These tests showed that the sample containing 0.75% P retained 95% of its original tearing strength and 100% of its original tensile strength, whereas the sample containing the 1.57% P retained 88% of

TABLE I. Influence of Processing Variables Upon the Properties of Fabric Treated with Solutions Made with Chloromethylphosphonic Dichloride

Wt. of materials in water solution, %	Cure, temp. ° C.	Cure time, min.	Wt. P, %	Cation exchange capacity, meq./g.	Strip burn angle, degrees, NH_4 salt form
10% NaOH	Room temp.	1440	0.02	0.06	0
O	110	5	0.02	0.06	0
‖	110	30	0.03	0.08	0
15% $ClCH_2P—(ONa)_2$	140	5	0.05	0.08	0
10.5% NaCl	140	30	0.13	0.12	0
10% NaOH	Room temp.	1440	0.02	0.07	0
O	110	5	0.03	0.06	0
‖	110	30	0.04	0.05	0
30% $ClCH_2P—(ONa)_2$	140	5	0.03	0.05	0
21.0% NaCl	140	30	0.10	0.10	0
25% NaOH	110	5	0.14	0.16	0
O	110	30	0.88	0.65	135
‖	140	5	0.90	0.66	135
5% $ClCH_2P—(ONa)_2$	140	30	0.90	0.68	135
3.5% NaCl					
25% NaOH	110	5	0.75	0.44	90
O	110	30	1.57	1.05	110
‖	140	5	1.61	1.07	170
10% $ClCH_2P—(ONa)_2$	140	30	1.57	1.08	180
7.0% NaCl					
25% NaOH	Room temp.	1440	0.02	0.10	0
O	110	5	1.54	0.98	160
‖	110	30	1.82	1.18	180
15% $ClCH_2P—(ONa)_2$	140	5	1.99	1.28	180
10.5% NaCl	140	30	1.96	1.29	180
25% NaOH	110	5	0.94	0.62	160
O	110	30	1.60	1.00	180
‖	140	5	1.78	1.11	180
30% $ClCH_2P—(ONa)_2$	140	30	1.45	0.93	180
21.0% NaCl					

its original tear strength and all of its breaking strength.

Phosphonomethylation Using Chloromethylphosphonic Acid as Starting Material

Small samples of 48×48 sheeting were padded through the treating solutions prepared by Method II using 2 dips and 2 nips, with a light squeeze roll pressure. The wet fabrics were then heated as specified in Table II. In these experiments the solution contained 25% free NaOH, but the concentration of disodium chloromethylphosphonate was varied from 2% to 15%. Cure times were varied from 5 min. to 18 hr., and the temperatures were varied from room temperature to 140° C. Phosphorus analyses, cation exchange capacities, and strip burn angles of the ammonium salt forms were obtained. Data from these experiments are reported in Table II. Wet pick-ups of the above fabrics ranged between 145–175%. The data indicate that preparation of the solution by Method II may give slightly better results according to degree of substitution. On comparing the samples prepared by using 25% NaOH and 15% $ClCH_2P(=O)(ONa)_2$ following Method I and Method II, using the optimum conditions of 5 min. at 140° C., it was found that only 1.99% P was introduced using Method I, whereas 2.23% P was introduced using Method II. This difference may be due to less hydrolysis of the chlorine on the alkyl group in the latter process or to the presence of the sodium chloride in the first process.

Repeated Phosphonomethylation of Cotton

Cotton sheeting was phosphonomethylated with a solution containing 25% unreacted NaOH and 15% disodium chloromethylphosphonate according to Method II and heated at 140° C. for 30 min. The phosphorus content of the fabric was 1.84% and the cation exchange capacity was 1.075 meq./g. This cation exchange value was in agreement with the value calculated on the basis of the phosphorus content. The resultant fabric was retreated in the same way except that an alcohol–water solution, 20–80 parts by volume, was used to wash the fabric. It then had a phosphorus content of 3.95% and a cation exchange capacity of 2.333 meq./g. This fabric had a DS of 0.25 phosphonomethyl groups per anhydroglucose unit. In the ammonium salt form, even before the retreatment, the fabric passed

TABLE II. Influence of Processing Variables Upon the Properties of Fabric Treated with Solutions Made with Chloromethylphosphonic Acid

Wt. of materials in water solution, %	Cure temp., °C.	Cure time, min.	Wt. P, %	Cation exchange capacity, meq./g.	Strip burn angle, degrees, NH_4 salt form
25% NaOH	110	5	0.36	0.30	45
	110	30	0.44	0.34	90
	140	5	0.42	0.33	100
2% $ClCH_2P(=O)(ONa)_2$	140	30	0.42	0.36	110
	Room temp.	1080	0.02	0.07	0
25% NaOH	110	5	0.15	0.17	0
	110	30	0.76	0.57	135
	140	5	0.81	0.57	135
5% $ClCH_2P(=O)(ONa)_2$	140	30	0.87	0.58	135
	Room temp.	1020	0.02	0.06	0
25% NaOH	110	5	0.92	0.59	90
	110	30	1.72	1.11	175
	140	5	1.62	1.07	175
10% $ClCH_2P(=O)(ONa)_2$	140	30	1.50	1.00	140
	Room temp.	1080	0.01	0.07	0
25% NaOH	110	5	2.0	1.31	180
	110	30	2.25	1.45	180
	140	5	2.23	1.40	180
15% $ClCH_2P(=O)(ONa)_2$	140	30	*	—	—

* Dissolved when washed in water after the cure.

the 180° strip flame test. This phosphorus content is possibly lower than might be obtained, since the fabric was jellylike and much of the more highly reacted portions went into solution. Washing this fabric in a higher ratio of alcohol-to-water mixture would eliminate the dissolution and result in a fabric with higher phosphorus content.

Phosphonomethylation of Cotton to Produce Water-Soluble Cotton

Cotton yarn (12's/4) which had been scoured, bleached, and mercerized was padded with a solution consisting of 35.1 parts by weight $ClCH_2P(=O)(OH)_2$, 96.5 parts by weight of NaOH, and 180 parts by weight of water to a wet pickup of 196%. (Note that the acid was not converted to the sodium salt before use.) The yarn was heated in a forced draft oven for 30 min. at 140° C. and washed in a 20% ethanol–water solution and then dried. The yarn had a weight increase of 13%. A sample of this yarn when placed in tap water dissolved immediately. The phosphorus content was 2.12%. The yarn passed the 90–110° angle flame test in the sodium salt form.

A sample of 48×48 cotton sheeting was treated in the same manner. It was also water soluble, but took longer to go into solution. It contained 2.4% P. The flammability was the same as that of the yarn.

Evaluation of Ion Exchange Capacity at Various pH Levels

Phosphonomethyl cotton is a cation exchange cotton of the strong acid type. It should behave like a dibasic acid. Its ionization characteristics can be measured by pH at half capacity and should be similar to those of the two hydrogens of chloromethylphosphonic acid.

The fabric used in this study contained 2.0% P. This is a degree of substitution of 0.12 phosphonomethyl groups per anhydroglucose unit. It was prepared by Method II. The cation exchange capacity of this fabric as a function of pH was determined by the method reported by Hoffpauir and Guthrie [6, 7]; see Figure 1. From the resulting curves, the total capacity and the pH at which the fabric exhibits one-half of the total capacity were obtained. The pH at half capacity is a good measure of the acidic or basic strength of an ion exchange material and may be used as a measure of the pK_a of the functional groups [7]. As shown in Figure 1, the pH at half capacity for the first hydrogen is approximately 1.9 and for the second hydrogen is 7.0, with total capacities of 0.6 and 1.1 meq./g. respectively. These pK_a values are in good agreement with what would be expected from the reported pK_a values for $ClCH_2P(=O)(OH)_2$. In the case of the chloromethylphosphonic acid the pK_a for the first hydrogen is 1.40 and for the second hydrogen is 6.30 [4]. The acidity of the hydrogen on the phosphonomethyl cellulose would be expected to be slightly less than that of the chloromethylphosphonic acid due to the presence of the halogen in the latter. The pH value at half capacity for phosphorylated cotton is approximately 1.5 for the first hydrogen and 7.5 for the second hydrogen [6].

Summary

A new phosphorus-containing ether of cotton cellulose has been made by reacting cotton with disodium chloromethylphosphonate in the presence of sodium hydroxide. The starting reagent may be either chloromethylphosphonic dichloride or chloromethylphosphonic acid. In either case the reagent is first dissolved in just enough NaOH solution to form the disodium salt of the acid. The solution is held at 30° C. or below during the neutralization to prevent hydrolysis of halogen from the chloromethyl group. After this, more sodium hydroxide is added and then the solution is used to treat cloth or yarn. Fabric is treated by padding with the solution and then heating. The degree of substitution can be varied widely by varying the concentration of the phosphonomethylating agent and of the sodium hydroxide and by varying the time and temperature of the cure. Fabric containing up to 3.96% phosphorus was produced by giving the fabric a double treatment. At this degree of substitution the textile was quite soluble in water. Up to 2.25% phosphorus was introduced by a single treatment. Generally, the modified cotton becomes water soluble when about 2.0% phosphorus is introduced. A permanently starched effect is produced with phosphorus contents of approximately 1%. At this degree of substitution there is little or no change in the breaking strength of the fabric. Modified cotton containing between 1%

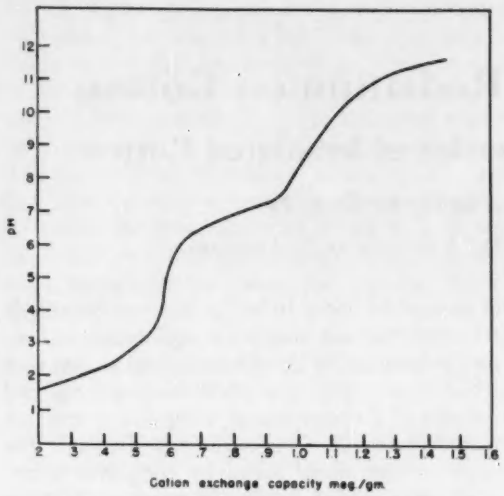

Fig. 1. Cation exchange capacity of phosphonomethylated cotton.

and 2% phosphorus has greatly increased swelling properties in water.

The phosphonomethyl cotton is produced as the sodium salt. It can be converted to the free acid form by soaking or rinsing in dilute mineral acid. The pK_a values for the first and second ionizations are 1.9 and 7.0, respectively. When in the ammonium salt form, the phosphonomethylated cotton has good flame resistance.

Acknowledgment

Acknowledgment is made to James A. Harris for phosphorus determinations and cation exchange capacities and to Harold P. Pastor for nitrogen determinations.

Literature Cited

1. ASTM D 1424–56T.
2. Chance, L. H., Warren, Jane, and Guthrie, J. D. (to Secretary of Agriculture of the United States), U. S. Patent 2,743,232 (April 24, 1956).
3. Coppick, S. and Hall, W. P., in "Flameproofing Textile Fabrics," edited by R. W. Little (A.C.S., Monograph 104), pp. 179 ff., New York, Reinhold (1947).
4. Crofts, P. C. and Kosolapoff, G. M., *J. Am. Chem. Soc.* **75**, 5738–5740 (1953).
5. Ford, F. M. and Hall, W. P. (to Joseph Bancroft & Sons Co.), U. S. Patent 2,482,755 (Sept. 27, 1949).
6. Guthrie, J. D., *Ind. Eng. Chem.* **44**, 2187–2189 (1952).
7. Hoffpauir, C. L. and Guthrie, J. D., TEXTILE RESEARCH JOURNAL **20**, 617–620 (1950).
8. Kabachnik, M. I. and Medved, T. Ya., *Izvest. Akad. Nauk S.S.S.R.*, Otdel. Khim. Nauk **1951**, 95–97, through *Chem. Abs.* **46**, 421 (1952).
9. Pons, W. A., Jr., Stansbury, M. F., and Hoffpauir, C. L., *J. Assoc. Offic. Agr. Chemists* **36**, 492–504 (1953).
10. Reeves, W. A., McMillan, O. J., Jr., and Guthrie, J. D., TEXTILE RESEARCH JOURNAL **23**, 527–532 (1953).
11. Reid, J. D. and Mazzeno, L. W., Jr., *Ind. Eng. Chem.* **41**, 2828–2831 (1949); Reid, J. D., Mazzeno, L. W., Jr., and Buras, E. M., Jr., *Ibid.* 2831–2834.
12. U. S. Federal Supply Service, "Textile Test Methods," Federal Specifications CCC-T-191b, Method 5902. U. S. Govt. Print. Off., Washington, D. C. (1951).
13. Yakubovich, A. Ya. and Ginsburg, V. A., *Zhur. Obshchĕi Khim.* **22**, 1534–1542 (1952) through *Chem. Abs.* **47**, 9255b (1953); *J. Gen. Chem. (U.S.S.R.)* **22**, 1575–1582 (1952) (Engl. translation), through *Chem. Abs.* **48**, 4435 (1954).

Manuscript received October 27, 1958.

The Effects of Gamma Radiation on Cotton

Part III: Base Exchange Properties of Irradiated Cotton

Robert J. Demint and Jett C. Arthur, Jr.

Southern Regional Research Laboratory,[1] New Orleans 19, Louisiana

IT HAS been reported that the principal reaction which cotton undergoes on exposure to gamma radiation is oxidation to yield reducing groups, chain cleavages, and carboxyl groups in the approximate ratio of 20:1:1 [1, 3]. The base exchange properties of gamma irradiated cotton cellulose, using radioactive tracer techniques, offer a sensitive means to indicate changes in the cotton. The base exchange properties of cotton, receiving gamma dosages ranging from zero to 100 megaroentgens, are reported.

Experimental

Gamma Irradiated Cotton Cellulose

Raw Deltapine cotton was purified and irradiated in an acidic form in an atmosphere of oxygen as previously described [3]. The gamma irradiations were performed at the National Reactor Testing Station, using fission products in spent MTR fuel elements, and at the Southern Regional Research Laboratory, using a kilocurie Co^{60} source.

Materials

The radioactive materials, $Ca^{45}Cl_2$ in 0.9% HCl solution, specific activity about 74 mc./g. and 54.6 mg. of Ca/ml., and $Co^{60}Cl_2$ in about neutral HCl solution, specific activity about 17 c./g. and 0.118 mg. of Co/ml., were obtained from the Oak Ridge National Laboratory. Stock solutions were prepared by diluting the above solutions about 500-fold with calcium or cobalt acetate solutions of desired molarity. Other chemicals used were C.P. or reagent grade.

Radioassay

Cotton (0.2 g.), ground to pass a 20-mesh screen, was suspended in 10 ml. of the desired salt solutions and agitated for about 16 hr. It had been previously established that salt absorption equilibrium was attained in less than 16 hr. The test solution was then clarified by centrifuging at 25,000 times gravity, and an aliquot of the supernatant solution was dried on a planchet and counted in a gas flow counter. The change in radioactive count, as compared to the control, was related to the micromoles of cation absorbed by the cotton. The use of a similar assay technique, using ion exchange cotton fabrics, has been reported [2]. Also, Moncrieff-Yeates and White [4] used a change in radioactive count to determine the interaction of simple salt solutions with cellulosic fibers.

The relative affinities of irradiated cottons for different cations were determined by measuring the extent of exchange between cations on the cotton and those in solution. Ca^{45} and Co^{60} were used for purposes of radioassay. The cotton was suspended in a solution of 0.002 *M* radioactive calcium acetate or cobalt acetate. Then, competing cations were added. The change in tagged ion in the solution was taken as a measure of its replacement on the cotton by the competing ion.

Data and Discussion

Exchange Reactions Involving Replacement of H^+ by Ca^{++}

The cotton had been purified, treated with acetic acid, and washed with water prior to irradiation, in order that the oxidized cellulose would exist in the free acid form. Then, when the irradiated cotton was suspended in solutions of calcium acetate, the hydrogen ions of the carboxyl groups formed on the cotton could be replaced by the calcium ions. The results of the direct determination of the Ca^{++} replacing H^+, using the radioassay technique, are shown in Figure 1.

[1] One of the laboratories of the Southern Utilization Research and Development Division, Agricultural Research Service, U. S. Department of Agriculture.

The Ca^{++}, interacting with the insoluble fraction of irradiated cotton, reached a maximum at about a 3-fold excess [2] of Ca^{++} for the cotton receiving a dosage of 100 megaroentgens and was about constant to at least a 6-fold excess of Ca^{++}. For the cotton receiving a dosage of 50 megaroentgens, the range was from about a 5-fold to a 12-fold excess of Ca^{++}. For the cotton receiving a dosage of 10 megaroentgens, the range was from about an 8-fold to a 20-fold excess of Ca^{++}. The unirradiated control sample of cotton had a small but measurable exchange of Ca^{++} with H^+.

Exchange Reactions Involving Replacement of Ca^{++} by H^+

Purified cotton, receiving a dosage of 50 megaroentgens, was suspended in 0.002 *M* calcium acetate; the aqueous suspension had a pH of 5.00. Under these conditions, the cotton absorbed about 20 micromoles of Ca^{++} per gram of cotton. As shown in Figure 2, when the H^+ concentration was increased by addition of acetic acid, the H^+ replaced the Ca^{++}. For example, at a mole ratio of 10 moles of acetic acid per mole of calcium acetate, H^+ replaced about half of the Ca^{++}. When the H^+ concentration was decreased by addition of ammonium hydroxide, the amount of Ca^{++} absorbed by the cotton increased. Apparently, the NH_4^+ offered little competition for Ca^{++}.

[2] That is, there was about three times as much Ca^{++} available in the solution as was apparently bound by the cotton.

Exchange Reactions Involving Replacement of Metallic Ions by Metallic Ions

The replacement of Ca^{++}, absorbed on cotton, by cations from dilute salt solutions is shown in Figure 3. The dotted curve, labelled "free exchange," would have been obtained experimentally if the competing ions and Ca^{++} had equal affinity for the binding sites on the irradiated cotton. That is, in making the calculation, it was assumed that the quantity of a given cation bound by the cotton was in direct proportion to its concentration relative to other cations in the solution. The Ca^{++} appears to be the most tightly bound cation. Under the experimental conditions, the relative order of affinity

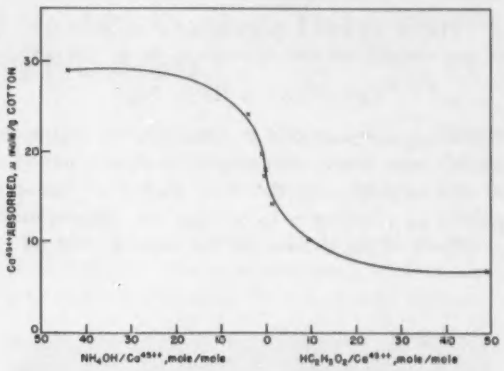

Fig. 2. Exchange reactions of cotton involving replacement of Ca^{++} by H^+. Cotton received 50 megaroentgens of gamma radiation.

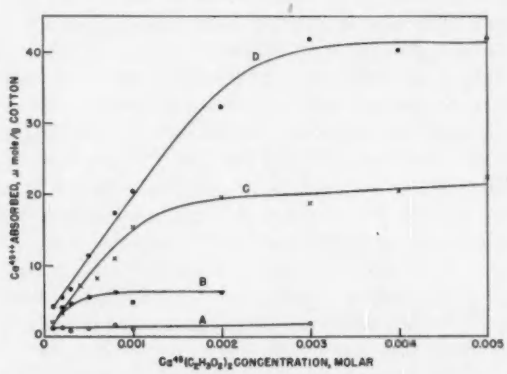

Fig. 1. Exchange reactions of cotton involving replacement of H^+ by Ca^{++}. Cotton A, control; B, gamma irradiated to 10 megaroentgens; C, to 50 megaroentgens; D, to 100 megaroentgens.

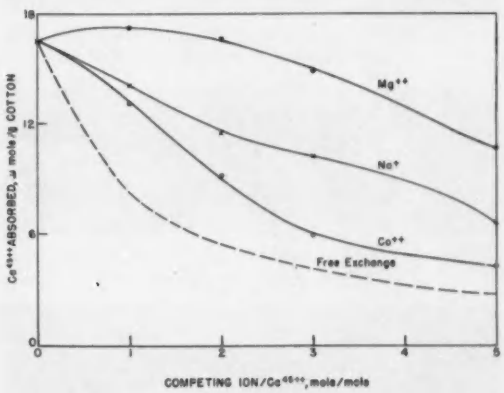

Fig. 3. Exchange reactions of cotton involving replacement of Ca^{++} by Na^+, Mg^{++}, or Co^{++}; 0.002 *M* $Ca(C_2H_3O_2)_2$ used. Cotton received 50 megaroentgens of gamma radiation.

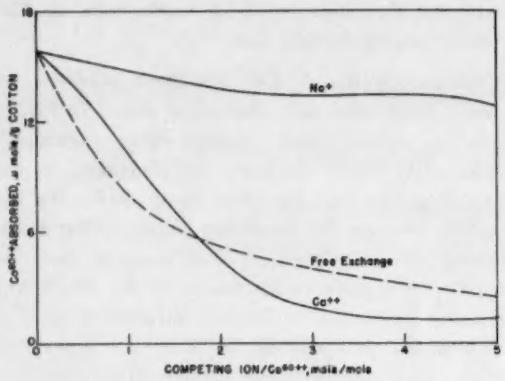

Fig. 4. Exchange reactions of cotton involving replacement of Co^{++} by Na^{+} or Ca^{++}; 0.002 *M* $Co(C_2H_3O_2)_2$ used. Cotton received 50 megaroentgens of gamma radiation.

of the metallic cations appears to be as follows:

$$Ca^{++} > Co^{++} > Na^{+} > Mg^{++}$$

The replacement of Co^{++}, absorbed on cotton, by cations from dilute salt solutions is shown in Figure 4. As in Figure 3, the "free exchange" curve is plotted as a reference to indicate the relative order of affinity of the cations for the binding sites on irradiated cotton. Under the experimental conditions, the relative order of affinity of the cations appears to be as follows:

$$Ca^{++} > Co^{++} > Na^{+}$$

Summary

It has been demonstrated, using radioactive cations, that cottons subjected to gamma radiation have base exchange properties. The number of groups on the cottons exhibiting these properties increased with increasing radiation dosage. Salt bonds were probably the major linkages involved, since any cation could be replaced with another cation by varying relative concentrations.

Literature Cited

1. Arthur, J. C., Jr., TEXTILE RESEARCH JOURNAL **28**, 204–6 (1958).
2. Arthur, J. C., Jr. and McLemore, T. A., *J. Am. Chem. Soc.* **78**, 4153–5 (1956).
3. Blouin, F. A. and Arthur, J. C., Jr., TEXTILE RESEARCH JOURNAL **28**, 198–204 (1958).
4. Moncrieff-Yeates, M. and White, H. J., Jr., *Am. Dyestuff Reptr.* **46**, P87–96 (1957).

Manuscript received November 10, 1958.

Letters to the Editor

Short communications in the form of Letters to the Editor are intended to provide prompt publication of significant new research results and to permit an exchange of views on papers previously published in the JOURNAL. These communications are not submitted to formal review as are research papers, and the editors do not assume any share of the author's responsibility for the information given or the opinions expressed. When work previously published in the JOURNAL is the subject of critical comment, the authors of the original paper are given an opportunity to submit a reply, which will be published concurrently when possible.

A Useful Stain for Inclusion and Surface Damage Detection in Viscose Rayon Filaments

Microscopical Laboratory
American Enka Corporation
Enka, N. C.
November 19, 1958

To the Editor

TEXTILE RESEARCH JOURNAL

Dear Sir:

We have found that an innovation in Gram's bacterial stain is quite useful in detecting certain defects in viscose rayon filaments.

In the course of examination of certain deposits on the surface of viscose rayon yarn suspected to be bacterial in origin, we found that on using Gram's stain, the yarn, following the final rinse in alcohol, not only showed the stained surface deposit, but certain localized areas within the individual filaments also had stained a brilliant blue or red color. These areas for the most part were of a general elongated oval shape, the elongation being in the direction of the filament axis. They consisted of an apparently amorphous aggregation of fine particles. Cross-sectioning of the stained filaments show the stained inclusions to be confined to the filament core.

Such stained areas are most frequently found in yarns which on testing are lower in strength than normal. In the past year we have not found any textile yarns of weak strength with which we have not been able to demonstrate such areas by this method. This statement, of course, does not include samples which were obviously weak because of mechanical damage, as seen by surface abrasion and cuts.

We have found similar areas in some "normal" strength yarns. Where these occur, however, they are usually confined to a very few of the filaments.

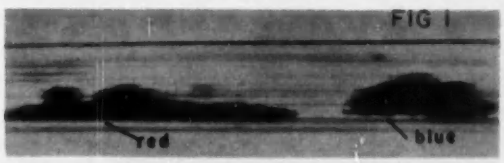

Fig. 1. Single filaments showing red and blue stained spun-in inclusions (inhomogeneities).

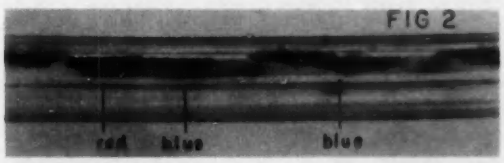

Fig. 2. Single filaments showing red and blue stained spun-in inclusions (inhomogeneities).

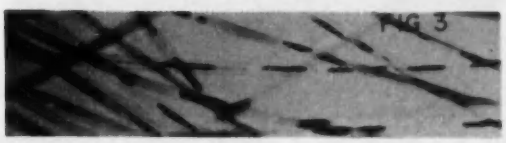

Fig. 3. Several stained filaments from the same thread.

Since the staining procedure is somewhat more simplified than the complete Gram technique, the following outline of the method is given.

Reagents

1. *Ehrlich's Aniline Gentian Violet*
   Saturated alcoholic solution of gentian violet 6 cc.
   Absolute alcohol 5 cc.
   Aniline water 50 cc.
   (Aniline water may be prepared by shaking 2 cc. of aniline with 98 cc. of water for several minutes.)
2. *Gram's Iodine*
   Iodine 1 g.
   Potassium iodide 2 g.
   Water 300 cc.
3. *95% Alcohol*

For use, 500 cc. of the Aniline Gentian Violet is prepared as a stock solution.

Note that no counter stain is used, as in the normal Gram technique.

Procedure

Aniline Gentian Violet (100 cc.) is placed in a 250-cc. glass beaker and brought gradually to a gentle boil.

A small skein is now entered into the dye and stained for 5 min. at the boil, the yarn being kept in constant motion during the dyeing.

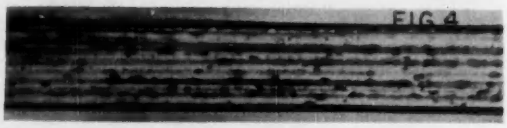

Fig. 4. Single filaments showing red and blue stained spun-in inclusions (inhomogeneities).

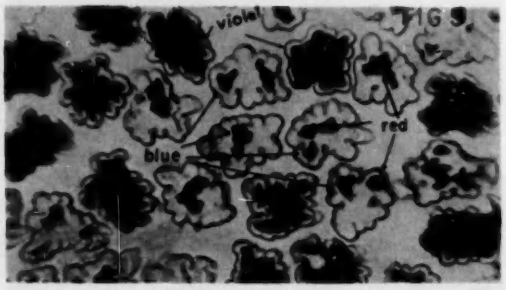

Fig. 5. Cross sections of filaments showing confinement of stained areas to core of filaments.

The sample is next removed from the dyebath and washed under a cold water tap until no evidence of color in the wash water may be seen.

Gram's Iodine (100 cc.) is placed in a 250-cc beaker and the wet sample entered into the cold solution, staining with agitation for 5 min.

The sample is then removed from the iodine bath, allowed to drain, and then entered into the first of three 100-cc. alcohol rinses, the first two being for 10 min. each, the last for 30 min. A variation in the time of the alcohol rinse may be made as desired in order to leave the body of the individual filaments, outside the stained inclusions, more or less colored by the dye.

We have used this method of staining for some time and have found the following facts connected with these phenomena.

Detection of Spun-In Inhomogeneities

1. Stained regions easily detectable in the filaments after staining are not previously detectable microscopically, either in transmitted light, using various mounting media of different refractive index, by swelling methods with polarized light, or with the phase microscope. We have found instances where small pieces of viscose skin, spun in the yarn with the material of the stained areas, but not stained intensely themselves, could be easily seen with the phase microscope. However, other areas which were afterwards easily found by staining with the outlined procedure were not detectable with the phase microscope.

On the other hand, where filaments containing the stained areas were subjected to a controlled bleaching until almost entirely colorless, the formerly stained areas and their granular particulate divisions could be detected easily with the phase microscope.

It would appear from the above that the stained areas within the filament have approximately the same optical and physical density as the known cellulose areas of the filament. Similarly, there is no great difference in optical reaction between this region before staining and the rest of the filament core.

2. If filaments containing the stained inclusions are now cross-sectioned, the stained areas will be confined to the core of the individual filaments.

3. If cross sections of filaments from a sample whose yarns by trials have been found to exhibit stained areas are made before staining, and these cross sections are then stained by the above proce-

dures, stained areas will again be found to develop in the core of the filaments.

4. While the areas made visible by staining are not easily detected before staining due to their close approximation in density and optical character to the rest of the filament, they are much more resistant after staining to cellulose solvents than their surround. Thus if a filament containing stained areas is placed in cold concentrated H_2SO_4 and observed under the microscope, it will be found that the surround completely dissolves well before the stained area starts to disintegrate. When this finally occurs it is seen as an apparent peptization, the area breaking up into many fine particles. Similar particles may also be observed as a residue after complete disintegration, in the same way, of unstained filaments from the same sample. In this instance, however, the comparative unstained areas, which are stained under the dyeing procedure, do not maintain their individuality sufficiently long after their surround to be distinguished as such.

5. The stained areas differ greatly in size and in number among different samples. Instances have been found where a single area occupied most of the filament diameter and extended for lengths of several hundred microns. Similarly, other samples have contained areas of 5μ or less in greatest diameter, the number of such separate areas being, however, much higher than in the first instance, and well distributed throughout the filaments' cores. Individual areas may be stained blue or red, and may be found well spaced or close together.

6. The appearance and structure of the stained areas found by this procedure in the filaments indicate that they are spun-in materials, probably cellulosic in some relation, and originate with the viscose or one of its components.

Detection of Mechanical or Chemical Damage

If rayon yarn seems weak in strength and low on elongation, the use of this staining procedure is particularly helpful.

Any damage to the filament which penetrates to a depth equivalent to its skin thickness may be distinguished quickly by the use of this staining technique.

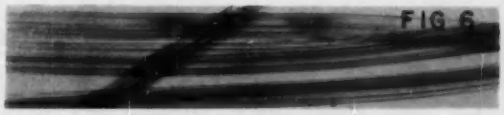

Fig. 6. The detection of surface damage.

Fig. 7. The detection of surface damage.

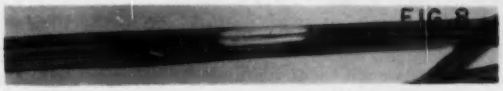

Fig. 8. The detection of surface damage.

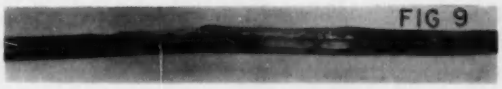

Fig. 9. The detection of surface damage.

After the yarn is stained as outlined above, it is removed from the last alcohol rinse, and a length approximately 2½ in. cut out with scissors.

One end of this length of yarn is held with the left thumb in contact with the surface of a clean glass microscope slide, while the other is spread evenly over the slide surface, using a jet of water from a water tap or a laboratory water bottle. When this end has been opened the slide is reversed, the open end being held in place with the thumb and the other end spread out with the jet of water.

The excess of water is now drained off carefully and the preparation covered with a glass cover slide.

The preparation is now placed on the stage of the microscope; an examination may be quickly made. Damaged areas and the cut ends of filaments will be found to have lost the stain and appear white or clear, the rest of the fibers being stained.

The above phenomena are illustrated by the accompanying photomicrographs.

E. CORWITH JOLLIFF

A Note on the Degradation of Jute Cellulose on Storage

Technological Research Laboratories
Indian Central Jute Committee
Calcutta 40, India
September 18, 1958

To the Editor

TEXTILE RESEARCH JOURNAL

Dear Sir:

In the course of investigations on the degree of polymerization (DP) of alpha-cellulose from jute fiber, the measurement of the solution viscosity of a particular sample was repeated at some months' interval to check the results obtained previously. The marked fall observed in the viscosity (hence, DP), contrary to expectation, provided an incentive to the present study. Various workers have shown that cellulose fiber is degraded by exposure to light [1, 6, 7, 9], heat [12, 13], microorganisms [4, 8, 10], and by storage [10]. But there is little evidence on record to show whether or not pure cellulose extracted from bast fibers deteriorates in storage under ordinary conditions. The importance of this study cannot be overemphasized. High-grade viscose rayon pulp is imported into this country from abroad, and it may be necessary to stock this material in good condition for a fairly long time against any emergency cut in the supply. The facts relating to the sensitivity of pure cellulose to oxidation and hydrolysis in humid air under the prevailing indoor conditions need be clearly understood before a suitable remedy can be found. Preliminary results on the deterioration of alpha-cellulose upon aging in storage are reported here.

Replicate preparations of alpha-cellulose were made with 17.5% caustic soda solution by the ACS method from the chlorite holocellulose of each sample of jute fiber. Portions taken from each preparation were immediately analyzed for copper number, acid value, and relative viscosity (hence, DP) at 0.5% concentration in cuprammonium solution. The methods of estimation were described earlier [2]. The remaining materials—jute fiber and cellulose preparations—were loosely wrapped in paper and left in the prevailing conditions (RH 50–85%, average 70%) inside the laboratory. At approximate intervals of time, chosen at random, samples were drawn out from storage and analyzed for the characters of alpha-cellulose as before. Some old preparations were treated with 5% caustic soda solution (1:100) at 30° C. for 1 hr., and loss in weight was determined. Some samples were heated in an air-oven at 105° C.; they were also analyzed before and after treatment.

The results are summarized in Table I. Each value represents the mean of several estimations. Quite a significant drop in the viscosity and DP of alpha-cellulose preparation takes place on storage, accompanied by an increase in its reducing power and acidity, as indicated by copper number and acid value. On the other hand, viscosity DP of alpha-cellulose *in situ* remains practically unchanged on prolonged storage of the jute fiber, perhaps because the associated noncellulosic constituents protect the alpha-cellulose. The fresh preparation, originally white, turns brown upon aging, more so on the surface than in the bulk. This discoloration is a clear symptom of chain degradation. The coloring matter, about 4% of low molecular oxycellulose, was completely removed by mild alkaline treatment and the copper number as well as acid value reduced, but the viscosity DP was not changed appreciably, the error of estimate being 5%. McIntyre [11] found with bleached sulfite pulp that the rate of discoloration upon aging rises linearly with relative humidity above 20%. Alpha-cellulose is gradually degraded when heated to dryness in an air-oven, producing oxycelluloses of the reducing type. This effect was also observed by Norman [12] with his isolated plant celluloses containing hemicellulose and by Demus [5].

From observations on the deterioration of jute fiber under ordinary conditions of storage, Macmillan and Bose [10] concluded that oxidation and not hydrolysis was the main effect. The present results will show that the deterioration of pure cellulose preparations under similar conditions is the combined effect of oxidation and hydrolysis of the cellulose chain, as characterized by a rise in the acid value and copper number, and a fall in the viscosity DP. Freshly prepared alpha-cellulose contains small amounts of free carboxyl groups as an artifact of the preparative treatment. These acid groups, in the presence of sensitizers (moisture etc.), tend to set up hydrogen-ion (auto-) hydrolysis of the cellulose molecules at the neighboring glucosidic linkages

TABLE I. Effect of Various Treatments on Jute Alpha-Cellulose

Sample and treatment	Time, months	Acid value, meq./100 g.		Copper number, g. Cu/100 g.		Rel. viscosity, $\eta_{0.5}$		DP		
		Initial	Final	Initial	Final	Initial	Final	Initial	Final	% Fall
Alpha-cellulose stored										
4144 *C* (a)	7	—	—	—	—	4.93	4.10	808	710	12.1
(b)	8	—	—	—	—	5.19	4.40	834	746	10.6
4577 *C*	12	5.32	6.30	0.36	0.76	6.00	3.31	912	596	34.6
5% NaOH at 30° C. (1 : 100), 1 hr., Loss—3.26%	0	6.30	2.89	0.76	0.56	3.31	3.58	596	637	−6.9
4589 *C*	10	3.63	5.64	0.39	0.57	5.77	3.64	890	646	27.4
5% NaOH at 30° C. (1 : 100), 1 hr., Loss—4.45%	0	5.64	3.34	0.57	0.42	3.64	3.59	646	638	1.2
4787 *O*	12	4.18	4.80	0.51	0.64	5.85	4.08	898	707	21.4
5% NaOH at 30° C. (1 : 100), 1 hr., Loss—3.25%	0	4.80	2.65	0.64	0.46	4.08	4.00	707	696	1.6
4929 *C*	13	—	5.34	—	0.70	5.89	3.92	902	686	23.9
5% NaOH at 30° C. (1 : 100), 1 hr., Loss—4.00%	0	5.34	2.90	0.70	0.58	3.92	3.71	686	656	4.4
Jute fiber stored										
3122 *C*	60					5.31	5.01	846	816	3.5
3267 *C*	60					5.56	5.76	872	888	−1.8
4787 *O*	14					5.85	5.75	898	888	1.1
	Time, hr.									
Alpha-cellulose heated in air-oven at 105° C.	6	—	—	—	—	4.87	4.25	800	728	9.0
4582 *C*	24	4.03	3.83	0.30	0.67	4.87	3.13	800	566	29.3
	5	—	—	—	—	5.75	5.32	888	848	4.5
4787 *O*	22	—	—	—	—	5.75	4.07	888	706	20.5

C = capsularis; *O* = olitorius.

during aging, so that a fall in viscosity DP and a rise in copper number would occur as with acidic oxycelluloses from cotton [3]. Alternatively, if it is a case of microbiological degradation, then also cellulose will be hydrolyzed by the secreted enzymes, resulting in depolymerization and an increase in copper number [8]. That the viscosity of the stored material does not show any significant decrease after alkali treatment possibly shows that it was subject to acid action (hydrolysis) and/or oxidation in storage followed by alkaline hydrolysis in cuprammonium solution. Further work on these lines is in progress to elucidate the nature of this degradation and the ways to check it.

Our thanks are due to Dr. P. B. Sarkar, Director, for his keen interest in this work.

Literature Cited

1. Bot, A. C. W. and van Vreeswijk, A. C., *Textilber.* **20**, 115, 181 (1939).
2. Chatterjee, H. et al., TEXTILE RESEARCH JOURNAL **24**, 43 (1954).
3. Davidson, G. F. et al., *J. Textile Inst.* **42**, T141 (1951); **46**, T407 (1955); **47**, T439 (1956).
4. Dean, J. D. and Worner, R. K., *Am. Dyestuff Reptr.* **36**, 405 (1947).
5. Demus, H., *Faserforsch. und Textiltech.* **1**, 357 (1956).
6. Egerton, G. S., *J. Soc. Dyers Colourists* **65**, 764 (1949).
7. Egerton, G. S., TEXTILE RESEARCH JOURNAL **18**, 659 (1948).
8. Greathouse, G. A., TEXTILE RESEARCH JOURNAL **20**, 227 (1950).
9. Launer, H. F. and Wilson, W. K., *J. Am. Chem. Soc.* **71**, 958 (1949).
10. Macmillan, W. G. and Bose, S. N., *J. Textile Inst.* **38**, T350 (1947).
11. McIntyre, J. W., *Paper Trade J.* **109**, 317 (1939).
12. Norman, A. G., *Biochem. J.* **30**, 2054 (1936).
13. Waller, R. C. et al., *Ind. Eng. Chem.* **40**, 138 (1948).

H. CHATTERJEE
A. K. MAZUMDAR

The Hydrogen→Deuterium Exchange Reaction in Stretched Keratin

Wool Textile Research Laboratories
Commonwealth Scientific and
Industrial Research Organization
Australia
November 10, 1958

To the Editor

TEXTILE RESEARCH JOURNAL

Dear Sir:

It has been shown previously [1] that the hydrogen → deuterium exchange reaction in wool may be studied by means of infrared spectra in the range 4000–6000 cm.$^{-1}$. The extent to which hydrogen has been replaced by deuterium in the peptide linkages may be estimated from the optical density of the absorption peak at 4860 cm.$^{-1}$, which is a combination of the 3300 cm.$^{-1}$ peptide NH stretching mode and a second peptide mode *ca.* 1540 cm.$^{-1}$. The transition moment associated with this combination mode is approximately perpendicular to the N—H bond so that the observed perpendicular dichroism (see Figures 1a and 1b) is consistent with the presence of α-helices preferentially oriented parallel to the fiber axis. In Figure 1b, where the exchange reaction has been carried out to equilibrium in the unstretched fibers, there is a considerable reduction in the optical density of the 4860 cm.$^{-1}$ band accompanied by an increase in dichroic ratio, indicating that the residual peptide hydrogens occur predominantly in the well oriented and presumably crystalline regions. The wool was then stretched at room temperature in D_2O by steps of 1% up to an extension of 40% over a period of 8 hr. and held at this extension for one day. The spectrum obtained from this wool after relaxing in D_2O and drying is shown in Figure 1c. Both the peak and the perpendicular dichroism at 4860 cm.$^{-1}$ are virtually eliminated, suggesting that the exchange of hydrogen by deuterium is almost complete in this instance. It appears therefore that during extension of the wool fibers to 40% all the peptide linkages are able to enter into a hydrogen → deuterium exchange. This means that the whole of these fibers including the oriented regions is accessible to water.

This is in contrast with results obtained when fibers are extended to 40% and relaxed in H_2O and then reacted to equilibrium with D_2O; the absorption spectrum (not shown) is similar to that of unstretched fibers (Figure 1b). It is also in contrast with tests [2] on fibers containing a large amount of β-keratin, when only partial hydrogen → deuterium

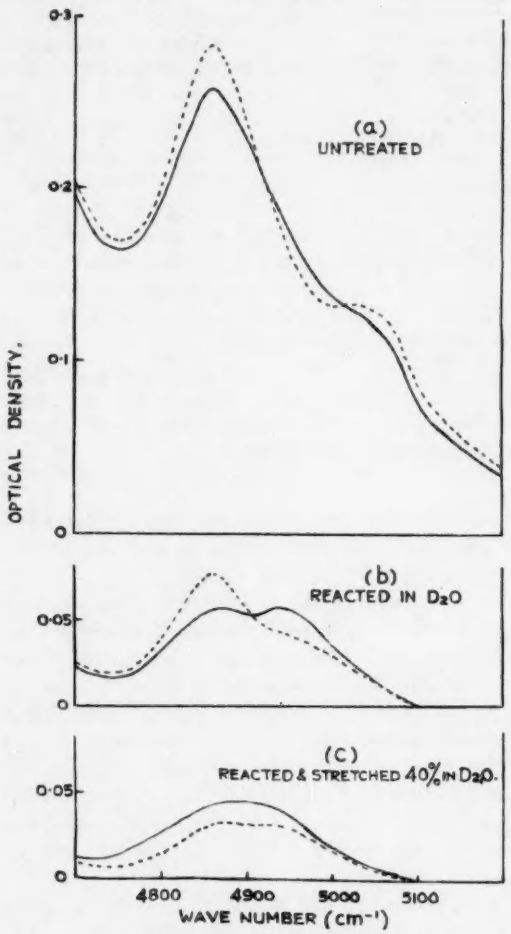

Fig. 1. Infrared spectra of dry aligned Lincoln wool fibers. (a) Untreated, (b) reacted to equilibrium in D_2O, (c) stretched to 40%, reacted to equilibrium, and relaxed in D_2O. The solid line is the spectrum obtained with electric vector vibrating parallel, and the dotted line, perpendicular, to the fiber axis.

exchange is obtained. In both these cases, therefore, it is likely that the oriented regions of the fiber are only partially accessible to H_2O.

The experiment was repeated at an extension of 5%, but the peak at 4860 cm.$^{-1}$ in Figure 1b showed a small reduction with no noticeable change in the perpendicular dichroism, indicating little increase in the hydrogen → deuterium exchange as against an unstretched fiber.

The origin of the residual broad parallel band at 4900 cm.$^{-1}$ is uncertain at present, but may be due to the first overtone of the N—D stretching vibration or the second overtone of the C—O stretching vibration.

Literature Cited

1. Fraser, R. D. B. and MacRae, T. P., *J. Chem. Phys.* **28**, 1120 (1958).
2. Fraser, R. D. B. and MacRae, T. P., *J. Chem. Phys.* **29**, 1024 (1958).

E. G. BENDIT
M. FEUGHELMAN
R. D. B. FRASER
T. P. MACRAE

The Occurrence of 4-*O*-Methyl-D-glucuronic Acid in Jute Hemicellulose

Department of Chemistry
University of British Columbia
Vancouver, Canada
November 24, 1958

To the Editor

TEXTILE RESEARCH JOURNAL

Dear Sir:

Your correspondents Das Gupta and Sarkar have reported [1] the occurrence of 3-*O*-methyl-D-glucuronic acid in jute hemicellulose, this identification being based on the paper chromatographic behavior of the monomethylglucose obtained by lithium aluminum hydride of the uronic acid. In view of the known difficulty of unequivocally identifying the monomethylglucoses on paper because of their very similar R_f values, we have repeated this identification. The 4-*O*-methyl-D-glucuronic acid is now well known in nature, but the occurrence of the 3-methyl ether has never been proved.

Graded hydrolysis of the hemicellulose with sulfuric acid gave an aldobiouronic acid which was cleaved with methanolic hydrogen chloride. The resulting uronic ester glycoside was characterized as its crystalline amide, and by mixed melting point (234–236° C.) was shown to be identical with methyl 4-*O*-methyl-α-D-glucopyranuronamide [3]. A second portion of the aldobiouronic acid was reduced and hydrolyzed and the monomethylglucose identified as the crystalline osazone and N-phenylglucosylamine. When the former derivative (m.p. 159–160° C.) was mixed with authentic 4-*O*-methyl-D-glucosazone, the m.p. was 158–159° C. [3]; when mixed with 3-*O*-methyl-D-glucosazone, the m.p. was 146–164° C. The N-phenylglucosylamine derivative had m.p. 156–158° C. and 156–159° C. when mixed with an authentic sample from 4-*O*-methyl-D-glucose. These results conclusively show that the uronic acid is 4-*O*-methyl-D-glucuronic acid, and this is confirmed by the paper of Srivastava and Adams [4] which appeared as this work was being completed. Experimental details will be published elsewhere [2], together with evidence that the aldobiouronic acid is 2-*O*-(4-*O*-methyl-α-D-glucopyranosiduronic acid)-D-xylose.

Literature Cited

1. Das Gupta, P. C. and Sarkar, P. B., TEXTILE RESEARCH JOURNAL **24**, 1071 (1954).
2. Dutton, G. G. S. and Rogers, I. H., *J. Am. Chem. Soc.* **81** (March 1959).
3. Smith, F., *J. Chem. Soc.* 2646 (1951).
4. Srivastava, H. C. and Adams, G. A., *Chem. and Ind.* 921 (1958).

G. G. S. DUTTON
I. H. ROGERS

Book Reviews

Chemical Publications; Their Nature and Use, Third Edition, New York, McGraw-Hill, 1958. 327 pages. Price $7.00.

The first revision of this standard text since 1940 is a welcome one. The general outline of former editions is followed; however, much new material and updating of the old has been included. Although meant primarily for students, the book should be of great help to chemists and technical librarians about to undertake a literature search. Sources of information are divided into primary (periodicals, institutional publications, patent literature, dissertations, manufacturers' technical publications), secondary (abstracting journals, reviews, bibliographies, reference works, monographs, textbooks), and tertiary (guides and directories). Also included are helpful suggestions on the mechanics of the actual search, as well as a short history of the development of chemical literature.

Automatic Control: Principles and Practice. Werner G. Holzbock. New York, Reinhold, 1958. 252 pages. Price $7.50.

Reviewed by E. J. Bernet, Institute of Textile Technology, Charlottesville, Virginia

Mr. Holzbock, who is Chief Engineer of the Askanis Regulator Company, has prepared an excellent primer on the basic fundamentals of automatic control in pneumatic systems. Starting with careful definitions of such terms as set point, primary feedback, summing point, off-set, dead time, etc., the first chapters also include typical static characteristics and dynamic behavior.

Beginning with the simplest type of two-position automatic control action, the examples and descriptions advance through single-spaced floating action, proportional-speed floating action, proportional-position action, proportional plus reset action, and, finally, proportional plus reset plus rate action. In almost completely nonmathematical terms, these types are first considered as applied to simple processes with and without selfregulation. The method used is graphical, i.e., showing what happens at various points in the control loop as a function of time, with step changes being made in the actuating signal or load.

Next, the same types of automatic control action are analyzed from the standpoint of frequency response, bringing in a thorough description of analysis by means of both the Nyquist and Bode diagrams. Although Mr. Holzbock has attempted to prepare this text without using differential equations, he has included a wealth of formulas and data tables which the practical worker in this field will find useful.

Following chapters are on mechanical components, special nonlinear devices, and various types of controllers, with particular emphasis on two devices: the flapper-nozzle and the jet pipe. These two devices are described in great detail, and are used in many of the examples of automatic control systems. A short chapter on electrical components describes potentiometers, differential transformers, and selsyns, touching only momentarily on electronic and magnetic amplifiers. The concluding chapters are devoted to descriptions of final control elements and complete present-day pneumatic control systems in industrial applications.

The many figures in this book are well drawn and helpful, and the explanations and descriptions are written in a simple and understandable manner. At strategic points throughout the book, the author has inserted concise paragraphs of summary and conclusions, a useful feature worthy of more widespread use.

In this reviewer's opinion, the title should include the word "pneumatic," since this is the primary content of the book. Automatic Control is no longer a single specialized field, but a group of specialized fields including pneumatic, hydraulic, electrical, electronic, etc.